NASA CR-120880

DEVELOPMENT OF OXIDATION RESISTANCE IN THORIATED NICKEL-CHROMIUM BASE ALLOYS

by

M. S. Seltzer, B. A. Wilcox, and R. I. Jaffee

BATTELLE
Columbus Laboratories

prepared for

NATIONAL AERONAUTICS AND SPACE ADMINISTRATION

Technical Management
NASA Lewis Research Center
Contract NAS 3-14326
Cleveland, Ohio

1. Report No.	2. Government Accession No.	3. Recipient's Catalog No.

4. Title and Subtitle	5. Report Date
Development of Oxidation Resistance in Thoriated Nickel-Chromium Base Alloys	December 31, 1971
	6. Performing Organization Code

7. Author(s)	8. Performing Organization Report No.
M. S. Seltzer, B. A. Wilcox, and R. I. Jaffee, BATTELLE, Columbus Laboratories, and J. Stringer, University of Liverpool, England	
	10. Work Unit No.

9. Performing Organization Name and Address	11. Contract or Grant No.
BATTELLE Columbus Laboratories 505 King Avenue Columbus, Ohio 43201	NAS3-14326
	13. Type of Report and Period Covered
12. Sponsoring Agency Name and Address	Contractor Report
National Aeronautics and Space Administration Washington, D. C. 20546	14. Sponsoring Agency Code

15. Supplementary Notes

Project Manager, Dr. Gilbert Santoro, Materials and Structures Division, NASA Lewis Research Center, Cleveland, Ohio

16. Abstract

A pack process has been developed which permits the introduction of nearly 6 weight percent aluminum into solid solution in the near-surface region of TDNiCr (Ni-20Cr-2ThO_2). At this aluminum concentration an adherent alumina scale is produced on the alloy surface upon exposure to an environment of 1.33×10^3 N/m^2 (10 torr) or 1.01×10^5 N/m^2 (760 torr) air at temperatures of 1093°C (2000°F) and 1204°C (2200°F). Room temperature mechanical properties of the aluminized alloys compare favorably with those of as-received TDNiCr.

While diffusivities for aluminum are a factor of three higher than those for chromium in TDNiCr or Ni-20Cr, the diffusion rates are similar for either of these elements in the thoriated or unthoriated alloy for a given temperature and grain size.

17. Key Words (Suggested by Author(s))	18. Distribution Statement
Aluminized TDNiCr Oxidation Diffusion	Unclassified – Unlimited

19. Security Classif. (of this report)	20. Security Classif. (of this page)	21. No. of Pages	22. Price*
Unclassified	Unclassified	72	$3.00

* For sale by the National Technical Information Service, Springfield, Virginia 22151

FOREWORD

This report was prepared by the personnel of Battelle-Columbus, Columbus, Ohio, and describes original work performed under Contract NAS3-14326.

The contract was awarded to Battelle-Columbus by the NASA-Lewis Research Center. Technical monitoring was provided by the Project Manager, Dr. G. Santoro, of the Materials and Structures Division of the NASA-Lewis Research Center.

M. S. Seltzer of Battelle-Columbus served as Principal Investigator.

The authors wish to acknowledge helpful discussions with Professor R. A. Rapp of The Ohio State University throughout the course of this program. Thanks are also due to Battelle's Columbus Laboratories for sharing a portion of the cost of this study.

The contract work was performed over the period from December 3, 1970, to November 30, 1971.

TABLE OF CONTENTS

	Page
SUMMARY	1
INTRODUCTION	2
OXIDATION STUDIES	3
Previous Work	3
Characterization of TDNiCr and Ni-20Cr	7
Aluminizing of TDNiCr and Ni-20Cr	7
Experimental Procedure	20
Results and Discussion	20
Kinetics	20
X-Ray Diffraction	41
Electron Probe Microanalysis	42
Metallography	47
MECHANICAL PROPERTIES	59
Bend Tests	59
Tensile Tests	60
DIFFUSION OF ALUMINUM AND CHROMIUM IN TDNiCr AND Ni-20Cr	60
Introduction	60
Experimental Procedures	61
Results and Discussion	63
CONCLUSIONS	69
REFERENCES	70
APPENDIX A. NEW TECHNOLOGY	A-1
APPENDIX B. DISTRIBUTION LIST FOR SUMMARY REPORT	B-1

LIST OF FIGURES

Figure 1.	Microstructure of As-Received TDNiCr Sheet	8
Figure 2.	Microstructure of As-Received Ni-20Cr Sheet	9
Figure 3.	Transmission Electron Micrographs of As-Received TDNiCr and Ni-20Cr	10
Figure 4.	ThO_2 Particle Size Distribution in TDNiCr Sheet	12
Figure 5.	Porosity Beneath Surface of Aluminized TDNi-Cr After Aluminizing Treatment 1	14

LIST OF FIGURES
(Continued)

Page

Figure 6. Pore-Free Specimens of TDNi-Cr After Aluminizing Treatment 2 . . 14

Figure 7. Electron Microprobe Data for Aluminum and Chromium in TDNiCr After Aluminizing by Treatment 2 at 1210°C (2210°F) for 16 Hours 15

Figure 8. Electron Microprobe Data for Aluminum and Chromium in Ni-20Cr After Aluminizing by Treatment 2 at 1210°C (2210°F) for 16 Hours 16

Figure 9. Microstructure of TDNiCr-5.8Al 17

Figure 10. Electron Microprobe Data for Aluminum, Chromium, and Nickel in TDNiCr After Aluminizing Run 4 – 1260°C (2300°F) for 3.34 Hours . 18

Figure 11. Weight Change for TDNiCr and TDNiCr-Al Isothermally Oxidized at 1093°C (2000°F) and 1.33×10^3 N/m^2 (10 Torr) Air. 28

Figure 12. Weight Change for TDNiCr and TDNiCr-Al Oxidized Isothermally at 1093°C (2000°F) and 1.01×10^5 N/m^2 (760 Torr) Air 29

Figure 13. Weight Change for TDNiCr and TDNiCrAl Oxidized at 1204°C (2200°F) and 1.33×10^3 N/m^2 (10 Torr) Air 30

Figure 14. Weight Change for TDNiCr and TDNiCr-5.8Al Oxidized at 1204°C (2200°F) and 1.01×10^5 N/m^2 (760 Torr) Air 31

Figure 15. Weight Change for Cyclic Oxidation of TDNiCr and TDNiCr-5.8Al at 1093°C (2000°F) and 1.33×10^3 N/m^2 (10 Torr) Air. 32

Figure 16. Weight Change for Cyclic Oxidation of TDNiCr and TDNiCr-Al at 1093°C (2000°F) and 1.01×10^5 N/m^2 (760 Torr) Air 33

Figure 17. Weight Change for Cyclic Oxidation of TDNiCr and TDNiCr-Al at 1204°C (2200°F) and 1.33×10^3 N/m^2 (10 Torr) Air. 34

Figure 18. Weight Change for Cyclic Oxidation of TDNiCr and TDNiCr-Al at 1204°C (2200°F) and 1.01×10^5 N/m^2 (760 Torr) Air 35

Figure 19. Microstructure of TDNiCrAlY 36

Figure 20. Weight Gain for TDNiCr-2Al Tested at 1204°C (2200°F) and 1.01×10^5 N/m^2 (760 Torr) Air 38

Figure 21. Weight Change for TDNiCr-5.8Al and Ni-Cr-5.8Al Tested at 1204°C (2200°F) and 1.01×10^5 N/m^2 (760 Torr) Air 39

Figure 22. Weight Change for Ni-Cr-5.8Al Isothermally Tested at 1204°C (2200°F) and 1093°C (2000°F) 40

LIST OF FIGURES
(Continued)

		Page
Figure 23.	Concentration Profiles for Aluminum in TDNiCr-5.8Al Before and After Cyclic Oxidation at 1204°C (2200°F) for 50 Hours	43
Figure 24.	Concentration Profiles for Aluminum in TDNiCr-4.95Al Before and After Cyclic Oxidation at 1204°C (2200°F) for 50 Hours	44
Figure 25.	Concentration Profiles for Aluminum in Ni-20Cr-5.8Al Before and After Oxidation at 1204°C (2200°F) for 50 Hours	45
Figure 26.	Concentration Profiles for Aluminum in TDNiCrAlY Before and After Isothermal Oxidation at 1204°C (2200°F) for 50 Hours	46
Figure 27.	Cross Section of the Metal/Oxide Interface From a Specimen of Ni-20Cr Cyclically Oxidized at 1204°C (2200°F) for 50 Hours in Air at 1.01×10^5 N/m^2 (760 Torr) Pressure	48
Figure 28a.	Surface of a TDNiCr Specimen Cyclically Oxidized at 1204°C for 50 Hours in Air at 1.01×10^5 N/m^2 (760 Torr) Pressure	49
Figure 28b.	Detail of the Scale Surface Shown in Figure 28a	49
Figure 28c.	Cross Section of the Same Specimen	50
Figure 29.	Cross Section of a Specimen of TDNiCr Cyclically Oxidized at 1204°C in Air at 1.33×10^3 N/m^2 (10 Torr) Pressure for 50 Hours	50
Figure 30a.	Surface of a Specimen of TDNiCr-4.95Al Cyclically Oxidized at 1204°C in Air at 1.01×10^5 N/m^2 (760 Torr) Pressure for 50 Hours	51
Figure 30b.	Cross Section of the Specimen Shown in Figure 30a	51
Figure 30c.	Detail of the Interface From Figure 30b Showing the Fine-Grained Layer	52
Figure 30d.	Another Section From the Same Specimen, Unetched, Showing a Local Oxide Growth	52
Figure 30e.	Another Section From the Same Specimen, Unetched, Showing Internal Oxidation, Apparently Beneath High Spots on the Metal Surface	52
Figure 31a.	Cross Section of a Specimen of TDNiCr-4.95Al Cyclically Oxidized at 1204°C in Air at 1.33×10^3 N/m^2 (10 Torr) Pressure for 50 Hours	54

LIST OF FIGURES
(Continued)

Page

Figure 31b. Another Section of the Same Specimen, Showing a Region Where Scale Failure has Occurred During the Test and a New Protective Layer Has Developed 54

Figure 31c. Another Section from the Same Specimen, Showing Internal Oxidation Beneath a Breakdown of the Protective Scale 54

Figure 32a. Cross Section of a Specimen of TDNiCr-5.8Al Cyclically Oxidized at 1204°C in Air at 1.3×10^3 N/m^2 (10 Torr) Pressure for 50 Hours, Showing Breakdown of the Oxide Over High Spots, and Associated Internal Oxidation 55

Figure 32b. Detail of the Metal/Oxide Interface From the Specimen Shown in Figure 32a 55

Figure 33. Cross Section of a Specimen of TDNiCr-4.3Al Oxidized Isothermally at 1093°C (2000°F) in Air at 1.01×10^5 N/m^2 (760 Torr) Pressure for 50 Hours 56

Figure 34. Cross Section of a Specimen of TDNiCr-4.95Al Oxidized Isothermally at 1093°C in Air at 1.01×10^5 N/m^2 (760 Torr) Pressure for 50 Hours 56

Figure 35. Cross Section of a Specimen of TDNiCr-5.8Al Oxidized Isothermally at 1093°C (2000°F) in Air at 1.01×10^5 N/m^2 (760 Torr) Pressure for 50 Hours 57

Figure 36. Cross Section of TDNi-Cr Before and After Isothermal Oxidation, 600X 58

Figure 37. Penetration Profiles for the Diffusion of ^{51}Cr in TDNiCr and Ni-20Cr at 1204°C (2200°F) 62

Figure 38. Aluminum Diffusion in TDNi-Cr and Ni-20Cr at 1210°C (2210°F) . 64

Figure 39. Microstructure of Fine-Grained TDNiCr 65

Figure 40. Diffusion Coefficients Versus Reciprocal of Absolute Temperature for Chromium Diffusion in Ni-20Cr Alloys With and Without Dispersoid 67

LIST OF TABLES

		Page
Table 1.	Chemical Analyses and Particle Parameters of As-Received Experimental Alloys	11
Table 2.	Surface Chemical Composition for Aluminized TDNiCr	19
Table 3.	Summary of Oxidation Tests for 50 Hours at Temperature	21
Table 4.	Room Temperature Mechanical Properties of TDNiCr and Aluminized TDNiCr (5.8Al at Surface)	60
Table 5.	Diffusion Coefficients for ^{51}Cr In TDNiCr, TDNiCr-5.8Al, Ni-20Cr-5.8Al, and Ni-20Cr for 50 Hours in 1 Atm Argon	66

DEVELOPMENT OF OXIDATION RESISTANCE IN THORIATED NICKEL-CHROMIUM-BASE ALLOYS

by

M. S. Seltzer, J. Stringer, B. A. Wilcox, and R. I. Jaffee

ABSTRACT

A pack process has been developed which permits the introduction of nearly 6 weight percent aluminum into solid solution in the near-surface region of TDNiCr ($Ni-20Cr-2ThO_2$). At this aluminum concentration an adherent alumina scale is produced on the alloy surface upon exposure to an environment of $1.33 \times 10^3 N/m^2$ (10 torr) or $1.01 \times 10^5 N/m^2$ (760 torr) air at temperatures of 1093°C (2000°F) and 1204°C (2200°F). Room-temperature mechanical properties of the aluminized alloys compare favorably with those of as-received TDNiCr.

While diffusivities for aluminum are a factor of three higher than those for chromium in TDNiCr or Ni-20Cr, the diffusion rates are similar for either of these elements in the thoriated or ThO_2-free alloy for a given temperature and grain size.

SUMMARY

The major objective of this research program was to develop a pack process to be used to introduce sufficient aluminum into solid solution in the near-surface region of TDNiCr ($Ni-20Cr-2ThO_2$) so that a protective Al_2O_3 scale would form upon oxidation, without serious degradation of the mechanical properties of TDNiCr. A second objective was to determine the effect of dispersed ThO_2 on the diffusion of aluminum and chromium in nickel-chromium-base alloys.

Various aluminum concentration gradients were produced in alloys containing 4.3, 4.95, and 5.8 weight percent aluminum at the surface. This was accomplished by annealing in an argon atmosphere for 3 to 16 hours in the temperature range of 1210-1260°C (2210-2300°F) in a pack consisting of 1% NaCl, 1% Urea, 85.11% Al_2O_3 (-100, +200 mesh) and 12.89% of a Ni-Cr-Al alloy powder (about 2% total aluminum in the pack). The aluminized samples had no intermetallic coating, and there was no evidence of internal porosity.

Both isothermal and cyclic oxidation tests were conducted at 1093°C (2000°F) and 1204°C (2200°F) at 1.33×10^3 N/m^2 (10 torr) and 1.01×10^5 N/m^2 (760 torr) air. Auxiliary evaluation techniques included metallography, X-ray diffraction and electron microprobe analysis. Selected room-temperature tensile tests and bend tests were performed on as-received, aluminized, and oxidized samples. Electron microprobe analysis was used to determine aluminum-diffusion data and aluminum- and chromium-concentration profiles after oxidation. A radioactive tracer technique, using ^{51}Cr, was employed to determine chromium diffusivities.

Under all oxidation conditions Cr_2O_3 was the major oxide formed on as-recieved TDNiCr. The measured weight change with time was a combination of a parabolic or higher-order growth step, a linear volatilization step, and, for cyclic tests, a small contribution due to spallation. A net wieght loss usually resulted after 50 hours at 1204°C (2200°F).

In contrast, Al_2O_3 was the primary scale constituent formed on TDNiCr containing 4.95 or 5.8 weight percent aluminum. Volatilization and spallation were minimized in these alloys and weight gains were always observed after 50 hours at temperature in isothermal or cyclic tests. Room-temperature mechanical properties of the aluminized alloys compared favorably with those of as-received TDNiCr.

While diffusivities for aluminum were a factor of three higher than those for chromium in TDNiCr or Ni-20Cr, the diffusion rates were similar for either of these elements in the thoriated or unthoriated alloy for a given temperature and grain size.

INTRODUCTION

Among the candidate materials for use in the outer skin or thermal protection system (TPS) of the reusable space-shuttle vehicles are various thoriated nickel-chromium-base alloys. In particular, the Ni-20Cr-2ThO_2 alloy produced by Fansteel Metallurgical Corporation under the name of TDNiCr has received considerable attention for use in the temperature range of 982-1204°C (1800-2200°F). Initial experiments in static air suggested that this alloy would exhibit excellent oxidation resistance and relatively high strength at the temperatures of interest. Later isothermal tests[1]* cyclic tests[31], and tests in arc-jet facilities[2], involving high flow rates, revealed serious weight loss and depletion of chromium from this alloy as the result of rapid volatilization of the protective Cr_2O_3 oxide scale as CrO_3. It therefore became apparent that in order to utilize thoriated nickel-chromium-base alloys for multiple reentries under conditions were skin temperatures approach 1204°C (2200°F) it would be necessary to improve the oxidation resistance of TDNiCr.

One approach that is being taken to solve this problem is adding sufficient aluminum directly to TDNiCr during production of the alloy to produce a protective Al_2O_3 scale upon oxidation.[3] This type of alloy is under development and is not as far advanced asTDNiCr. A number of factors being considered are cost; the possibility that aluminum as a uniform addition [particularly if γ' (Ni_3Al) forms] may have detrimental effects on the mechanical properties, particularly the fabricability of the alloy; and development of thermomechanical processing to produce microstructures that are optimum for high-temperature strength, e.g., a highly elongated grain structure (high grain-aspect ratio).

As an alternative approach to direct alloying, one of the objectives of this research program was to enrich only the near-surface region of TDNiCr with aluminum so that a protective Al_2O_3 scale would form upon oxidation, and such that the mechanical strength of the nonaluminized alloy was maintained over much of the alloy thickness. TDNiCr and Ni-20Cr were aluminized by pack-cementation and diffusion annealing. To characterize the scale formed on the various alloys, both isothermal and cyclic oxidation tests were conducted at 1093 and 1204°C (2000 and 2200°F) at 1.33×10^3 N/m^2 (10 torr) air and 1.01×10^5 N/m^2 (760 torr) air. Auxiliary evaluation techniques included optical metallography, X-ray diffraction, and electron microprobe analysis.

* See Reference list at end of report.

Thoria additions are reported to modify the nature of scales produced on nickel-chromium-base alloys. In particular thoria appears to promote the selective oxidation of chromium in the Ni-20Cr base alloy.[4] Results of some recent diffusion experiments with alloys containing a dispersoid[5] led to the suggestion that the thoria serves to enhance chromium diffusion in TDNiCr, as compared with diffusion in Ni-20Cr. A second objective of this investigation was therefore to determine the effect of dispersed ThO_2 on the diffusion of aluminum and chromium in nickel-chromium-base alloys. Electron microprobe analysis was used to determine aluminum-diffusion data and chromium- and aluminum-concentration profiles after oxidation. A radioactive tracer technique, using ^{51}Cr, was employed to determine chromium diffusivities.

OXIDATION STUDIES

Previous Work

Early work on the oxidation of dispersion strengthened nickel alloys was discussed in detail by Stringer, Wright, Wilcox, and Jaffee[6], and this review, not available in the open literature, is presented here, along with a discussion of more recent studies[2, 7, 29, 30] on the oxidation of TDNiCr in high-gas-flow environments.

Wallwork and Hed[4] have examined the oxidation of TDNiCr between 900 and 1200°C (1652 and 2192°F), using a metallographically polished surface, in dry, slowly flowing oxygen at 1.33×10^4 and 1.01×10^5 N/m^2 (100 and 760 torr) pressure. At 900°C (1652°F) the scale consisted of three distinct layers, varying in thickness, and not continuous. At 1100 and 1200°C (2012 and 2192°F) the oxidation front and the scale were much more uniform. At 1000 and 1200°C (1832°F and 2192°F) the scales were essentially Cr_2O_3, with minor amounts of $NiCr_2O_4$ spinel; unfortunately no X-ray data are quoted for the three-layer scale formed at 900°C (1652°F), but microprobe results show an outer layer of spinel, an intermediate layer of NiO, and an inner layer of Cr_2O_3. It is extremely difficult to interpret this distribution of phases.

The growth rates of the scales are compared with those for Ni-30Cr and Co-35Cr, which also give substantially Cr_2O_3 scales, and it is clear that the rate of growth is very substantially smaller on TDNiCr. For all alloys forming Cr_2O_3 scales, the overall weight change involves two terms: an increase due to the growth of the scale and a decrease due to the oxidation/volatilization of Cr_2O_3, according to the equation

$$Cr_2O_3(s) + \frac{3}{2}O_2(g) = 2CrO_3(g) \quad . \tag{1}$$

Lewis first demonstrated that for pure chromium, the overall rate curve could be interpreted in terms of a parabolic thickening of the scale and a linear volatilization of the oxide;[8] the analytic form of the rate law was first expressed by Tedmon[9]. These rate laws make clear that the scale will eventually thicken to a point at which the rate of thickening due to transport will equal the rate of thinning due to volatilization, and the thickness will then remain constant; the overall weight of the specimen will increase initially and then decrease, and the rate of weight loss will approach the volatilization rate.

For pure chromium and the simple binary alloys, the maximum in the weight-versus-time curves is at times well in excess of 100 hours at 1100 and 1200°C (2192°F), but, for TDNiCr, Wallwork and Hed report weight losses after a few hours. This implies either a decrease in the rate of growth of Cr_2O_3 or an increase in the volatilization rates.

Platinum markers were found at the scale/oxygen interface for a TDNiCr specimen oxidized for 75 hours at 1100°C (2012°F) in 1.33×10^4 N/m^2 (100 torr) oxygen, in the oxidation of Ni-30Cr, the markers were found at the scale. metal interface: this clearly implies a change in the transport process in the scale. The back-scattered electron mode in a scanning electron microscope (BSE-SEM) shows the thoria particles as easily detected bright points; this shows that the scale consisted of two layers with thoria particles in the inner layer but not in the outer.

While Cr_2O_3 scales formed on Ni-Cr alloys are often separated from the metal and convoluted, those formed on TDNiCr were always extremely tenacious. Wallwork and Hed did not present a mechanistic interpretation of their results.

Lowell, et al examined the oxidation of TDNiCr at 800, 1000, and 1200°C (1472, 1832, and 2192°F) in static air.[10] Polished specimens first formed NiO, followed by Cr_2O_3; later reaction between these two produced $NiCr_2O_4$. Ground specimens formed only Cr_2O_3; both groups of specimens lost Cr_2O_3 by oxidation/volatilization, and metal-thickness measurements suggested that the overall oxidation of the polished specimens was less than that of the ground specimens.

At 800°C (1472°F), ground specimens gained weight linearly for the entire duration of the oxidation (100 hours) up to a total gain of 0.2 mg/cm^2; at 1000°C (1832°F), there was a small gain up to approximately 0.1 mg/cm^2 after 20 hours and little change for the remaining period; at 1200°C (2192°F), the specimen gained weight rapidly for 1 hour to a maximum of 0.2 mg/cm^2, and then lost weight, the weight loss rapidly becoming linear. For the polished samples, a rapid weight gain to approximately 0.6 mg/cm^2, was followed by very little change; the curves looked very similar for all three temperatures.

A careful and comprehensive study of the oxidation of TDNiCr in the temperature range 900-1200°C (1652-2192°F) in 1.01×10^5 N/m^2 (760 torr) static oxygen was conducted by Giggins and Pettit[11]. All specimens were polished through 600-grit SiC paper and cleaned. The surfaces of the oxidized specimens were covered with dark-green adherent scales with negligible relief: X-ray analysis showed that Cr_2O_3 and ThO_2 were always present; NiO was observed occasionally as porous mounds at the oxide/gas interface.

The rate curves showed little temperature dependence; a relatively rapid initial increase was followed by little change up to the 20-hour limit of most runs, and overall weight gains were in the range 0.15-0.36 mg/cm^2. At 1200°C (2192°F) the specimens were clearly losing weight after 10 hours or so; for one run at 1100°C (2012°F) the specimen started to lose weight after 3 hours, and the weight loss was linear after 10 hours. There was clearly a degree of irreproducibility in the form of the rate curves. A few runs performed with electropolished samples always showed the presence of NiO (in agreement with Lowell, et al), but there was little difference in the form of the rate curves.

Giggins and Pettit, using Tedmon's analysis to computer fit their rate curves and the volatilization data of Hagel[12], calculated a parabolic rate constant, k_p. This varied with time initially, but approached an asymptotic value, which was between 10 and 15 times smaller than the parabolic rate constant for the oxidation of Ni-30 Cr. In agreement with Wallwork and Hed[4], platinum markers were found at the oxide/oxygen interface for TDNiCr specimens, in contrast to Ni-30Cr; but the activation energies for the parabolic rate constants being approximately the same, it was considered unlikely

that there had been a radical change in reaction mechanism, or in particular that bulk diffusion of oxygen was involved.

Examination of surface replicas from a specimen oxidized for 1 hour did not show any ThO_2 particles, but after 20 hours many portions of the surface showed ThO_2 particles, and after 80 hours thoria particles were found on virtually all areas of the oxide surface, and some agglomeration of particles was apparent. From this, Giggins and Pettit concluded that there is both inward and outward growth of scale; the outer layer involving chromium transport and containing no thoria; but this layer is eventually removed by the oxide-volatilization process. During the growth of the outer layer, it is suggested that the thoria particles from the consumed metal accumulate at the metal/oxide interface and restrict the outward movement of chromium until, eventually, a dissociation reaction is initiated at the oxide/metal interface; the oxygen then diffuses through or around the ThO_2 particles and new Cr_2O_3 is formed incorporating the thoria.

Lowell used the scanning electron microscope to study the surface morphology of TDNiCr oxidized at 800, 1000, and 1200°C (1472, 1832, and 1292°F) for times up to 64 hours in air.[13] Surfaces abraded with 120 grit and oxidized in air at atmospheric pressure grew an oxide layer that developed large crystals of Cr_2O_3: after 64 hours the crystals were 5-μm diameter. Surfaces polished through 0.5-μm diamond paste oxidized differently over scratches and grain boundaries than over the rest of the specimen: the bulk of the surface was covered with faceted NiO, but the grain boundaries and scratches had Cr_2O_3 growing much more slowly than the NiO. Lowell considers that the large crystals of Cr_2O_3 result from vapor-phase growth – the Cr_2O_3 volatilizing and recondensing.

Davis, Graham, and Kvernes have studied oxidation of three experimental alloys: Ni-31.5Cr-1ThO_2, Ni-22.6Cr-1ThO_2, and Ni-33.7Cr-1ThO_2.[14] All specimens were abraded through 600 grit; some were further polished through No. 2 Al_2O_3. Most oxidations were conducted for 20-50 hours, but the total range of times studied was from 5 minutes to 150 hours. The oxidation was carried out in pure dry oxygen at a pressure of 2×10^4 N/m^2 (150 torr) and a flow rate of 12 cm^3/sec at temperatures of 1000 and 1200°C (1832 and 2192°F). The 33.7Cr alloy formed only a thin Cr_2O_3 layer at both temperatures for both surface conditions. The 22.6Cr alloy formed a thin Cr_2O_3 layer under all circumstances, but, in addition, the polished specimens showed a discontinuous spinel layer at both temperatures. The 13.5Cr alloy showed NiO, Cr_2O_3, and spinel; a thin Cr_2O_3 layer was the major feature for the abraded specimens.

That they too invoke a dissociation mechanism for the growth of NiO on the most dilute alloy suggests that the ThO_2 particles screen the chemical-bonding forces that are responsible for maintaining intimate contact between the metal and the scale.

For the two more-concentrated alloys, the general form of the rate curves is similar to that reported by Giggins and Pettit; very thin scales are formed, and at the higher temperature the specimens speedily start to lose weight overall because of the oxide volatilization that is more rapid due to the higher-gas-flow rate. The volatilization rates were determined and compared with data obtained by Graham and Davis for Cr_2O_3;[15] excellent agreement of the values indicates that the vaporization rate is unaffected by the presence of ThO_2.

In discussing the mechanism of reaction, Davis, et al, note that continuous Cr_2O_3 scales are formed on Ni-20Cr alloys only in the vicinity of alloy grain boundaries, but in this case they are formed over the whole specimen; they suggest therefore that

the ThO_2 is enhancing the diffusion of chromium.[14] Fleetwood has reported enhanced diffusion of chromium in a Ni-5ThO_2 alloy[5] (but, as discussed below, it has been shown in the present study that the diffusion rate of chromium in TDNiCr is identical to that in Ni-20Cr).

Davis, et al, applied Tedmon's analysis to their rate curves, but no satisfactory fit was obtained; as with Giggins and Pettit's results, k_p varied with time in the early stages, but Davis, et al, do not consider that this can be attributed to NiO growth in the early stages, as suggested by Giggins and Pettit. They point out that the initial value of k_p for the 33.7Cr alloy in the first 30 minutes of oxidation at 1000°C (1832°F) is essentially the same as that reported for Ni-30Cr, and comment that this is consistent with Giggins and Pettit's model for the initial growth before ThO_2 has accumulated at the interface.

Lowell and Sanders[29] have studied the oxidation of TDNiCr in a burner-rig apparatus operated at a combustion velocity of Mach 1 in both cyclic and an isothermal mode. Experiments were performed in a 1-atmosphere gas stream at 1204°C (2200°F) for times up to 50 hours. Neither surface preparation nor thermal cycling had an appreciable effect on the oxidation behavior. It was found that Cr_2O_3 was the initial primary constituent of the scale produced on TDNiCr. Rapid volatilization of this oxide led to a metal loss rate of 40 μm per hour. After about 1 hour the Cr_2O_3 broke down and NiO formed a continuous layer on the surface. This resulted in a metal loss rate of 2.5 μm per hour; limited by the diffusion of Cr through NiO.

Centolanzi and co-workers[2,30] have conducted a series of arc-jet tests on a series of dispersion-strengthened alloys including TDNiCr and TDNiCrAlY (a proprietary alloy containing Ni-16Cr-2ThO_2 with aluminum and yttrium) at temperatures of 982°C (1800°F) and 1204°C (2200°F) and under nominal surface pressures of 2.0×10^3 N/m^2 (15 torr) and 4.0×10^3 N/m^2 (30 torr). Each test consisted of a various number of 1800-second cycles, ranging in number from 28 to 50. The two types of flow employed were a stagnation flow where the air impinges on the sample at right angles to the planar surface, and a shear-type flow where the sample is embedded in the surface of a wedge having a locally supersonic boundary layer.

TDNiCr was found to lose weight steadily with time in the arc-jet tests; the loss was 14.8 mg/cm^2 after 50 cycles at 1204°C (2200°F) and 2.0×10^3 N/m^2 (15 torr) in the stagnation mode. In contrast, TDNiCrAlY lost only 1 mg/cm^2 under the same conditions after 40 test cycles. The scales formed on TDNiCr were primarily NiO, Cr_2O_3, and $NiCr_2O_4$, while Al_2O_3 is the main constituent of the scale formed on TDNiCrAlY. After long exposure to hypervelocity, air, TDNiCr was found to be severly depleted in chromium. This depletion was accompanied by internal porosity which was concentrated near the exposure surface. No depletion of chromium or internal porosity was observed for the TDNiCrAlY.

The only negative aspect of the TDNiCrAlY was that in-situ measurements of emissivity (0.70 ± 0.05) for the aluminum-containing alloy were considerably lower than the value of 0.85 ± 0.05 measured at 1204°C (2200°F) for TDNiCr.

The oxidation of TDNiCr in static, flowing, and dissociated oxygen has been studied by Gilbreath[7] at 1100°C (2012°F) and 130 N/m^2 (1 torr). In atomic oxygen, TDNiCr volatilizes faster and has a higher rate of oxide growth and a greater metal recession than occurs in molecular oxygen. The oxide scale formed in atomic oxygen was

essentially devoid of chromium and had a high-temperature emittance significantly lower than that from the oxides formed in molecular oxygen.

Characterization of TDNiCr and Ni-20Cr

Two square feet each of Ni-20Cr-2ThO_2(TDNiCr) and Ni-20Cr sheet were provided by NASA-Lewis Research Center. Both materials were made by Fansteel Metallurgical Corporation, and essentially the same processing methods were used for both alloys. While the nominal thickness of the TDNiCr sheet was 0.0292 cm (0.0115 in.), thickness varied from 0.024 to 0.033 cm (0.010 to 0.013 in.). The Ni-20Cr sheet varied in thickness from 0.0305 to 0.0457 cm (0.012 to 0.018 in.). Oxidation coupons of this alloy were taken from an area that had a thickness of 0.0394 cm (0.0155 in.).

The optical micrographs in Figures 1 and 2 show the microstructure of the as-received TDNiCr and Ni-20Cr, respectively, and transmission electron micrographs of each alloy are shown in Figure 3. The TDNiCr has a coarse, elongated, recrystallized grain structure with only four or five grains across the sheet thickness. The large, dark-etching particles in Figure 1 are probably Cr_2O_3. The transmission micrograph in Figure 3b shows that there is very little dislocation substructure, but there is a high density of fine annealing twins. In the longitudinal sheet thickness (View B in Figure 1) the average grain length of the TDNiCr is 0.056 cm (0.022 in.) and the average grain width is 0.00635 cm (0.0025 in.). This gives a grain-aspect ratio of 8.8.

The Ni-20Cr alloy has a fine, recrystallized grain structure (Figure 2) that is nearly equiaxed with a grain size of 0.00076 cm (0.0003 in.). This material appears to have much more Cr_2O_3 (dark-etching stringers in Figure 2) than the TDNiCr. The Ni-20Cr also has very little dislocation substructure and an abundance of fine annealing twins. Figure 3a shows a noncoherent twin boundary being blocked by a Cr_2O_3 particle.

The chemical analyses of both alloys are given in Table 1, together with the ThO_2 particle size and spacing in the TDNiCr. The particle size and spacing were determined using techniques described previously.[16, 17] A Zeiss Particle Size Analyzer was used to measure 2000 particle diameters from transmission electron micrographs, and the distribution is plotted in two ways in Figure 4. From the data in Figure 4b, the mean planar center-to-center particle spacing, d, was calculated from the following expression:[16, 17]

$$d^2 = \frac{2\pi}{3 \sum_i (f_i / r_{v_i}^2)} \quad . \tag{2}$$

Here, f_i is the volume fraction of particles in a limited size range having an average particle radius, r_{v_i}. Table 1 shows that the average ThO_2 particle diameter is 0.0125 μm (125 A) and that the spacing, d, is 0.1870 μm (1870 A).

Aluminizing of TDNiCr and Ni-20CR

The initial aluminizing (designated treatment No. 1) was conducted in a pack mix containing 1% Al powder, 1% NaCl, and 98% Al_2O_3 (-100, +200 mesh) contained in a

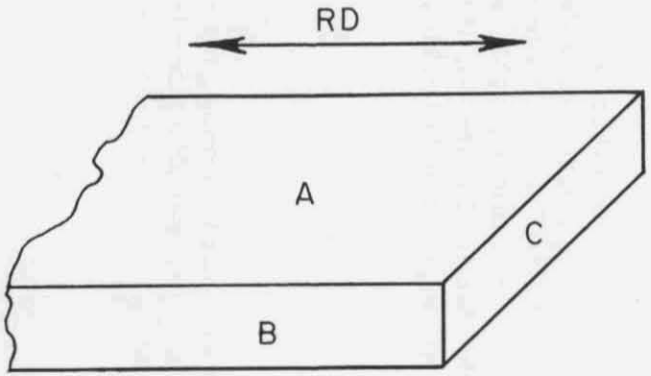

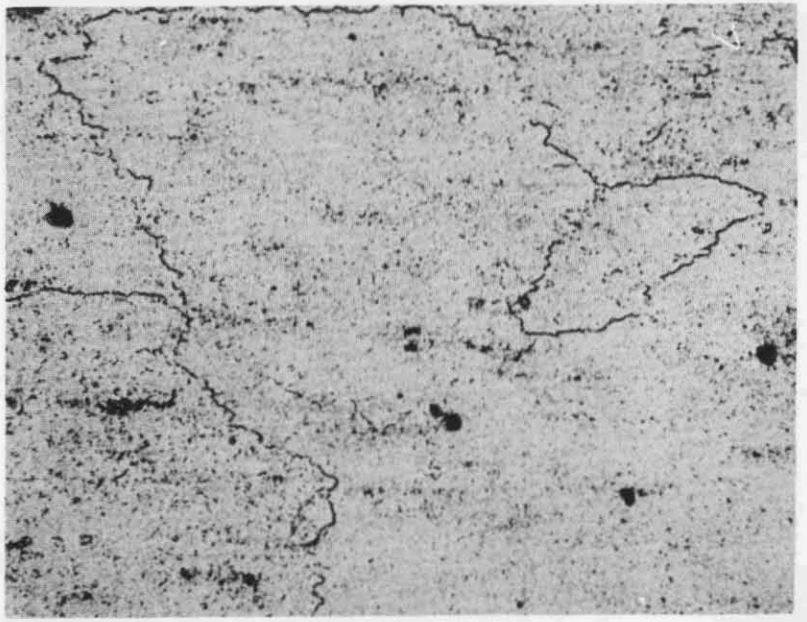

View A, 200X

View B, 200X

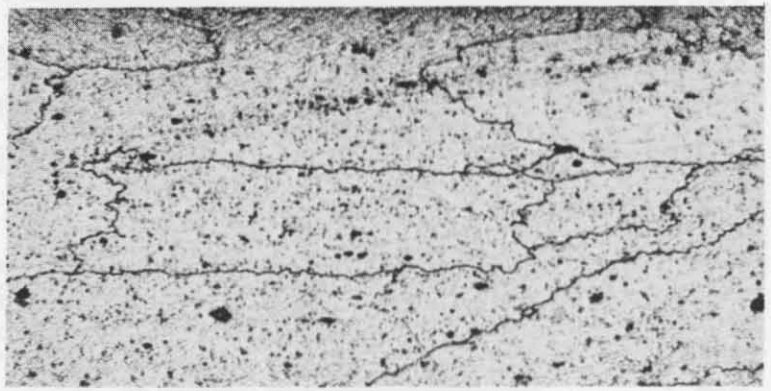

View C, 200X

FIGURE 1. MICROSTRUCTURE OF AS-RECEIVED TDNi-Cr SHEET

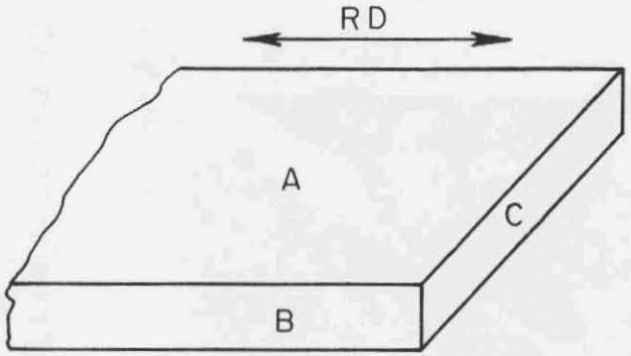

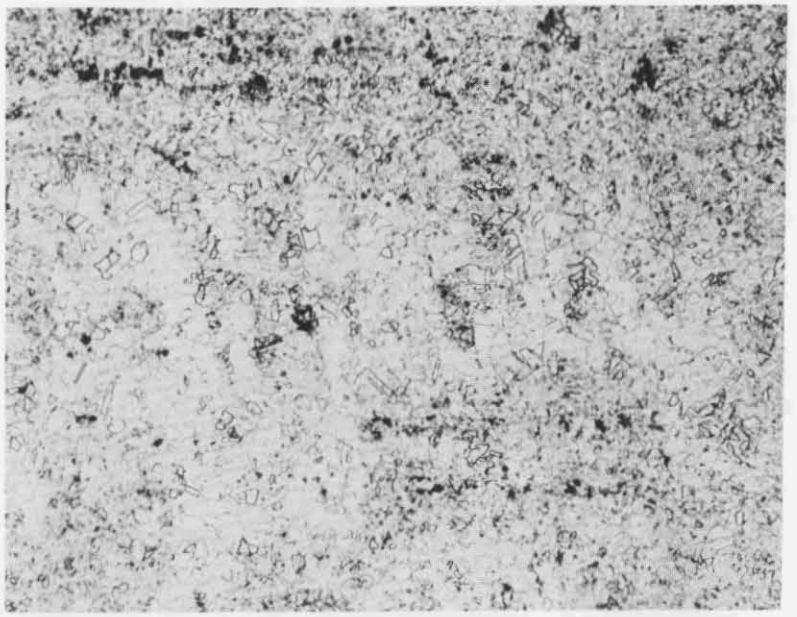

View A, 200X

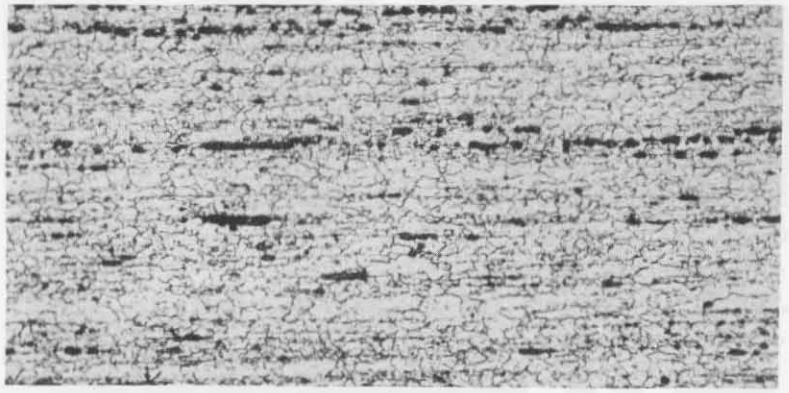

View B, 200X

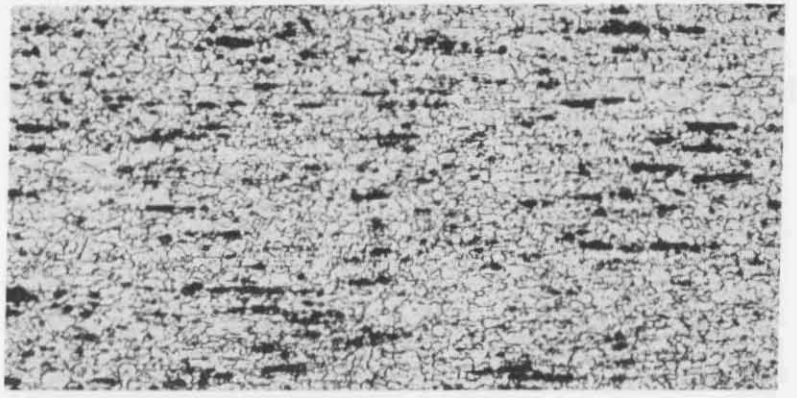

View C, 200X

FIGURE 2. MICROSTRUCTURE OF AS-RECEIVED Ni-20Cr SHEET

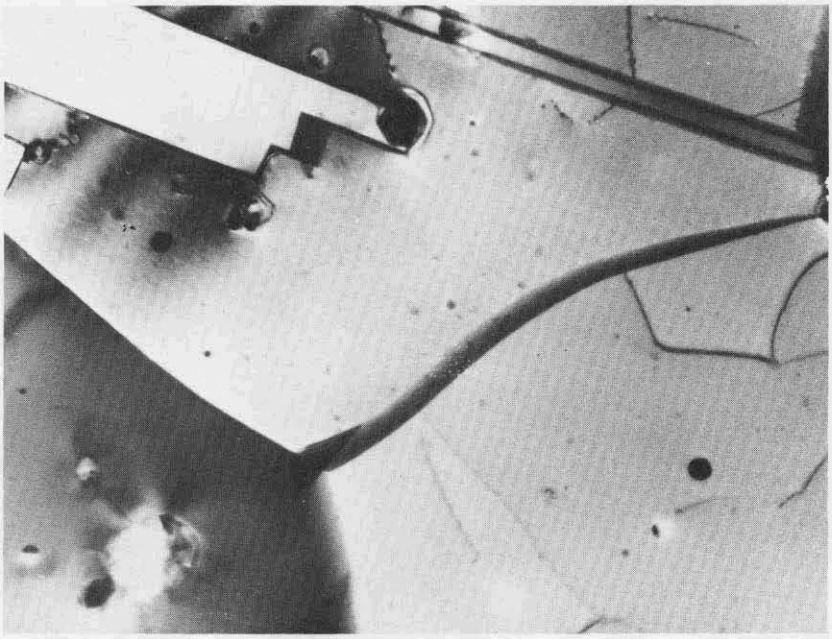

(a) Ni-20Cr 30,000X

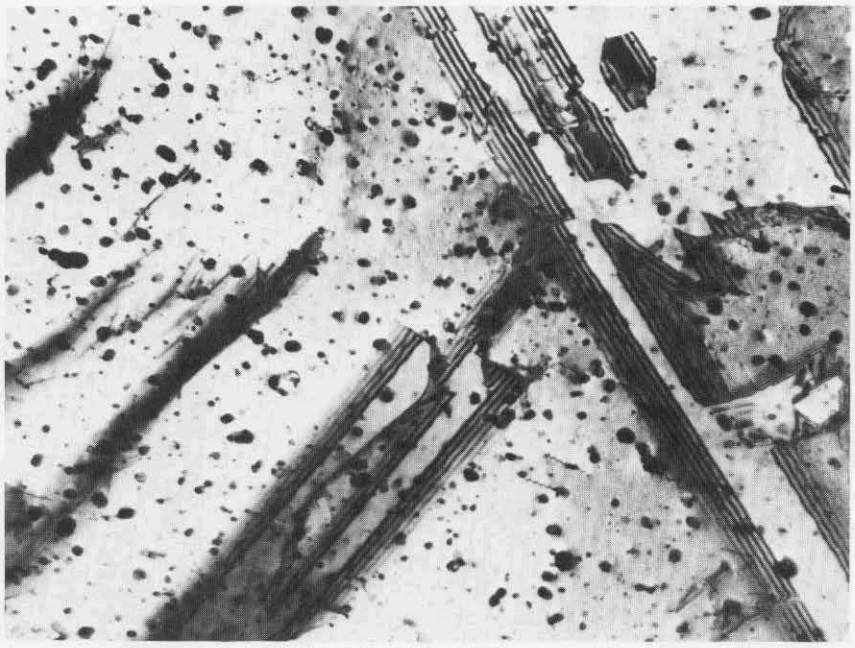

(b) Ni-20Cr-2ThO_2 30,000X

FIGURE 3. TRANSMISSION ELECTRON MICROGRAPHS OF AS-RECEIVED TDNi-Cr AND Ni-20Cr

TABLE 1. CHEMICAL ANALYSES AND PARTICLE PARAMETERS OF AS-RECEIVED EXPERIMENTAL ALLOYS

	Analyses		
Alloy	Wt.% Cr	Wt.% ThO_2	Vol.% ThO_2
Ni-20Cr	21.4	-	-
Ni-20Cr-2ThO_2	19.7	1.71	1.52

Particle Parameters in Ni-20Cr-2ThO_2

Parameters	Dimensions
Range of ThO_2 particle diameters	0.0093-0.1197 μm (93-1197 A)
Avg. ThO_2 particle diameter, $2r_v$	0.0125 μm (125 A)
Mean planar center-to-center particle spacing, d	0.1870 μm (1870 A)

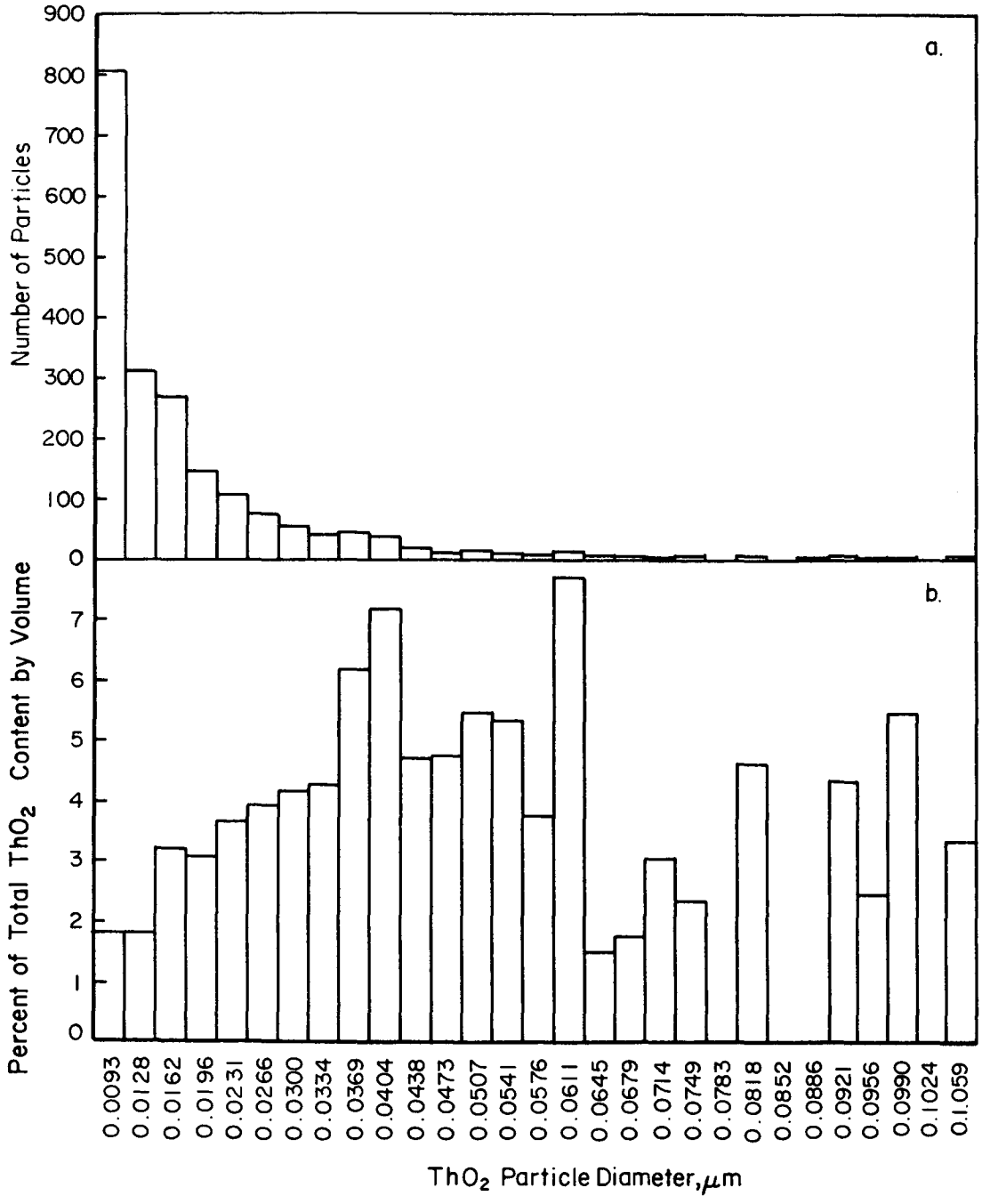

FIGURE 4. ThO_2 PARTICLE SIZE DISTRIBUTION IN TDNiCr SHEET

prefired graphite box, ID, 5.7 x 10.2 x 20.4 cm (2-1/4 x 4 x 8 in.). The specimens were first aluminized at 932°C (1710°F) for 12 hours in an argon atmosphere, then brought to room temperature, wet-brushed and weighed to determine the amount of aluminum pickup. This was followed by an homogenization treatment in which the specimens were annealed under argon in Ni-Cr baskets at temperatures up to 1204°C (2200°F) for periods of time to 16 hours.

Representative samples treated in this way were examined metallographically, by electron probe microanalysis, and by X-ray diffraction techniques. The samples were found to contain an outer skin that was rich in nickel (but of unknown structure), and Ni_3Al which could be peeled from the surface. Beneath this layer was an aluminum concentration profile whose shape depended on the aluminizing treatment. The concentrations of chromium and nickel were found to be uniform throughout the central portion of the specimen but decreased near the surface.

Optical microscopy revealed that a network of porosity had been developed about 0.00125 cm (0.0005 in.) from the surface of the samples after the diffusion process and again after homogenization (Figure 5). It is thought that these were Kirkendall-type voids formed by rapid out diffusion of chromium or nickel during the aluminizing process.

In an attempt to eliminate the undesirable internal porosity and intermetallic coatings found in the first groups of aluminized specimens, a series of TDNiCr and Ni-20Cr samples was aluminized in a pack containing an alloy of 74.7 Ni-15.5Al-9.7Cr (weight percent) (designated Treatment 2), instead of the pure aluminum used in the first packs. It was hoped that a one-step aluminizing process using an alloy of essentially Ni_3Al with sufficient chromium to maintain 20 weight percent chromium in the TDNiCr would eliminate both the porosity, and chromium and nickel surface depletion.

The following procedure was used for aluminizing Treatment 2, with the NiCrAl alloy as the source for aluminum. The specimens of TDNiCr and Ni-20Cr were acid cleaned (warm 50 percent HNO_3-laboratory reagent grade, 70 percent), rinsed, measured, and weighed. They were then placed in a graphite boat containing a pack which consisted of 600 grams Al_2O_3, 110 grams of the NiCrAl alloy, 6 grams of NaCl and 6 grams of urea. The boat was placed in an electrically heated tube furnace and brought up to 1210°C (2210°F) under a flowing argon atmosphere. The specimens were kept at temperature for 16 hours and then allowed to furnace cool to 300°C (572°F). The boat was then removed and the specimens were brushed, remeasured, and reweighed.

The specimens treated in this way were found to have a shiny surface, free of a visible oxide or intermetallic scale. Metallographic studies of several specimen cross sections revealed no internal porosity as was found after Treatment 1. Figure 6 is a typical cross section of TDNiCr aluminized by Treatment 2. Electron probe microanalyses (Figures 7 and 8) on these samples showed a typical diffusion-concentration profile for aluminum with a concentration of 4.3 weight percent aluminum at the surface dropping to zero at about 100 μm from the surface. At the same time, the chromium concentration decreased near the surface to approximately 17 percent. These profiles are discussed in more detail in the section on diffusion.

By repeating the above process on samples already aluminized, specimens were produced with 4.9 weight percent aluminum at the surface. These specimens had some aluminum over the entire cross section, however, and the chromium concentration at the surface had dropped to 16.2 weight percent.

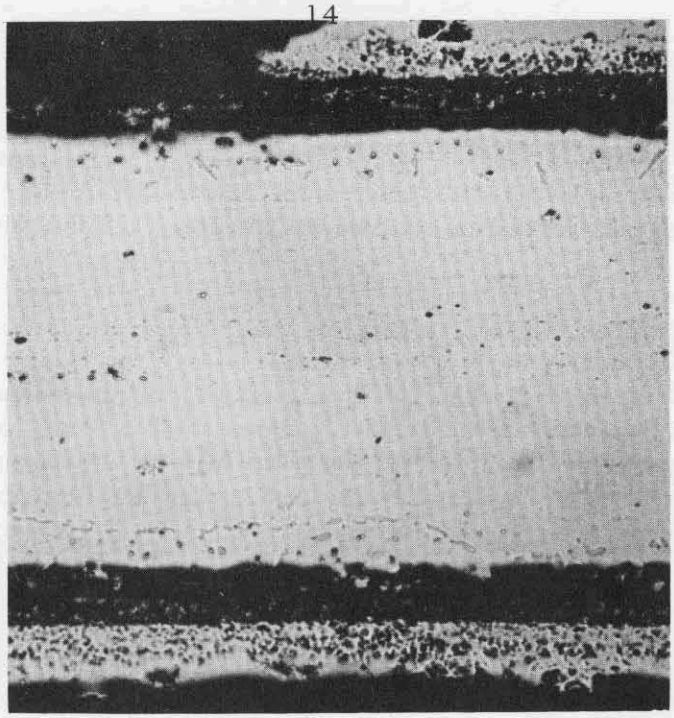

200X

FIGURE 5. POROSITY BENEATH SURFACE OF ALUMINIZED TDNi-Cr AFTER ALUMINIZING TREATMENT 1
Also shown is intermetallic skin which has peeled from surface.

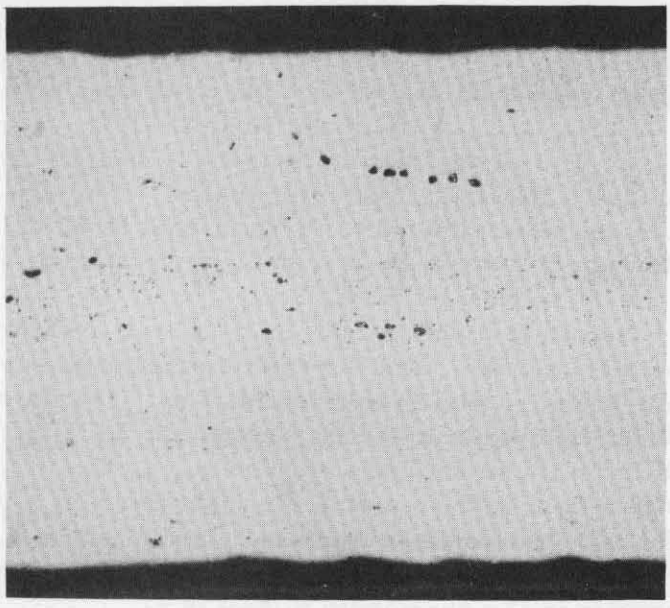

200X

FIGURE 6. PORE-FREE SPECIMENS OF TDNi-Cr AFTER ALUMINIZING TREATMENT 2

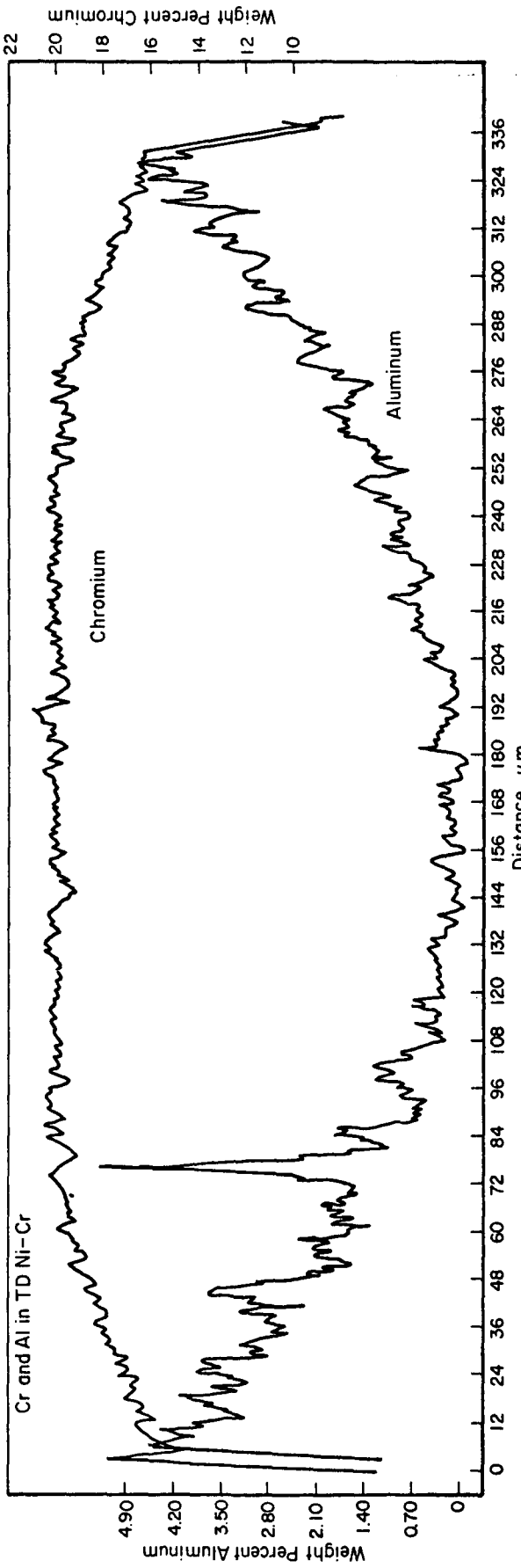

FIGURE 7. ELECTRON MICROPROBE DATA FOR ALUMINUM AND CHROMIUM IN TDNiCr AFTER ALUMINIZING BY TREATMENT 2 AT 1210°C (2210°F) FOR 16 HOURS

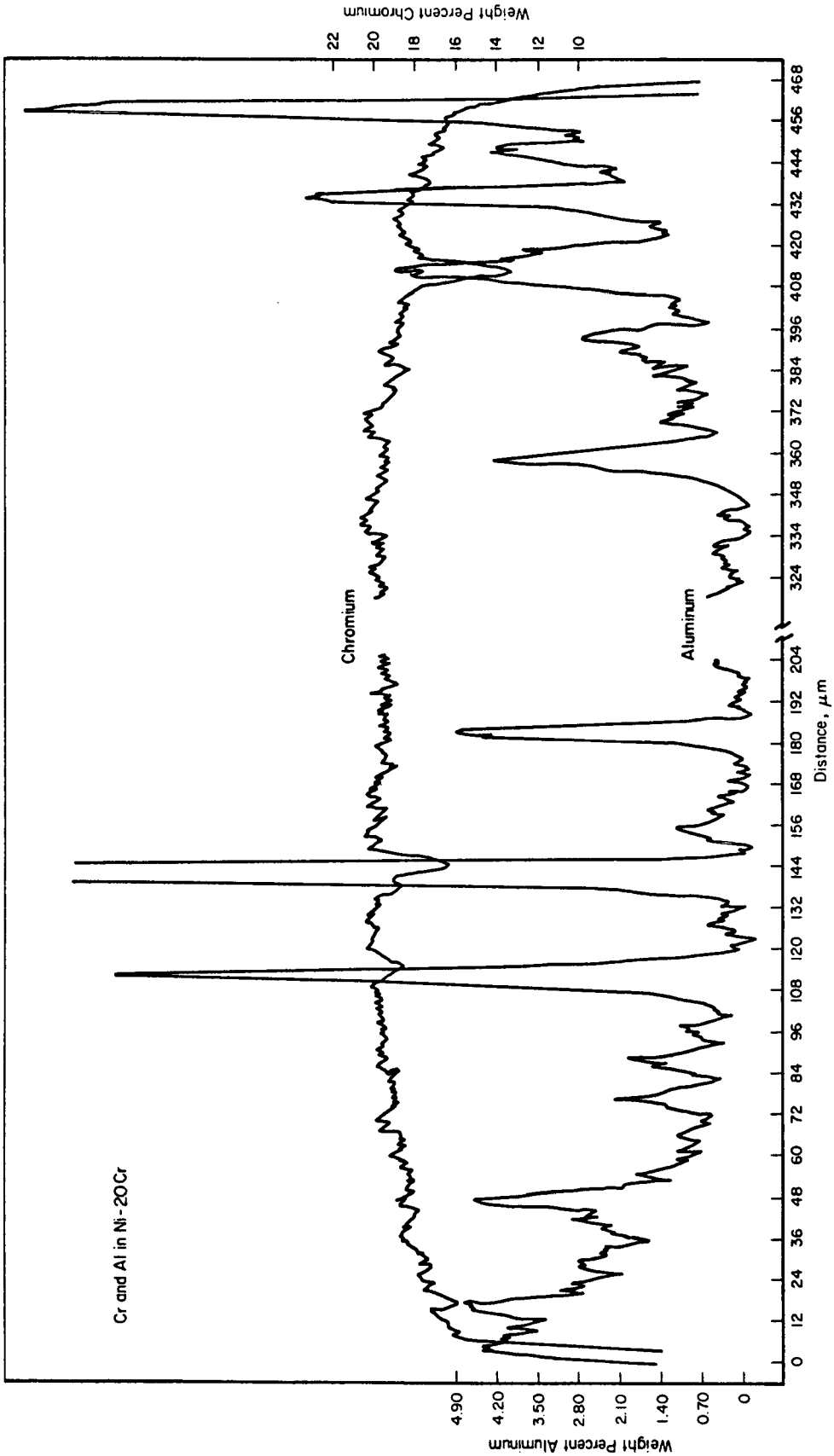

FIGURE 8. ELECTRON MICROPROBE DATA FOR ALUMINUM AND CHROMIUM IN Ni-20Cr AFTER ALUMINIZING BY TREATMENT 2 AT 1210°C (2210°F) FOR 16 HOURS

In an attempt to increase the concentrations of aluminum and chromium in the surface region while maintaining a sharp aluminum-concentration gradient, an alumizing treatment was conducted at 1260°C (2300°F) for 3.3 hours using powder of an alloy of 68Ni-15Cr-17Al (weight percent) in the pack. The alloy was prepared by arc melting a 400-gram ingot of the above composition in a water-cooled copper crucible, positive argon pressure arc melting furnace. The ingot was surface ground to remove scale, then crushed using a diamond mortar. The small pieces were then loaded in a steel-ball mill and ground for 25 hours to give -200 mesh powder.

Specimens of TDNiCr and Ni-20Cr were acid cleaned (warm 50 percent HNO_3-laboratory reagent grade, 70 percent) rinsed, measured, and weighed. Aluminizing was conducted in a pack mix containing 12.89% alloy powder (about 2% total aluminum in the pack), 1% NaCl, 1% urea, and 85.11% Al_2O_3 (-100, +200 mesh) contained in a prefired graphite cylinder boat. The aluminizing furnace was flushed with argon for 24 hours prior to heatup and a flow of 0.225 m^3/hr was maintained until the samples were removed from the furnace. The pack was charged cold, heated to 1260°C (2300°F) in 3 hours, held at temperature for 3 hours and furnace cooled to 66°C (150°F) at which time the pack was removed from the furnace and air cooled to room temperature. The specimens were then wet brushed to remove adhering Al_2O_3 particles, dried, and weighed. The samples had no intermetallic coating and there was no evidence of internal porosity. The optical micrograph in Figure 9 shows the microstructure of aluminized TDNiCr containing an aluminum surface concentration of 5.8 weight percent.

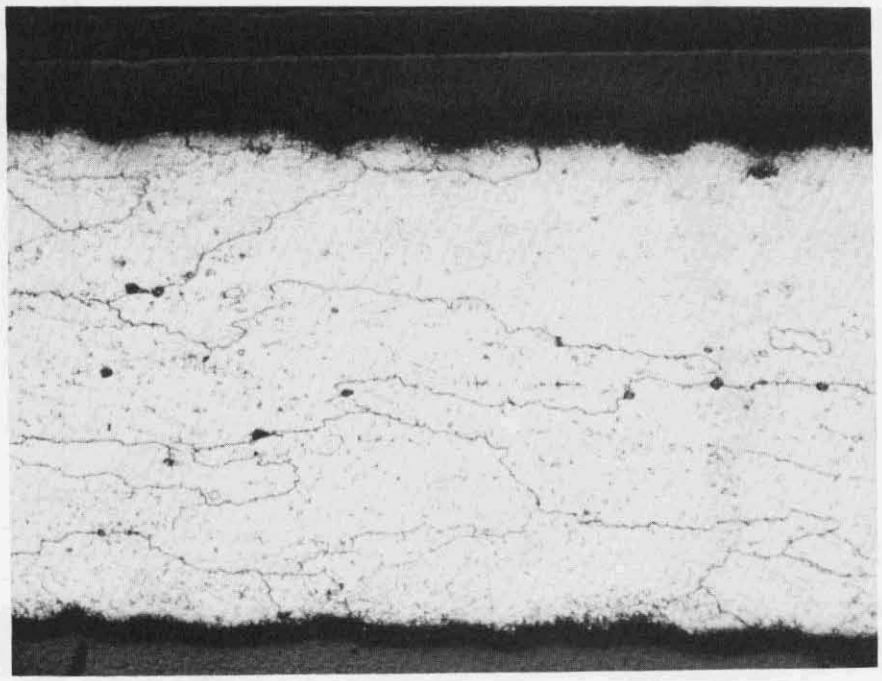

200X

FIGURE 9. MICROSTRUCTURE OF TDNi-Cr-5.8Al

Representative samples aluminized under the above conditions were mounted, and electron microprobe analysis was used to determine the concentrations and penetration profiles for nickel, chromium, and aluminum. As shown in Figure 10, the aluminum concentration in TDNiCr was found to reach the background level some 100 μm from the specimen surface. The nickel concentrations remained uniform across the specimens

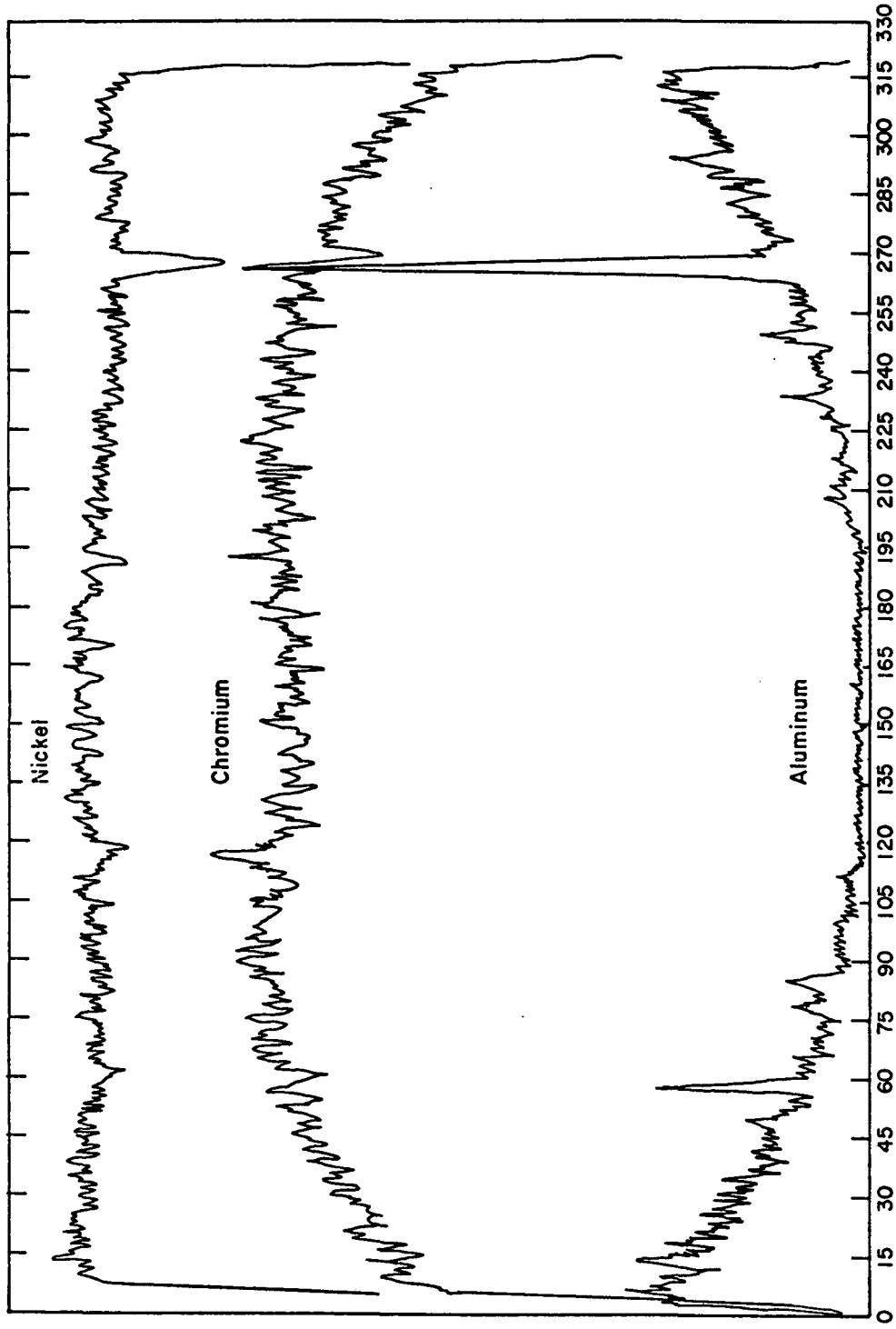

FIGURE 10. ELECTRON MICROPROBE DATA FOR ALUMINUM, CHROMIUM, AND NICKEL IN TDNiCr AFTER ALUMINIZING RUN 4 - 1260°C (2300°F) FOR 3.34 HOURS

Surface concentrations are 5.8Al-14.6Cr-76.6Ni (weight percent).

and the chromium levels dropped near the surface in proportion to the increasing aluminum concentrations.

As seen in Figures 7, 8, and 10, several peaks of high aluminum concentration are observed beneath the specimen surface, particularly in the Ni-20Cr base alloy. These are believed to reflect the presence of internal Al_2O_3 particles formed by a displacement reaction with initially present Cr_2O_3 particles.

Initially, surface concentrations for aluminum, chromium, and nickel were estimated by comparing the count rates for the various elements of the alloys with the counts for standards of pure chromium, aluminum, and nickel. In order to obtain more accurate data for the concentrations of the various constituents of the aluminized alloys, intensity data were collected from several specimens and computer corrected with MAGIC, a computer program for quantitative electron microprobe analysis. The program corrects all data for dead-time, background, absorption, and atomic number. Intensity data were obtained by taking five 10-second counts for nickel, chromium, and aluminum at 25 points along the surface of the samples. The averages of the five 10-second intensity counts for each element in each of the 25 areas were compared with intensities from the matrix of the material with a known chromium content. The matrix intensities for nickel and chromium were compared with 100 percent standards. For TDNiCr it was found that the computer program had not completely corrected for the fluorescence of chromium. An additional correction of the computer data for chromium was made using the chromium value for TDNiCr obtained by chemical analysis. Results of the corrected data are given in Table 2 with two sigma limits.

TABLE 2. SURFACE CHEMICAL COMPOSITION FOR ALUMINIZED TDNiCr

Run	Temp C	Temp F	Time, hrs	Weight Percent Ni	Cr	Al	ThO_2 (a)
3	1210	2210	16	77.22 ± 1.29	16.78 ± 1.82	4.30 ± 0.34	1.80
3 + 3A	1210	2210	32	77.51 ± 0.36	16.23 ± 0.45	4.95 ± 0.27	1.31
4	1260	2300	3.3	76.65 ± 0.78	14.60 ± 0.48	5.86 ± 0.35	2.89

(a) By difference.

Giggins and Pettit[18] reported the presence of γ' (Ni_3Al) in Ni-20Cr-6Al but not in Ni-20Cr-4Al. In the present study a replica technique was used to determine if γ' was present at room temperature in the aluminized specimens, which have more than 5 weight percent aluminum only in the near-surface region. At 30,000X no γ' could be detected. As shown in another section there was little difference between room-temperature mechanical properties of TDNiCr and TDNiCr-5.8Al.

Experimental Procedure

The as-received TDNiCr and Ni-20Cr had a fairly coarse belt-sanded finish, and this surface condition was used for all oxidation studies, except where noted. Similarly, no surface treatment was given to aluminized samples, other than wet brushing to remove adhering Al_2O_3 particles. Coupon samples cut from the as-received sheet were 2.54 x 1.27 cm (1 x 1/2 in.) or 2.54 x 2.54 cm (1 x 1 in.).

Isothermal tests, consisting of 50 hours at 1093°C or 1204°C (2000 or 2200°F), were followed continuously with either a Cahn type RG or type RH recording electronic microbalance. With the RG balance the specimens were suspended on a platinum wire and the reaction was initiated by raising a furnace (already at temperature) around the reaction tube. In this setup, the specimen takes approximately 20 minutes to reach reaction temperature. Specimens tested in the unit containing the RH balance were magnetically dropped into a furnace and reached temperature in several minutes. Except where noted all tests were performed in static air at 1.33×10^3 N/m^2 (10 torr) or 1.01×10^5 N/m^2 (760 torr).

Isothermal tests in which the RG balance was employed were terminated by lowering the furnace and allowing the specimen to cool in the test atmosphere; the specimens used in conjunction with the RH balance were magnetically raised from the hot zone and allowed to cool in the static air atmosphere. The specimens were then removed, visually examined, and weighed on an analytic balance as a check on the microbalance. The oxidized samples were examined using optical metallography, X-ray diffraction, and electron microprobe analysis.

Cyclic tests were performed by subjecting the specimens to 100 cycles of 30 minutes at temperature and 20 minutes of radiation cooling. The minimum temperature during the cooling cycle was 150°C (302°F). Continuous weight change was recorded with a Cahn type RG electronic microbalance. The specimen was suspended from a platinum wire in a mullite tube. The cyclic testing was accomplished by automatic raising and lowering a platinum-wound resistance furnace while the specimen remained stationary. The weight changes plotted for each cycle represent the value at the midpoint of the high-temperature portion of each cycle.

Results and Discussion

Kinetics

The experimental conditions for all oxidation tests performed in this study are presented in Table 3. The results of isothermal tests on TDNiCr and TDNiCrAl are plotted in Figures 11 to 14 as weight change versus time, and the results of cyclic tests on these materials are given in Figures 15 to 18 as weight change versus cycles at temperature. Since weight changes are the sum of various processes, including gains from oxidation and losses due to volatilization and spalling, few significant conclusions can be made on the basis of the weight-change data alone.

In general, the kinetic data point to parabolic or nearly parabolic behavior for the TDNiCr-5.8Al; continuous weight gains are observed in both isothermal and cyclic tests. Furthermore, the weight-change data are nearly identical for TDNiCr-5.8Al tested under the same conditions of temperature and oxygen pressure either in the cyclic

TABLE 3. SUMMARY OF OXIDATION TESTS FOR 50 HOURS AT TEMPERATURE

Specimen	Alloy	Type Test	Temperature °C	Temperature °F	Air Pressure N/m^2	Air Pressure Torr	Weight Gain: Microbalance, mg/cm^2	Weight Gain: Weight After Cooling, mg/cm^2	Comments[c]
1	TD NiCr	Isothermal	1093	2000	1.01×10^5	760	0.40	0.19[b]	
2	TD NiCr	Isothermal	1093	2000	1.01×10^5	760	0.84	-	
3	TD NiCr	Isothermal	1204	2200	1.33×10^4	100	0.63	-	
4	TD NiCr	Isothermal	1204	2200	1.01×10^5	760	0.51	-	
5	TDNi-Cr-XAl[a]	Isothermal	1204	2200	1.01×10^5	760	0.89	-	Intermetallic skin and internal porosity.
6	TDNi-Cr-XAl[a]	Isothermal	1204	2200	1.01×10^5	760	2.69		Ditto.
7	TDNi-Cr-XAl[a]	Isothermal	1204	2200	1.01×10^5	760	-	-	Ditto, hang wire broke.
8	TD NiCr	Cyclic	1093	2000	1.01×10^5	760	0.45	-	Minimum temperature was 480°C (896°F). No spalling observed.
9	TDNiCr-XAl[a]	Isothermal	1204	2200	1.01×10^5	760	2.36	-	As in Test 5.
10	TD NiCr						-	-	Test aborted.
11	Ni-20Cr	Cyclic	1093	2000	1.01×10^5	760	- 1.53	-	Minimum temperature was 480°C (896°F). No spalling observed.
12	TD NiCr	Isothermal	1093	2000	1.01×10^5	760	0.43	0.30	
13	Ni-20Cr	Cyclic	1093	2000	1.01×10^5	760	-	- 2.14	Minimum temperature was 150°C (302°F). Scale spalled at every cooling cycle.

TABLE 3. (Continued)

Specimen	Alloy	Type Test	Temperature °C	Temperature °F	Air Pressure N/m²	Air Pressure Torr	Weight Gain Microbalance, mg/cm²	Weight Gain Weight After Cooling, mg/cm²	Comments[c]
14	TD NiCr-4.3Al	Isothermal	1093	2000	1.01×10^5	760	0.16	0.27	$\alpha\ Al_2O_3 > NiAl_2O_4 \gg ThO_2 \gg Cr_2O_3$
15	TD NiCr-4.3Al	Isothermal	1093	2000	1.01×10^5	760	0.29	0.20	
16	TD NiCr-4.3Al	Isothermal	1093	2000	1.33×10^3	10	0.71	0.34	Large weight gain in last 5 hours.
17	TD NiCr-4.3Al	Isothermal	1093	2000	1.33×10^3	10	0.30	0.31	
18	TD NiCr-4.3Al	Cyclic	1093	2000	1.01×10^5	760	0.39	-	
19	TD NiCr	Isothermal	1093	2000	1.33×10^4	100	0.19	0.19	Oxygen.
20	TD NiCr	Cyclic	1093	2000	1.01×10^5	760	0.35	0.30	
21	TD NiCr-4.95Al	Isothermal	1093	2000	1.01×10^5	760	0.41	0.24	$\alpha\ Al_2O_3 \ggg ThO_2$.
22	TD NiCr-4.95Al	Isothermal	1093	2000	1.01×10^5	760	0.37	0.36	
23	TD NiCr	Isothermal	1093	2000	1.33×10^3	10	0.34	0.18	
24	TD NiCr-4.95Al	Isothermal	1093	2000	1.33×10^3	10	0.40	0.54	
25	TD NiCr	Isothermal	1093	2000	1.33×10^3	10	0.16	0.17	
26	TD NiCr-4.95Al	Isothermal	1093	2000	1.33×10^3	10	0.38	0.42	
27	TD NiCr	Cyclic	1204	2200	1.01×10^5	760	0.22	0.22	$Cr_2O_3 \ggg ThO_2$.
28	Td NiCr-4.95Al	Cyclic	1204	2200	1.01×10^5	760	0.67	0.57	$\alpha\ Al_2O_3 > NiAl_2O_4 > ThO_2$.

TABLE 3. (Continued)

Specimen	Alloy	Type Test	Temperature °C	Temperature °F	Air Pressure N/m²	Air Pressure Torr	Weight Gain Microbalance, mg/cm²	Weight Gain Weight After Cooling, mg/cm²	Comments[c]
29	Ni-20Cr	Cyclic	1204	2200	1.01×10^5	760	- 4.86	- 5.98	$Cr_2O_3 \gg NiCr_2O_4$.
30	TD NiCr	Cyclic	1204	2200	1.33×10^3	10	- 0.63	- 0.56	$Cr_2O_3 \ggg ThO_2$.
31	TDNiCr-4.95Al	Cyclic	1204	2200	1.33×10^3	10	0.40	0.26	$NiAl_2O_4 > \alpha\ Al_2O_3 > ThO_2$.
32	TDNiCr-5.8Al	Isothermal	1093	2000	1.01×10^5	760	0.35	0.53	$\alpha\ Al_2O_3 > NiAl_2O_4 \gg ThO_2 > NiCr_2O_4$.
33	TDNiCr-5.8Al	Isothermal	1093	2000	1.01×10^5	760	0.46	0.64	
34	TDNiCr-5.8Al	Isothermal	1204	2200	1.33×10^3	10	0.77	0.61,	
35	TDNiCr-5.8Al	Cyclic	1204	2200	1.33×10^3	10	0.76	-	$\alpha\ Al_2O_3 > Cr_2O_3 > NiAl_2O_4 > ThO_2$.
36	TD NiCr	Cyclic	1204	2200	1.33×10^3	10	- 0.54	- 0.61	Mechanically polished.
37	TDNiCr-5.8Al	Isothermal	1204	2200	1.33×10^3	10	0.64	0.67	
38	TD NiCr	Isothermal	1204	2200	1.33×10^3	10	- 0.18	0.02	Specimen stuck to wall.
39	TD NiCr	Isothermal	1204	2200	1.01×10^5	760	2.48		Specimen lost weight for 17 hours, then gained.
40	TDNiCr-5.8Al	Cyclic	1204	2200	1.01×10^5	760	0.94	0.84	
41	TDNiCr-5.8Al	Isothermal	1204	2200	1.01×10^5	760	0.68	0.84	
42	TDNiCr-5.8Al	Cyclic	1093	2000	1.01×10^5	760	0.49	0.60	Test aborted after 28 cycles.

TABLE 3. (Continued)

Specimen	Alloy	Type Test	Temperature °C	Temperature °F	Air Pressure N/m^2	Air Pressure Torr	Weight Gain Microbalance, mg/cm^2	Weight Gain Weight After Cooling, mg/cm^2	Comments[c]
43	TDNiCr-5.8Al	Isothermal	1093	2000	1.33×10^3	10	0.29	0.30	
44	TDNiCr-5.8Al	Cyclic	1093	2000	1.33×10^3	10	-	-	Test aborted.
45	TDNiCr-5.8Al	Isothermal	1093	2000	1.33×10^3	10	0.27	0.28	
46	TDNiCr-5.8Al	Isothermal	1204	2200	1.01×10^5	760	0.52	0.30	
47	TDNiCr-5.8Al	Cyclic	1093	2000	1.33×10^3	10	0.17	-	Test aborted after 19 cycles.
48	TDNiCr	Isothermal	1204	2200	1.01×10^5	760	- 0.33	- 0.67	
49	TDNiCr	Isothermal	1204	2200	1.01×10^5	760	- 0.09	-	
50	TDNiCr	Isothermal	1204	2200	1.33×10^3	10	0.10	0.21	
51	TDNiCr-5.8Al	Cyclic	1093	2000	1.33×10^3	10	0.46	0.43	
52	TDNiCr-5.8Al	Cyclic	1093	2000	1.33×10^3	10	0.48	0.43	
53	TDNiCr	Isothermal	1204	2200	1.33×10^3	10	- 0.27	- 0.08	
54	TDNiCr	Cyclic	1093	2000	1.33×10^3	10	0.28	0.17	
55	TDNiCr	Isothermal	1093	2000	1.33×10^3	10	0.24	0.15	
56	TDNiCr	Cyclic	1093	2000	1.33×10^3	10	0.19	0.27	
57	TDNiCr	Cyclic	1093	2000	1.01×10^5	760	0.28	0.15	

TABLE 3. (Continued)

Specimen	Alloy	Type Test	Temperature °C	Temperature °F	Air Pressure N/m^2	Air Pressure Torr	Weight Gain Microbalance, mg/cm^2	Weight Gain Weight After Cooling, mg/cm^2	Comments[c]
58	TDNiCr-5.8Al	Cyclic	1093	2000	1.01×10^5	760	0.44	0.39	Furnace was at temperature for 15 hours during two cycles.
59	TDNiCrAlY	Isothermal	1204	2200	1.33×10^3	10	1.12	1.01	
60	TDNiCr-4.3Al	Isothermal	1204	2200	1.33×10^3	10	0.66	0.58	
61	TDNiCr-4.3Al	Isothermal	1204	2200	1.01×10^5	760	0.29	0.59	Furnace burned out after 47 hours.
62	TDNiCr-5.8Al	Cyclic	1093	2000	1.01×10^5	760	0.59	0.53	
63	TDNiCr-4.9Al	Isothermal	1204	2200	1.33×10^3	10	0.75	0.32	
64	TDNiCr-4.9Al	Isothermal	1204	2200	1.01×10^5	760	0.74	0.66	
65	TDNiCr-5.8Al	Cyclic	1204	2200	1.01×10^5	760	0.37	0.36	Tube cracked during run.
66	TDNiCr	Cyclic	1204	2200	1.01×10^5	760	0.06	0.12	
67	TDNiCr-5.8Al	Cyclic	1204	2200	1.33×10^3	10	-	-	Test aborted.
68	TDNiCr	Cyclic	1204	2200	1.01×10^5	760	- 0.22	- 0.11	
69	TDNiCr	Isothermal	1204	2200	1.33×10^4	100-0_2	- 0.68	- 0.51	
70	TDNiCr-4.3Al	Isothermal	1204	2200	1.01×10^5	760	1.05	0.78	
71	TDNiCr-4.9Al	Cyclic	1204	2200	1.01×10^5	760	0.73	0.65	
72	TDNiCr-4.9Al	Isothermal	1204	2200	1.33×10^3	10	0.32	0.08	
73	TDNiCr	Isothermal	1204	2200	1.33×10^3	10	- 0.33	- 0.12	

TABLE 3. (Continued)

Specimen	Alloy	Type Test	Temperature °C	Temperature °F	Air Pressure N/m^2	Air Pressure Torr	Weight Gain Microbalance, mg/cm^2	Weight Gain Weight After Cooling, mg/cm^2	Comments[c]
74	TDNiCr	Isothermal	1204	2200	1.33×10^3	10	0.20	0.32	
75	Ni-Cr-5.8Al	Isothermal	1204	2200	1.01×10^5	760	-	-	Test aborted.
76	Ni-Cr-5.8Al	Isothermal	1204	2200	1.01×10^5	760	0.79	0.46	
77	Ni-Cr-5.8Al	Isothermal	1204	2200	1.33×10^3	10	0.76	0.67	
78	Ni-Cr-5.8Al	Isothermal	1204	2200	1.33×10^3	10	0.36	0.44	
79	Ni-Cr-5.8Al	Isothermal	1093	2000	1.01×10^5	760	-	-	Test aborted.
80	Ni-Cr-5.8Al	Isothermal	1093	2000	1.01×10^5	760	0.28	0.30	
81	Ni-Cr-5.8Al	Isothermal	1093	2000	1.33×10^3	10	0.17	0.34	
82	Ni-Cr-5.8Al	Isothermal	1093	2000	1.33×10^3	10	0.23	0.27	
83	Ni-Cr-5.8Al	Cyclic	1258	2300	1.01×10^5	760	0.39	0.11	Specimen was wrinkled and bent.
84	Ni-Cr-5.95Al	Cyclic	1093	2000	1.01×10^5	760	0.70	0.51	
85	TDNiCr	Cyclic	1258	2300	1.01×10^5	760	- 0.09	0.06	
86	TDNiCr	Cyclic	1093	2000	1.33×10^3	10	-	-	Test aborted.
87	TDNiCr-5.8Al	Isothermal	1204	2200	1.33×10^3	10	0.50	0.54	From aluminizing Treatment 5 (same as 4). #4).
88	TDNiCr	Isothermal	1204	2200	1.01×10^5	760	0.09	0.00	Specimen bent to 3T prior to oxidation.

TABLE 3. (Continued)

Specimen	Alloy	Type Test	Temperature °C	Temperature °F	Air Pressure N/m^2	Air Pressure Torr	Weight Gain Microbalance, mg/cm^2	Weight Gain Weight After Cooling, mg/cm^2	Comments[c]
89	TDNiCr-5.8Al	Isothermal	1204	2200	1.01×10^5	760	0.41	0.63	Specimen bent to 3T prior to oxidation.
90	TDNiCrAlY	Cyclic	1204	2200	1.33×10^3	10	1.28	0.92	Oxygen.

(a) This alloy, aluminized by Treatment 1, had an unknown aluminum surface concentration.

(b) The difference between the microbalance weight gain and the measured weight gain after cooling may be a measure of the scale lost by spalling.

(c) Where scale components are noted, they were determined by X-ray diffraction.

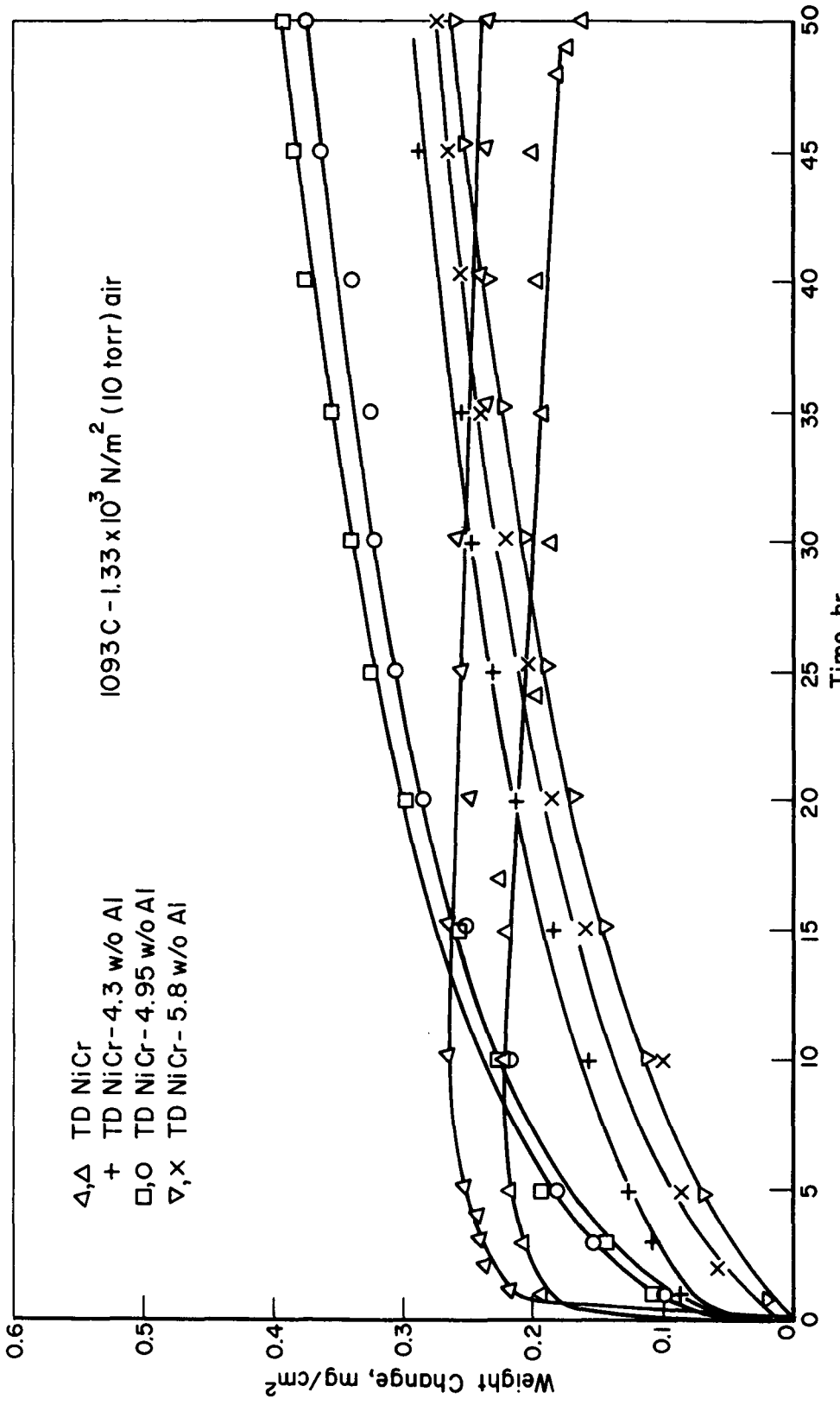

FIGURE 11. WEIGHT CHANGE FOR TDNiCr AND TDNiCr-Al ISOTHERMALLY OXIDIZED AT 1093°C (2000°F) AND 1.33 x 10^3 N/m^2 (10 TORR) AIR

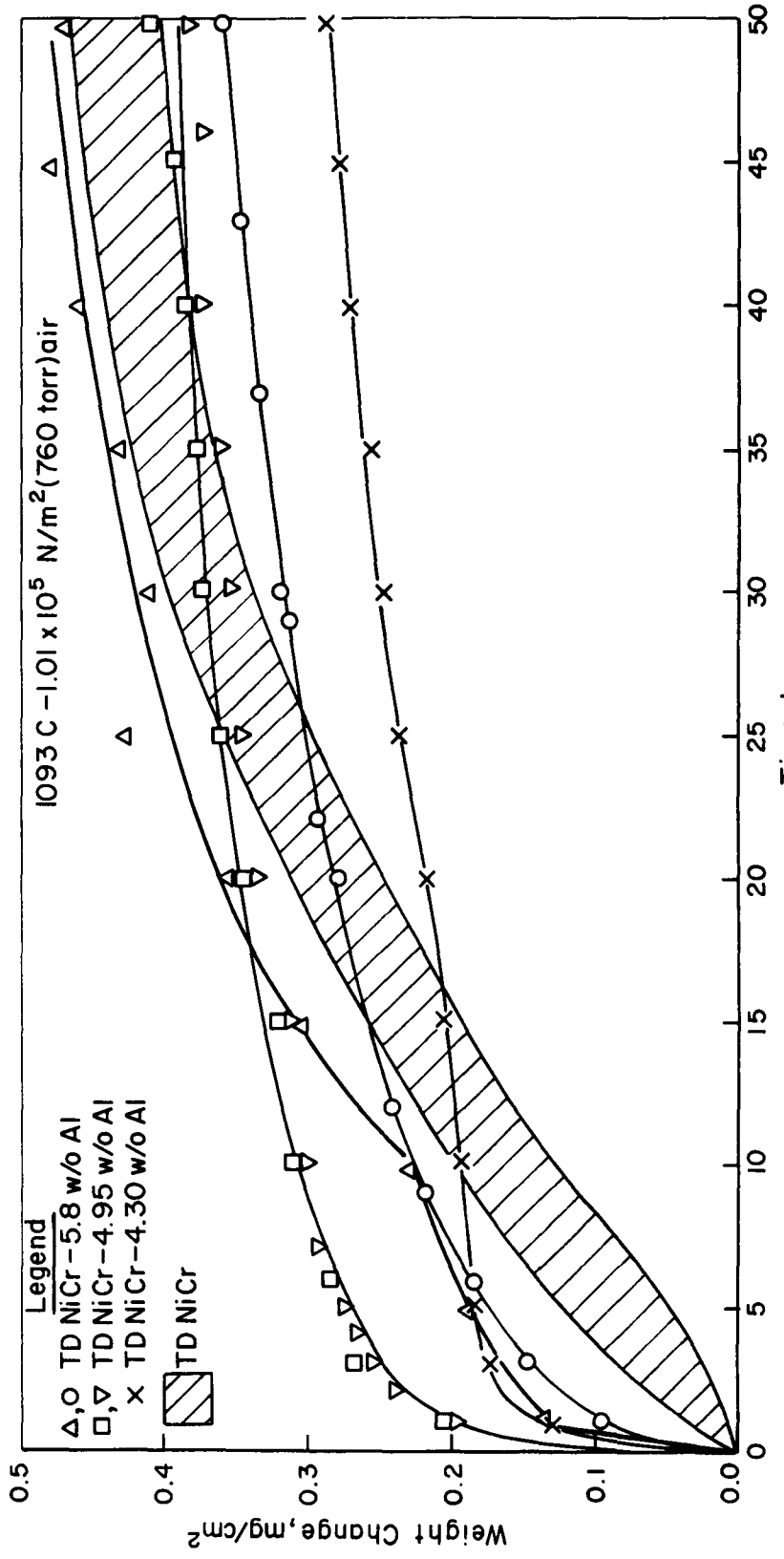

FIGURE 12. WEIGHT CHANGE FOR TDNiCr AND TDNiCr-Al OXIDIZED ISOTHERMALLY AT 1093 °C (2000 °F) AND 1.01 x 10^5 N/m^2 (760 TORR) AIR

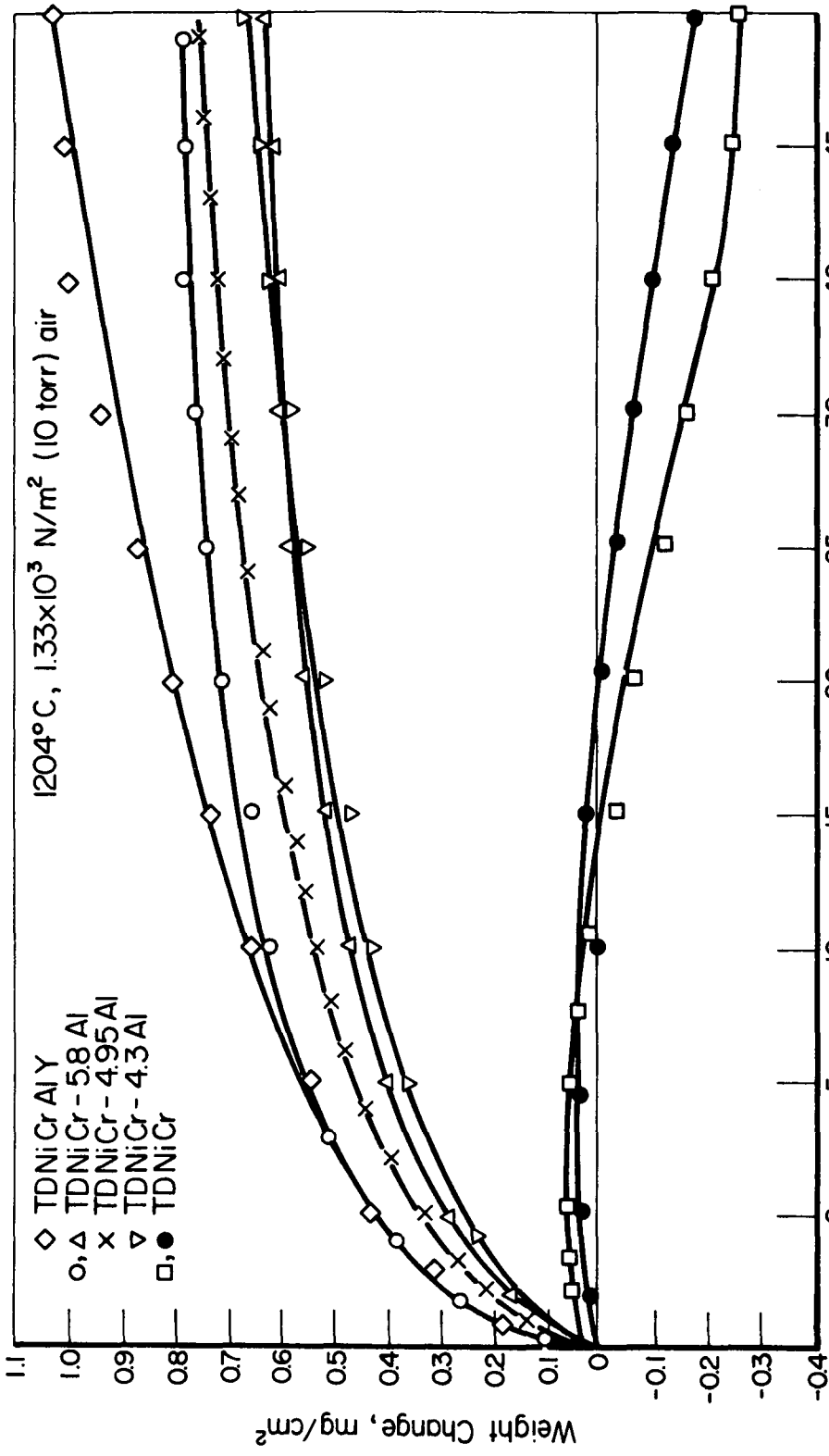

FIGURE 13. WEIGHT CHANGE FOR TDNiCr AND TDNiCrAl OXIDIZED AT 1204°C (2200°F) AND 1.33 x 10^3 N/m^2 (10 TORR) AIR

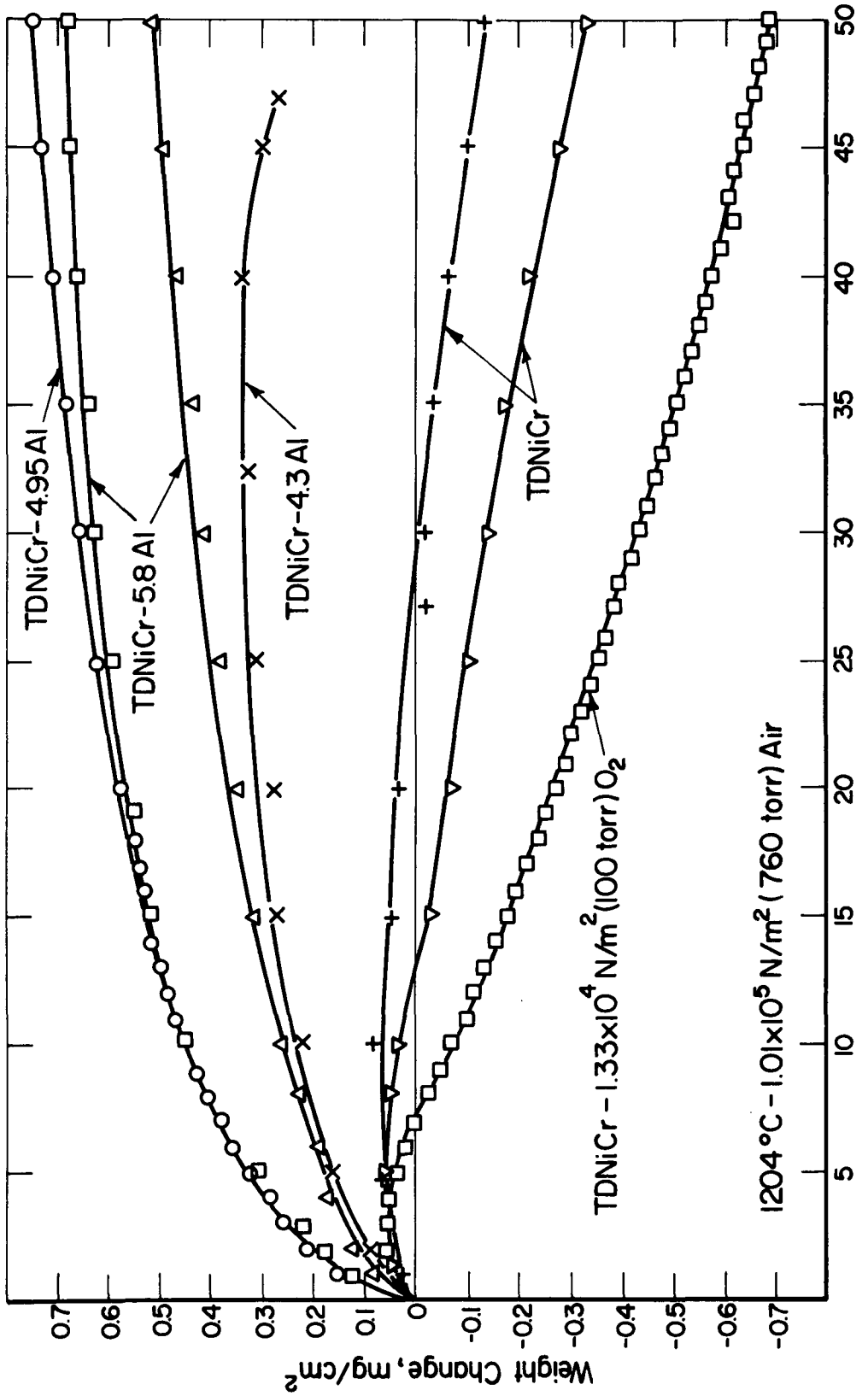

FIGURE 14. WEIGHT CHANGE FOR TDNiCr AND TDNiCr-5.8Al OXIDIZED AT 1204°C (2200°F) AND 1.01×10^5 N/m^2 (760 TORR) AIR

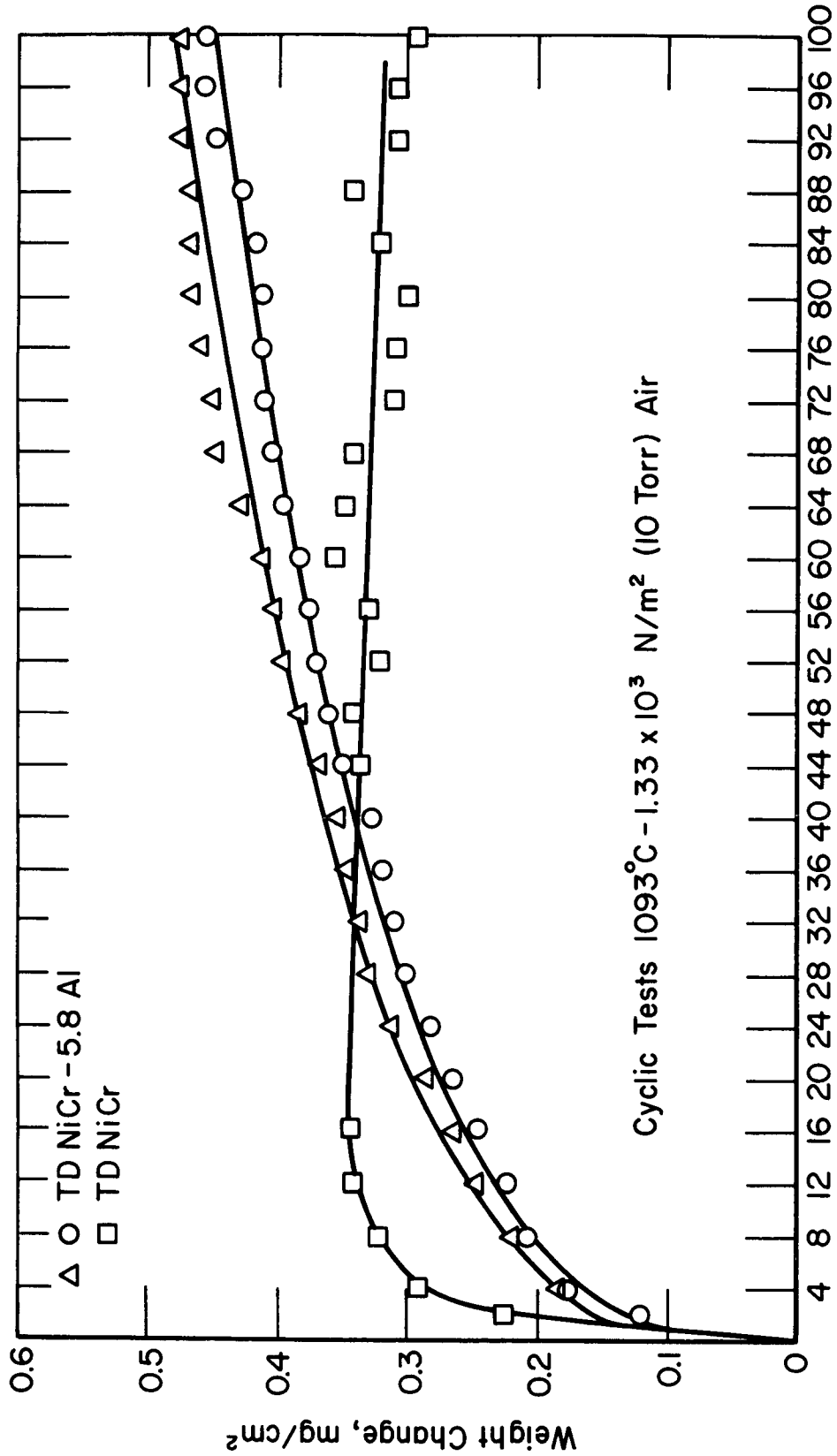

FIGURE 15. WEIGHT CHANGE FOR CYCLIC OXIDATION OF TDNiCr AND TDNiCr-5.8Al AT 1093°C (2000°F) AND 1.33 x 10^3 N/m^2 (10 TORR) AIR

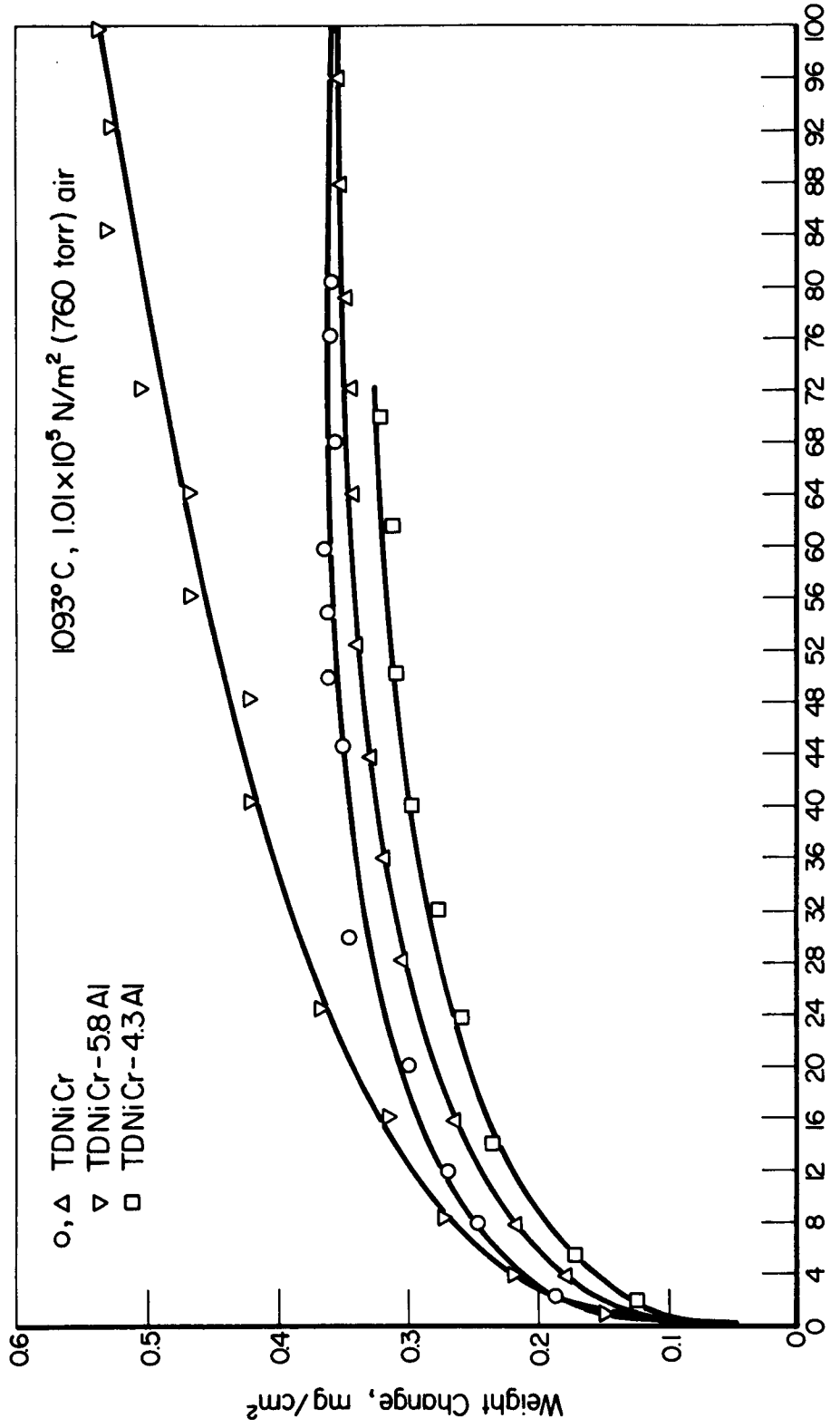

FIGURE 16. WEIGHT CHANGE FOR CYCLIC OXIDATION OF TDNiCr AND TDNiCr-Al AT 1093°C (2000°F) AND 1.01 x 10^5 N/m^2 (760 TORR) AIR

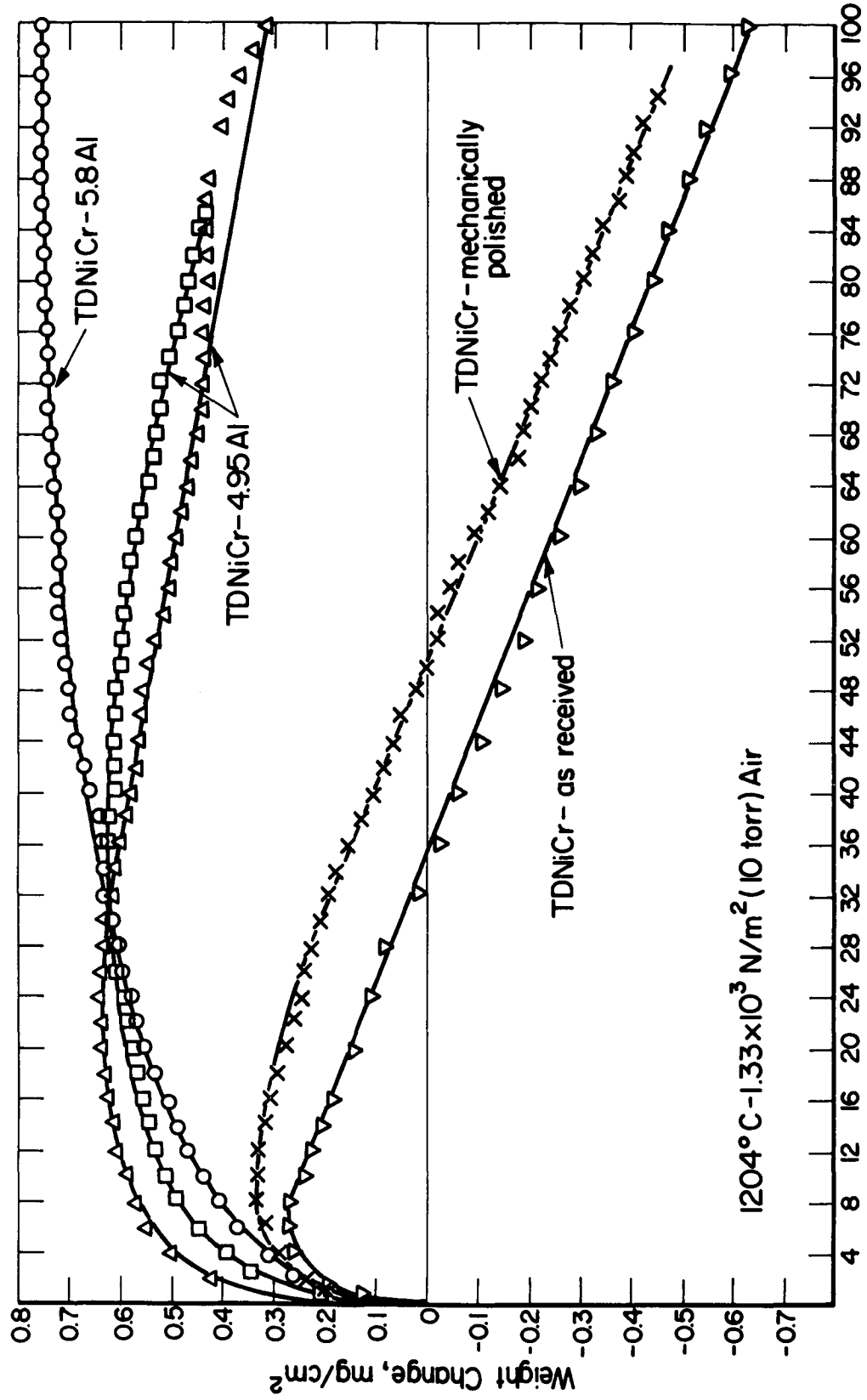

FIGURE 17. WEIGHT CHANGE FOR CYCLIC OXIDATION OF TDNiCr AND TDNiCr-Al AT 1204°C (2200°F) AND 1.33×10^3 N/m^2 (10 TORR) AIR

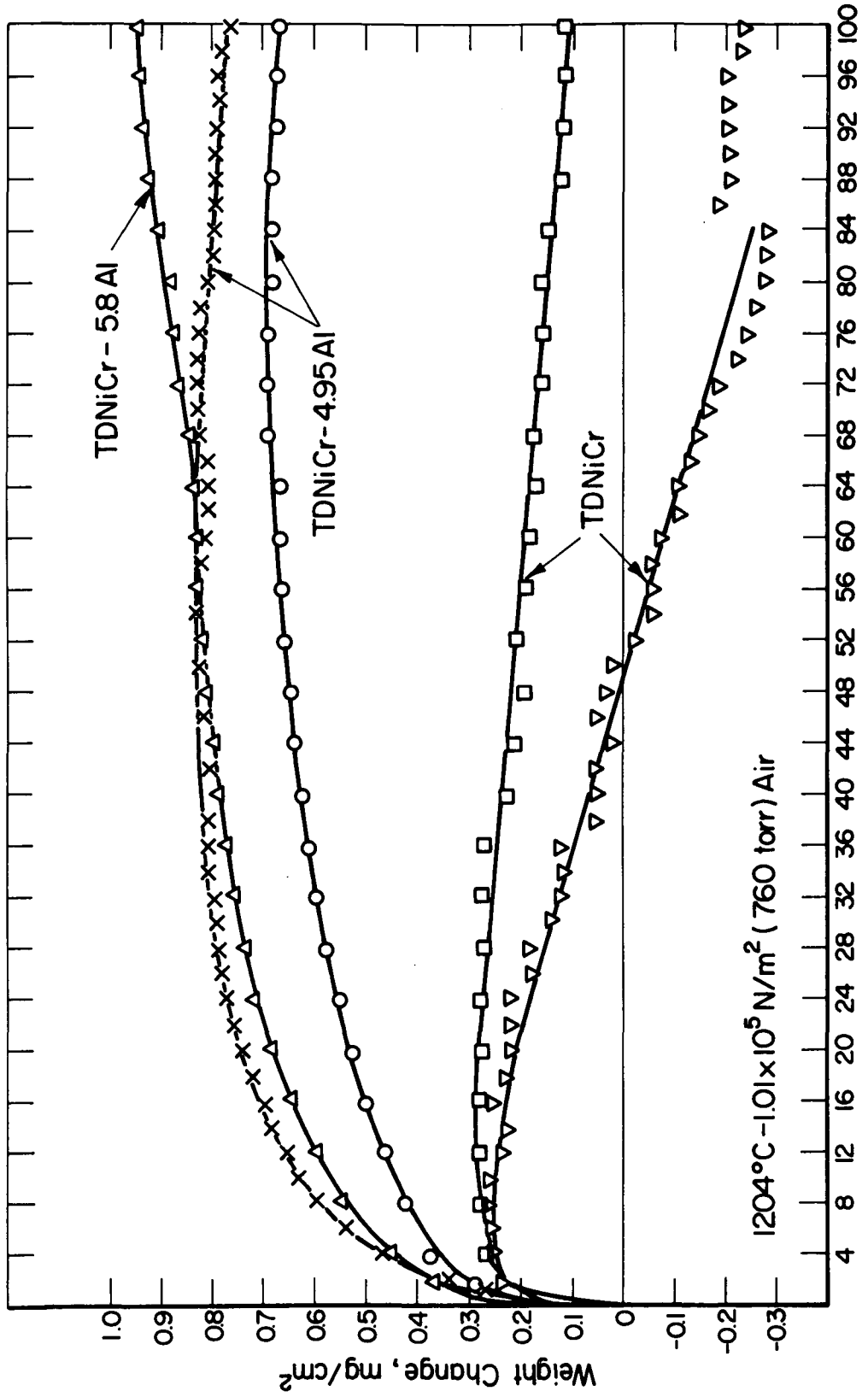

FIGURE 18. WEIGHT CHANGE FOR CYCLIC OXIDATION OF TDNiCr AND TDNiCr-Al AT 1204°C (2200°F) AND 1.01×10^5 N/m^2 (760 TORR) AIR

or isothermal mode. This suggests that little spalling occurs during the cyclic testing of TDNiCr-5.8Al.

For TDNiCr-4.95Al, continuous weight increases are observed over the duration of 50-hour isothermal tests, but weight losses were measured in cyclic tests at 1204°C (2200°F) at both 1.33×10^3 N/m^2 (10 torr) air and 1.01×10^5 N/m^2 (760 torr) air. These results suggest that some spalling has occurred for the TDNiCr-4.95Al specimens during cyclic oxidation. Further evidence for spalling of scales on the 4.95Al alloys was obtained from an analysis of the aluminum distribution before and after oxidation of aluminized specimens. This is discussed in another section.

The TDNiCr-4.3Al alloy appears to have insufficient aluminum to form pure alumina scales, and weight losses were observed in some instances for this alloy even in isothermal tests (see Figure 14). The weight losses that occur in isothermal tests are attributed to volatilization of Cr_2O_3 in the scale as CrO_3.

For TDNiCr without aluminum, the data suggest that, after an initial period during which scale formation occurs, volatilization of Cr_2O_3 scale as CrO_3 results in continuous weight loss of test specimens. This behavior is observed under all test conditions except 1093°C (2000°F) and 1.01×10^5 N/m^2 (760 torr) air. The slightly greater weight losses found for TDNiCr subjected to cyclic tests as compared with losses measured in isothermal tests may be attributed to spallation during cycling.

An analysis of the kinetic data for TDNiCr and some experimental Ni-20Cr-$2Y_2O_3$ alloys has been performed.[6] Results point to the fact that the oxidation of TDNiCr cannot be fit by a parabolic rate law in combination with the volatilization, but, rather, a high-order rate law such as a cubic or quartic must be used to obtain the best fit to the isothermal weight-change data.

As seen in Table 3, an isothermal, 50-hour test was performed at 1204°C (2200°F) and 1.33×10^3 N/m (10 torr) air on TDNiCrAlY (Specimen 59) prepared by Fansteel (Heat 3190). The optical micrograph in Figure 19 shows the relatively fine-grained

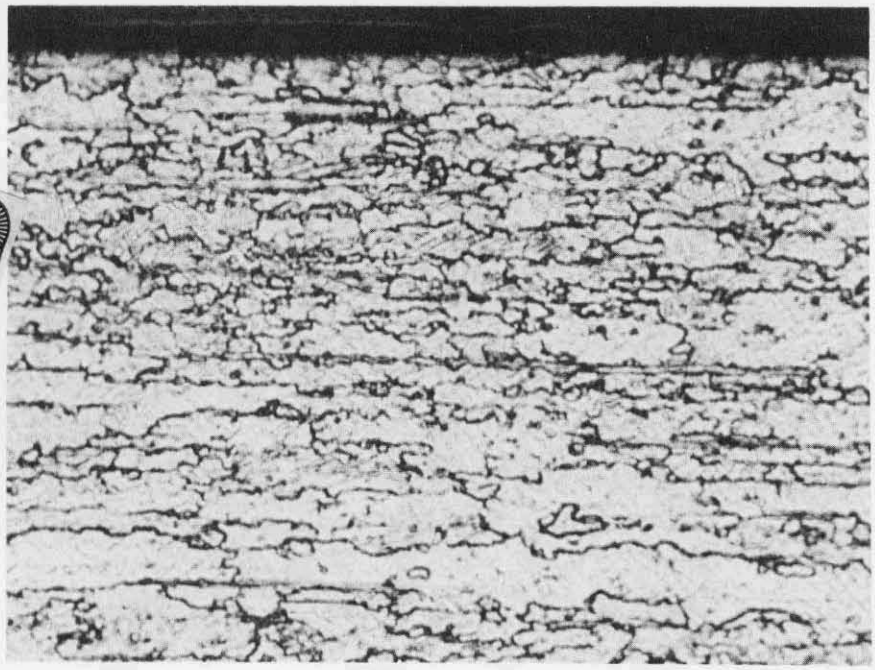

FIGURE 19. MICROSTRUCTURE OF TDNiCrAlY

somewhat-elongated microstructure of this alloy. The weight-change data for this specimen are included in Figure 13, along with data previously obtained at Battelle for TDNiCr and TDNiCr-5.8 w/o Al produced by the pack process. The continuous weight increase with time suggests that little or no volatilization has occurred from the TDNiCrAlY specimen. The scale appears to consist solely of Al_2O_3. Almost identical weight-change data were obtained for TDNiCrAlY (Sample 90) which was cyclically tested (100 cycles) at 1204°C (2200°F) and 1.33×10^3 N/m^2 (10 torr) oxygen.

Results obtained for specimens of TDNiCr ~2Al are presented in Figure 20. These specimens were obtained from the aluminization Treatment 1, in which pure aluminum was used in the pack. They were prepared by peeling off the intermetallic skin and removing the outer 12.7 to 25.4 μm (0.0005 to 0.001 in.) by grinding on 240 grit metallographic paper, in order to approximate the belt-sanded finish of the as-received TDNiCr. All specimens with low aluminum concentrations oxidized at a higher rate than the TDNiCr at 1204°C (2200°F) and in 1.01×10^5 N/m^2 (760 torr) air. The weight gain was particularly high for the specimens which had been reduced in thickness by 0.0025 cm (0.0001 in.) on each face. The aluminum concentration in all these specimens was, of course, too low to provide a continuous Al_2O_3 scale on the specimen surface. This was obvious from the appearance of a green Cr_2O_3 scale on the surface of the oxidized specimens.

Cook, Timbres, and Norris have found that aluminum additions on the order of 2 weight percent result in increased weight gain for Ni-20Cr-3ThO_2 at 1204°C (2200°F), compared with that for the unmodified alloy.[19] The observed increase in specific weight gain was of the same magnitude as shown in Figure 20 – from 0.3 mg/cm^2 for Ni-20Cr-2ThO_2 to 3.6 mg/cm^2 for the alloy containing 2 weight percent aluminum.

A series of tests on Ni-20Cr-5.8Al specimens had the twofold purpose of obtaining isothermal and cyclic oxidation data to compare with those of TDNiCr-5.8Al and determining diffusion rates for out-diffusion of aluminum from these alloys during oxidation. It was hoped that the latter information could be obtained from a comparison of aluminum-concentration profiles in aluminized specimens before and after oxidation.

The kinetic data are presented in Figures 21 and 22. Included in Figure 21 are data obtained at 1204°C (2200°F) and 1.01×10^5 N/m^2 (760 torr) air for 50 hour isothermal tests and 100 cycle cyclic experiments with TDNiCr-5.8Al and Ni-Cr-5.8Al. The isothermal data suggest similar oxidation behavior for the alloys with and without thoria. In both, continuous weight increases are observed after 50 hours at temperature and the scale formed is primarily light-gray Al_2O_3. Electron probe microanalysis confirms the presence of an Al_2O_3 scale with a slight amount of chromium as Cr_2O_3 or $NiCr_2O_4$ spinel. These results are in contrast, of course, to those obtained for TDNiCr and Ni-20Cr where great differences in oxidation behavior are observed under the above experimental conditions, and where weight losses occur during 50-hour tests due to volatilization of Cr_2O_3 as CrO_3.

The superior adhesion of Al_2O_3 scales on TDNiCr-5.8Al is revealed in the cyclic tests, where again a continuous weight increase is observed for TDNiCr-5.8Al after 100 cycles, while continuous weight loss occurs after 32 cycles for Ni-Cr-5.8Al. After 100 cycles, the ThO_2-free alloy was severely wrinkled and had a nearly black scale, as compared with the tightly adherent, gray Al_2O_3 on the thoriated alloys. It appears that the alumina scale that formed during the initial cycles on the unthoriated alloys spalled on cooling. Eventually, the alloy became depleted in aluminum, and

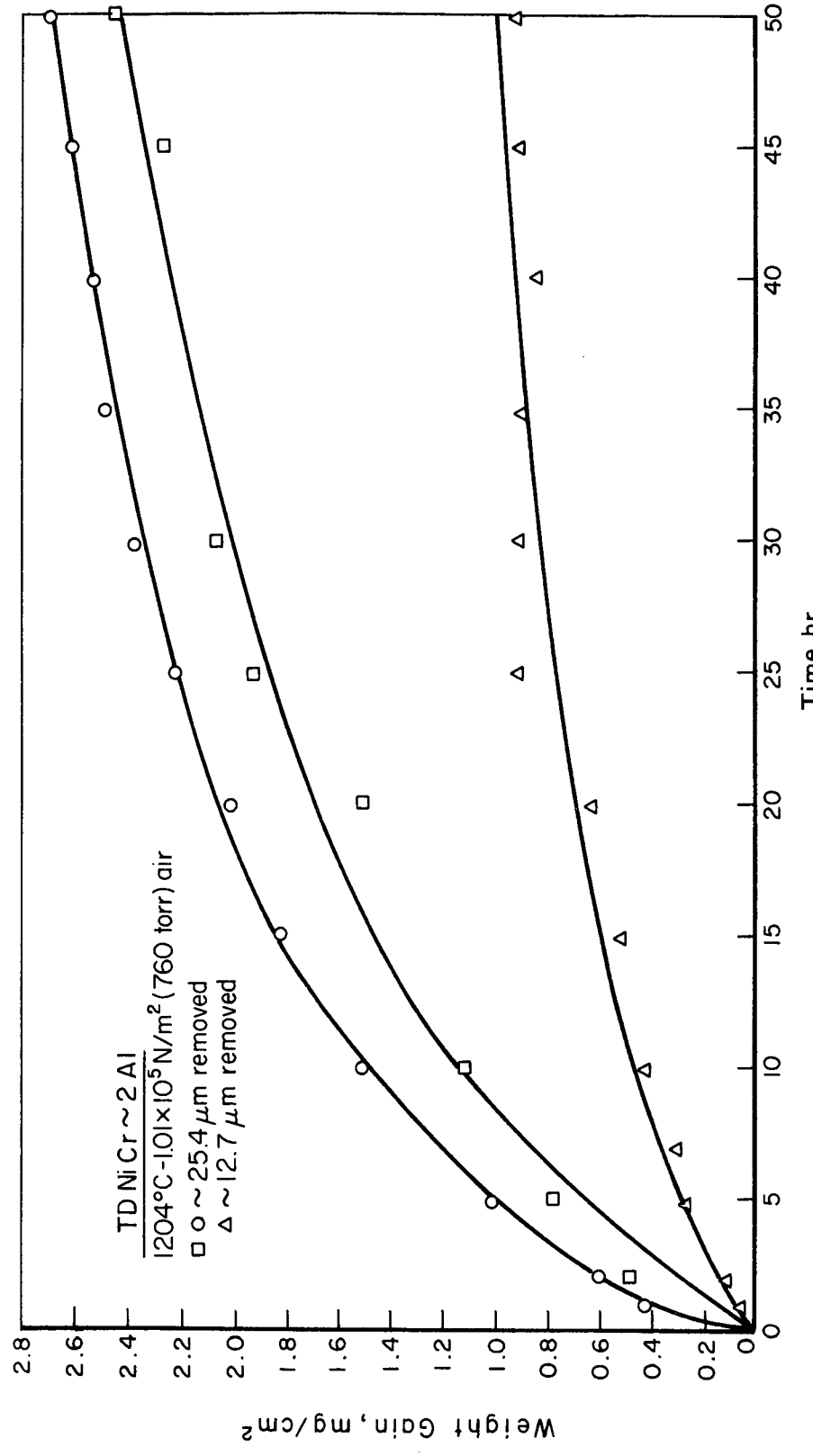

FIGURE 20. WEIGHT GAIN FOR TDNiCr-2Al TESTED AT 1204°C (2200°F) AND 1.01×10^5 N/m^2 (760 TORR) AIR

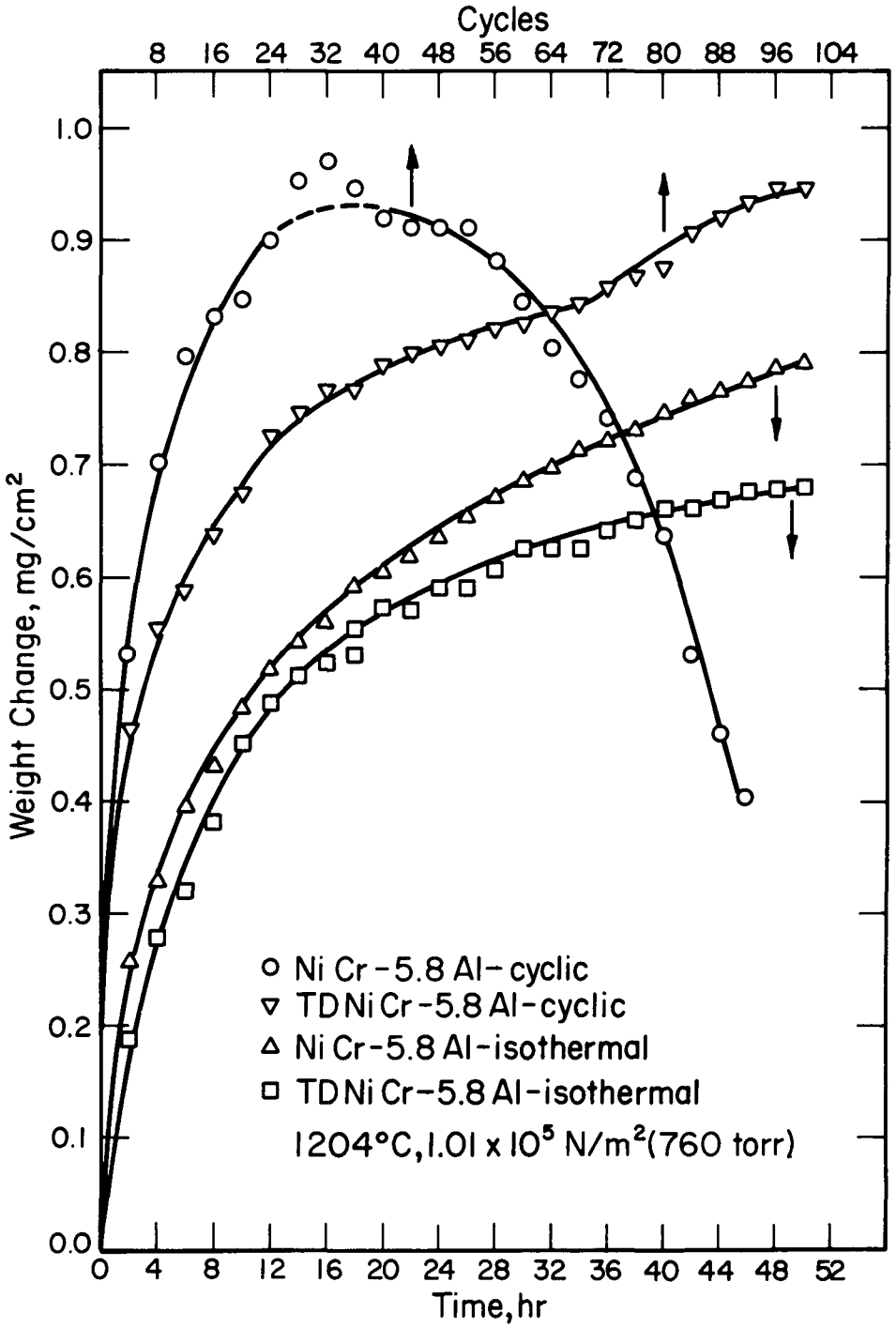

FIGURE 21. WEIGHT CHANGE FOR TDNiCr-5.8Al AND Ni-Cr-5.8Al TESTED AT 1204°C (2200°F) AND 1.01 x 10^5 N/m^2 (760 TORR) AIR

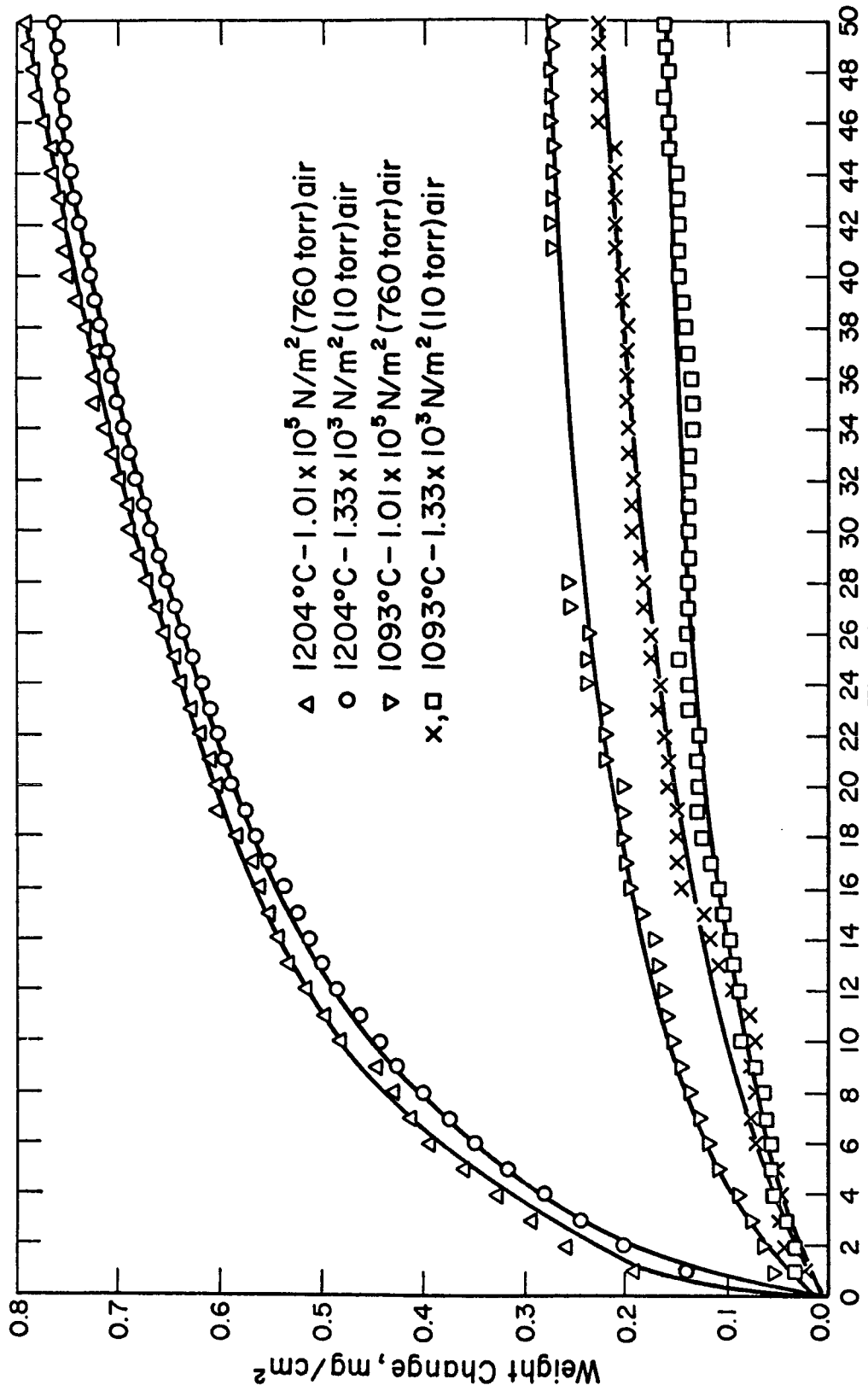

FIGURE 22. WEIGHT CHANGE FOR Ni-Cr-5.8Al ISOTHERMALLY TESTED AT 1204°C (2200°F) AND 1093°C (2000°F)

scales containing chromium and nickel were produced. Weight losses were then observed due to spalling and volatilization of the chromium-containing scale.

Isothermal data obtained for Ni-Cr-5.8Al at 1093°C and 1204°C (2000°F and 2200°F) at 1.01×10^5 N/m^2 (760 torr) and 1.33×10^3 N/m^2 (10 torr) air are presented in Figure 22. The oxidation behavior is nearly identical at both temperatures for the two oxygen pressures used, and again the data for ThO_2-free aluminized alloys are similar to those obtained for TDNiCr-5.8Al.

As noted in Table 3, specimens (88 and 89) were oxidized at 1204°C (2200°F) and 1.01×10^5 N/m^2 (760 torr) air after being bent on a die with a 0.79-mm (1/32 in.) radius. The purpose of these experiments was to determine the effect of a simulated fabrication operation on the oxidation resistance of pack-aluminized TDNiCr. The weight changes after 50 hours for both specimens were similar to those found for unbent specimens. Furthermore, the scale on either side of the bend in the aluminized specimen was found (by electron probe microanalysis) to consist entirely of Al_2O_3, with no evidence of chromium or nickel in the scale.

X-ray Diffraction

The constituents of the scales produced during the cyclic tests at 1204°C (2200°F) were determined from X-ray diffraction analyses after completion of the experiments. A diffractometer technique was used to analyze the scales in place on the surface of the specimens, and an evacuated Debye-Scherrer camera technique was used to analyze powder scraped from the specimen surface. The results obtained are included in Table 3. At 1204°C (2200°F) and 1.01×10^5 N/m^2 (760 torr), the scale formed on TDNiCr (Specimen 27) consisted of Cr_2O_3 with some ThO_2; for the TDNiCr-4.9Al alloy (Specimen 28), which showed little or no weight loss, the scale consisted of α Al_2O_3 with somewhat less $NiAl_2O_4$, and again ThO_2. For specimens tested at 1204°C (2200°F) and 1.33×10^3 N/m^2 (10 torr) the same scales were found on TDNiCr (Specimen 30) and TDNiCr-4.9Al (Specimen 31) as had been found at the higher air pressure. For the latter alloy, however, $NiAl_2O_4$ appeared to be predominant over α Al_2O_3. Surprisingly, the scale for TDNiCr-5.8Al (Specimen 35), which appeared to have the best weight change versus time characteristics, was found to contain some Cr_2O_3 although α Al_2O_3 was the primary constituent along with $NiAl_2O_4$ and ThO_2. It might be pointed out that chromium (in the form of $NiCr_2O_4$) was also found in TDNiCr-5.8Al (Specimen 32) oxidized at 1093°C (2000°F) and 1.01×10^5 N/m^2 (760 torr), but for the TDNiCr-4.9Al alloy (Specimen 21) tested under the same conditions, the scale consisted entirely of α Al_2O_3.

Two points must be made regarding these findings. First, the scales produced during cyclic tests are not uniform in appearance. For the aluminized samples, areas of green color, indicative of chromium-containing oxide, are dispersed in the light-gray-alumina scale. Thus the nature of the constituents found in the various scales may depend on the region of the specimens from which the samples are taken. In our analysis samples were taken by scraping a small amount of scale from an area about 0.254 cm (0.1 in.) square on the specimen surface. Second, the scales formed on the aluminized specimens have varying aluminum gradients. For TDNiCr-4.9Al the aluminum concentration slowly decreased from 4.9 weight percent at the surface to a minimum of about 2 weight percent at the center of the specimen. For the TDNiCr-5.8Al, the aluminum concentration dropped to zero some 100 μm from the surface. It is conceivable that depletion of aluminum in the alloys containing the higher concentrations or nonuniformity

of aluminum in these specimens could have resulted in the appearance of chromium-containing oxides in the scales. This point is discussed in greater detail in the next section.

Electron Probe Microanalysis

Several oxidized specimens of TDNiCr, NiCrAl, TDNiCrAl, and TDNiCrAlY have been examined by electron microprobe analysis. Profiles for chromium, nickel, aluminum, and thorium were obtained across the scale and the underlying alloy. Since the scales on these alloys are approximately 1 to 4 μm thick, whereas the resolution of the electron probe is three microns, no details of the scale composition variation could be obtained. For the TDNiCr (Specimen 30), cyclically oxidized at 1204°C (2200°F) under 1.33×10^3 N/m^2 (10 torr) air, chromium was the only metallic constituent that could be detected in the scale; for the TDNiCr-5.8Al sample oxidized under the same conditions, aluminum was the sole metallic constituent that could be detected in the scale. In both, these elements appeared simply as peaks at the specimen surface.

The concentrations of nickel and thorium in all specimens were found to be uniform across the alloy. The chromium concentrations of the TDNiCr-5.8Al and Ni-Cr-5.8Al alloys were also uniform, in contrast to the gradient from 20 at the center to 14 weight percent chromium at the surface which was present after aluminizing but prior to the oxidation test.

Concentration profiles for aluminum in TDNiCr-5.8Al, TDNiCr-4.9Al, Ni-Cr-5.8Al, and TDNiCrAlY before and after oxidation at 1204°C (2200°F) are presented in Figures 23 through 26. The data in Figures 23 and 24 were obtained from specimens cycled 100 times for 30 minutes at temperature under 1.33×10^3 N/m^2 (10 torr) air while the TDNiCrAlY and NiCrAl specimens of Figures 25 and 26 were isothermally tested for 50 hours at the same oxygen partial pressure.

A time of 50 hours at 1204°C (2200°F) is seen to be sufficient to produce a nearly homogeneous aluminum level in both the 5.8 and 4.95 weight percent aluminum alloys which initially contained relatively sharp concentration gradients. The low aluminum levels in the samples oxidized for 50 hours are probably insufficient to produce a protective alumina scale if the scale already formed is defected. The manner of change from the initial sharp to the final homogeneous profile is not known. It is apparent, however, that optimization of oxidation resistance and mechanical properties of TDNiCr aluminized by a pack process will require additional evaluation of the pack conditions. For example, it may be possible to obtain higher concentrations of aluminum at the surface and shallower gradients (more uniform composition) while still maintaining satisfactory fabricability.

As shown in Figure 26, the TDNiCrAlY specimens somewhat uniform aluminum concentration of about 5.5 weight percent before testing, was reduced to 4.2 to 4.6 weight percent after oxidation at 1204°C (2200°F) for 50 hours. It is not known if this lower level of aluminum would be sufficient to form a protective Al_2O_3 scale if the original scale were defected after a 50-hour test.

As mentioned above, based on the data contained in Figures 23 and 24, an analysis has been performed on the distribution of aluminum in the samples of TDNiCr-5.8Al and TDNiCr-4.95Al before and after oxidation. The TDNiCr-5.8Al specimens contained 2.105×10^{-3} g/cm^3 of aluminum before oxidation and 1.232×10^{-3} g/cm^3 after

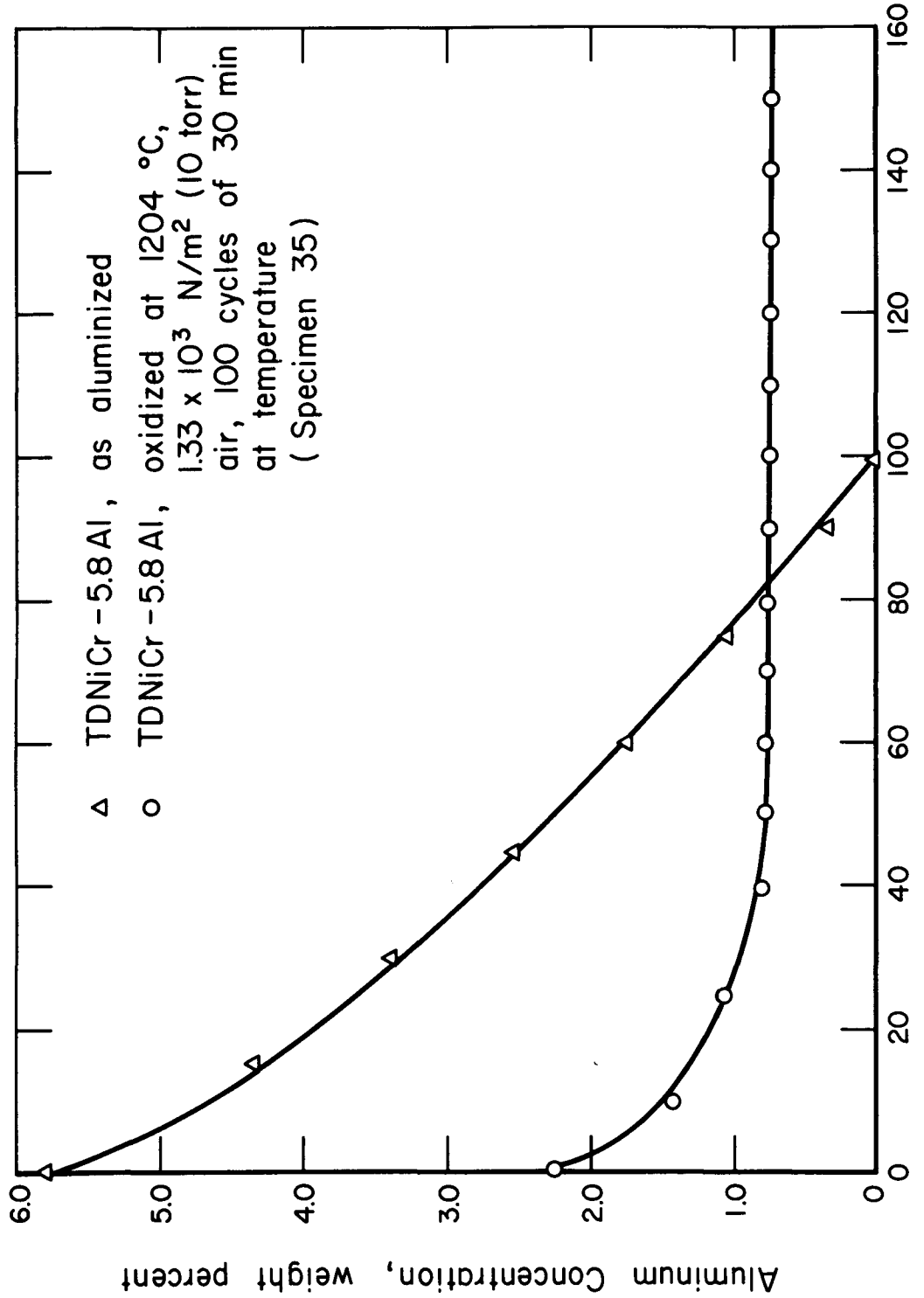

FIGURE 23. CONCENTRATION PROFILES FOR ALUMINUM IN TDNiCr-5.8Al BEFORE AND AFTER CYCLIC OXIDATION AT 1204°C (2200°F) FOR 50 HOURS

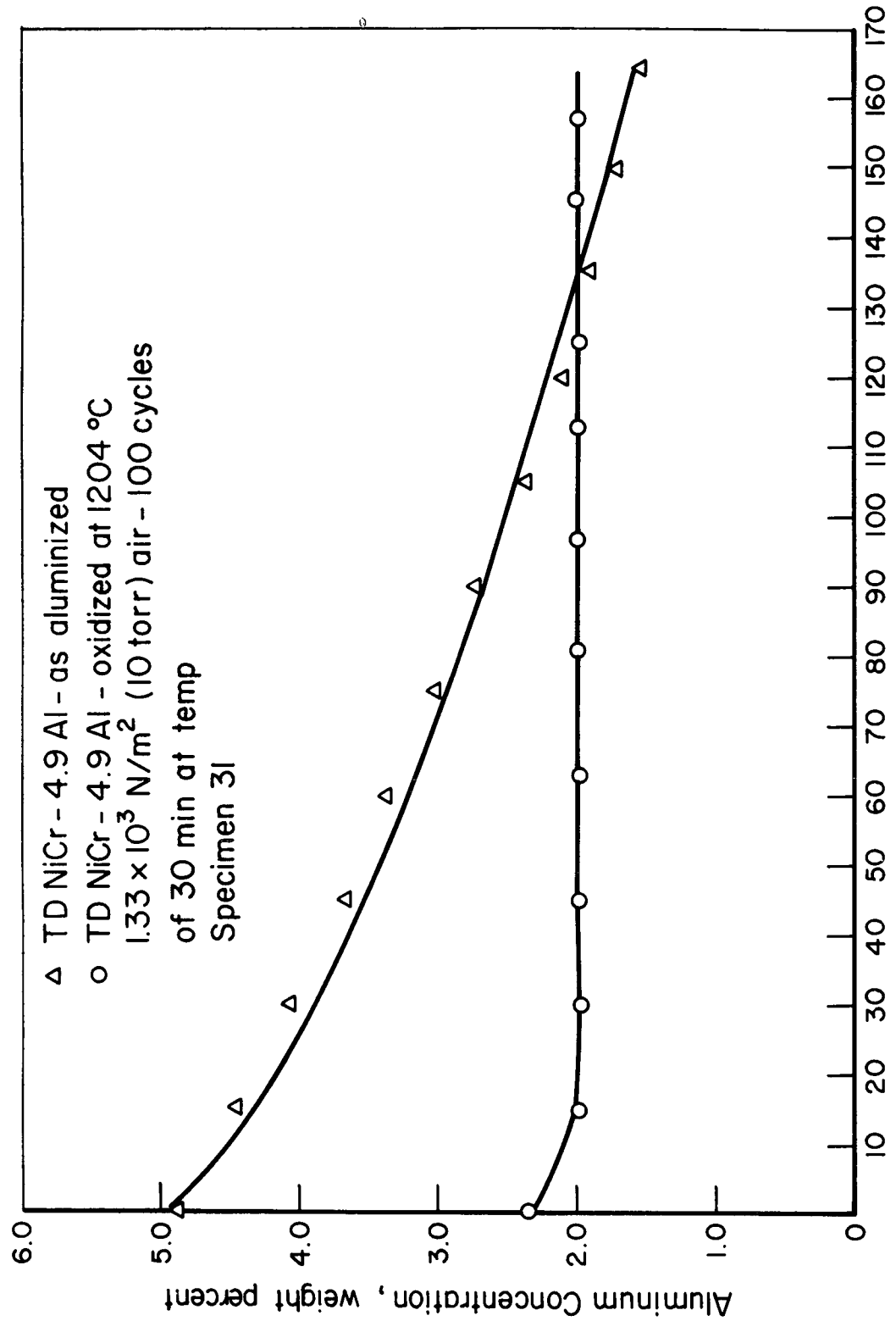

FIGURE 24. CONCENTRATION PROFILES FOR ALUMINUM IN TDNiCr-4.95Al BEFORE AND AFTER CYCLIC OXIDATION AT 1204°C (2200°F) FOR 50 HOURS

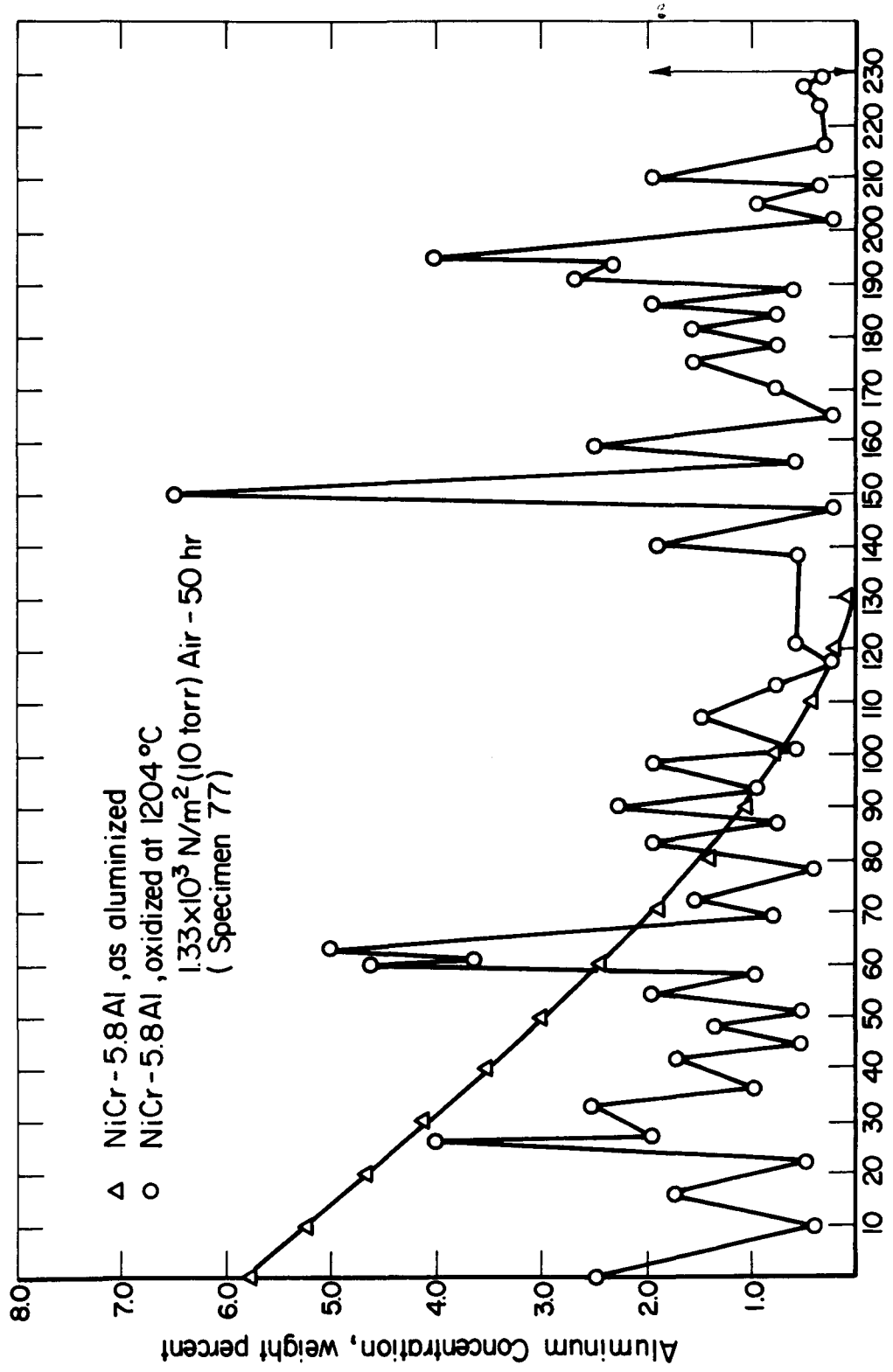

FIGURE 25. CONCENTRATION PROFILES FOR ALUMINUM IN Ni-20Cr-5.8Al BEFORE AND AFTER OXIDATION AT 1204°C (2200°F) FOR 50 HOURS

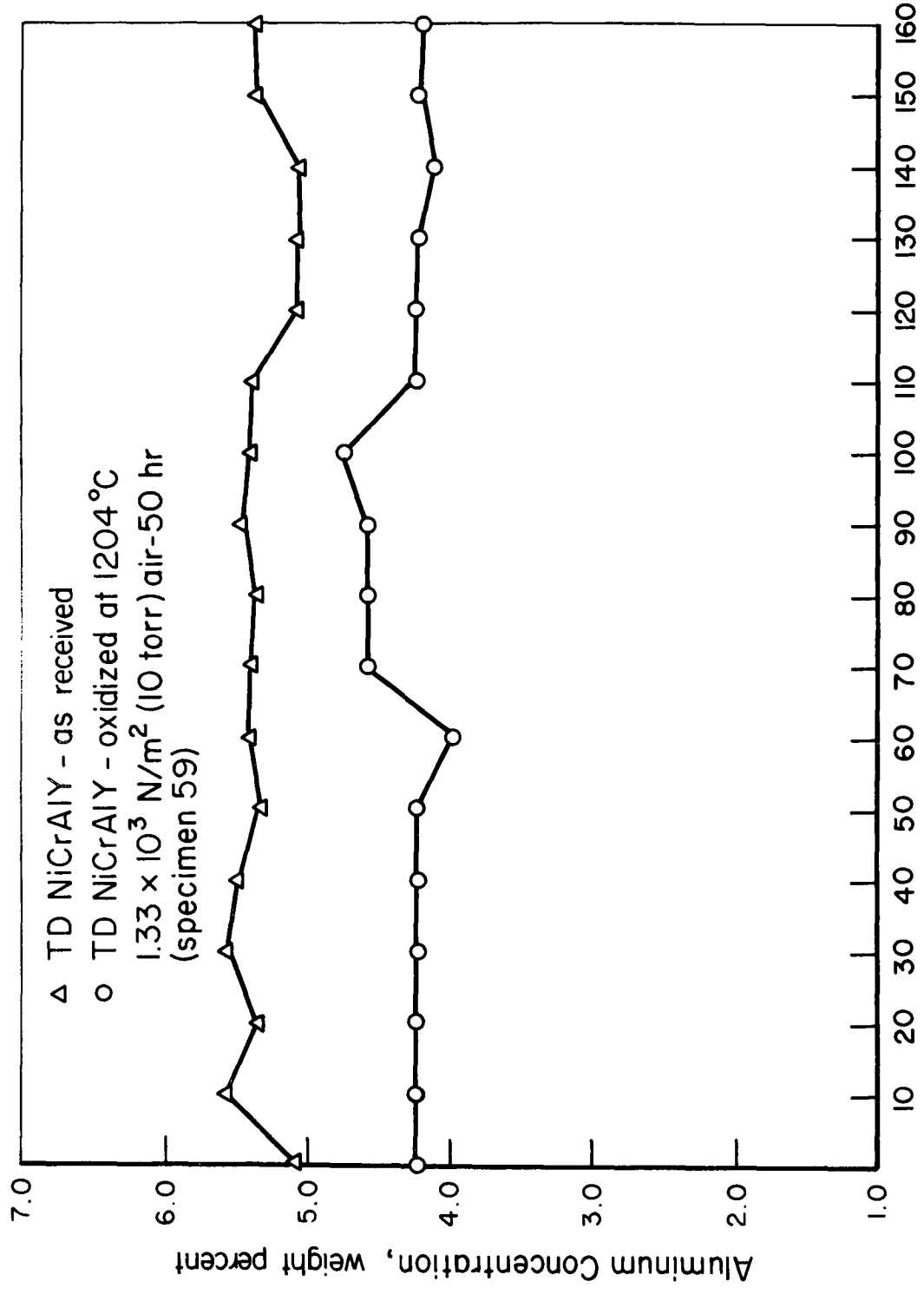

FIGURE 26. CONCENTRATION PROFILES FOR ALUMINUM IN TDNiCrAlY BEFORE AND AFTER ISOTHERMAL OXIDATION AT 1204°C (2200°F) FOR 50 HOURS

oxidation. Thus, the oxidation appears to have consumed 0.873 mg/cm^3 of aluminum, and if this was consumed as Al_2O_3, it corresponds to an oxygen gain of 0.773 mg/cm^2. As shown in Figure 18, this is nearly identical with the weight gain measured for TDNiCr-5.8Al after 100 cycles.

If the total weight of Al_2O_3 formed is 1.646 mg/cm^2 and the density of Al_2O_3 is taken as 3.9 g/cm^3, the thickness of the scale formed is estimated to be 4.22 μm. However, the external scale on this specimen is only about 2 μm. Examination of a cross section of this specimen (Figure 32b) reveals a large concentration of internal oxide immediately beneath the oxide surface. This is believed to be Al_2O_3 particles present in sufficient concentration to account for the total aluminum content of the TDNiCr-5.8Al. Evidence for the presence of internal Al_2O_3 is obtained from the electron-probe aluminum profiles, that show high aluminum peaks at distances well below the outer scale.

For TDNiCr-4.95Al, analysis of the concentration profiles given in Figure 24 indicates that the alloy contained 4.196 mg/cm^2 of aluminum before oxidation and 2.847 mg/cm^2 after oxidation. The 1.349 mg/cm^2 of aluminum which was consumed corresponds to 1.195 mg/cm^2 of oxygen absorbed. The total weight of 2.544 mg/cm^2 is equivalent to an Al_2O_4 scale of 6.5 μm. The actual scale thickness appears to be about 4 μm. As seen in Figure 31a, a second phase appears to be present in the scale formed on TDNiCr-4.95Al. The probe results on this specimen after oxidation, confirmed the presence of chromium in the surface of the scale formed on this specimen. As also seen in Figure 31a there is no evidence for internal oxidation in the 4.95 aluminum alloy. Thus, the scale on the surface of this alloy represents about 0.85 mg/cm^2 of oxygen absorbed. If the remainder has spalled, this means that 0.76 mg/cm^2 of scale has spalled, which would result in an apparent weight gain of 0.44 mg/cm^2. This is very close to the weight gain measured after completion of the 90-cycle test shown in Figure 17 for TDNiCr-4.9Al. As pointed out above, evidence for the suggestion that spallation has occurred in cyclic oxidation of this specimen is obtained from comparison of the isothermal and cyclic kinetic data (see Figures 13 and 17).

Metallography

Figure 27 shows a cross section of a specimen of Ni-20Cr cyclically oxidized at a temperature of 1204°C (2200°F) for 50 hours in air at 1.01 x 10^5 N/m^2 (760 torr) pressure (Specimen 29). By the end of the test, the specimen was severely bent, and this is generally indicative of an irregular oxidation front with penetrations into the metal and a degree of asymmetry with respect to the opposite faces of the specimen. As can be seen, there are indeed gross irregularities in the oxide/metal interface, but it proved to be difficult to establish positively the existence of asymmetry. The small gray particles in the metal are chromium oxide, Cr_2O_3, formed during manufacture; there appeared to be no additional internal oxidation during the test.

Figure 28a shows the surface of a TDNiCr specimen cyclically oxidized under the same conditions (Specimen 27). The surface markings lie parallel to the sanding grooves on the original metal surface; the white patches are regions where oxide has separated from the metal surface during the last cooling to room temperature. Figure 28b shows a detail of the surface: cracks running in the oxide along the high points of the metal surface can be seen along with a limited amount of associated scale separation. It is interesting that these cracks do not lead to a greater degree of scale spallation. Figure 28c shows a cross section of a similar region: the association of the cracks with

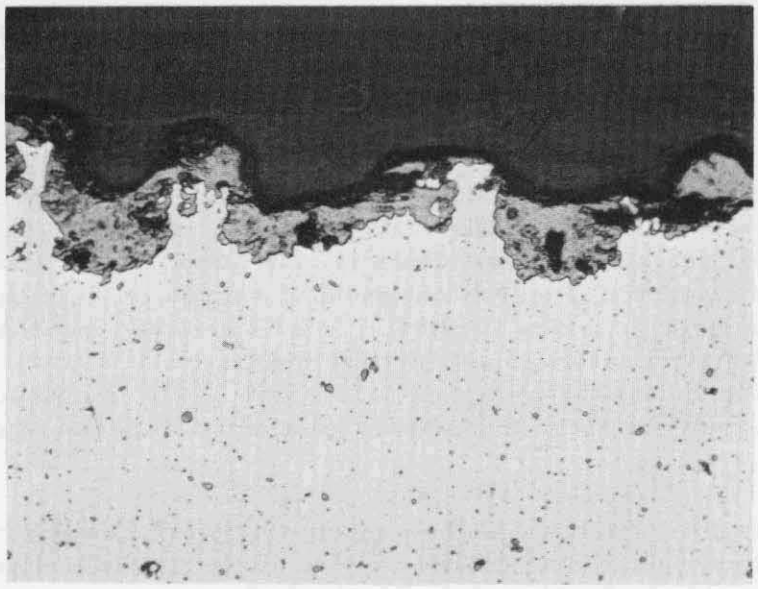

FIGURE 27. CROSS SECTION OF THE METAL/OXIDE INTERFACE FROM A SPECIMEN OF Ni-20Cr CYCLICALLY OXIDIZED AT 1204°C (2200°F) FOR 50 HOURS IN AIR AT 1.01×10^5 N/m^2 (760 TORR) PRESSURE

the high points on the metal surface is apparent, but it is clear that the "cracks" are related rather to the mode of growth of the oxide over the sharp corners (this has sometimes been referred to as "cruciform" oxidation or "edge effect" when observed at the corners of coupon specimens) than to mechanical fracturing of the oxide due to cycling stresses. This accounts for the very limited propagation into the surrounding oxide.

Cyclic oxidation of TDNiCr at 1204°C (2200°F) in air at 1.33×10^3 N/m^2 (10 torr) pressure for 50 hours (Specimen 30) produces a thinner scale with no apparent cracking. Although in some areas the scale is uniform, more typically it has the appearance shown in Figure 29, with local regions of oxide separated by regions in which the oxide is very thin or absent. This difference is rather difficult to rationalize.

Figure 30a shows the surface of a specimen of TDNiCr-4.95Al oxidized cyclically at 1204°C (2200°F) in air at 1.01×10^5 N/m^2 (760 torr) pressure for 50 hours (Specimen 28). Again, the bright regions are metal, corresponding to regions where the scale has spalled during the last cooling to room temperature. The darker regions are areas of thicker oxide, and it appears that possibly the spalled oxide may have come from these thicker areas. Figure 30b is a cross section, in which a reasonably uniform oxide film adhering to the metal surface is shown. Some parts of this film separated during metallographic preparation. Beneath the oxide, a region of relatively fine-grained metal can be seen. This is shown in more detail in Figure 30c, which also shows the presence of bright-appearing points in the adherent scale. This effect, seen in other scales formed on alloys containing dispersed phases, possibly may be due to the incorporation of dispersoid in the oxide. However, it may also be an artifact caused by the intrusion of polishing medium.

Figure 30d shows a locally thicker region of oxide, presumably similar to those shown in Figure 30a, and the generally looser appearance of the oxide is apparent. Figure 30e shows another region: scale has apparently fractured from the metal surface

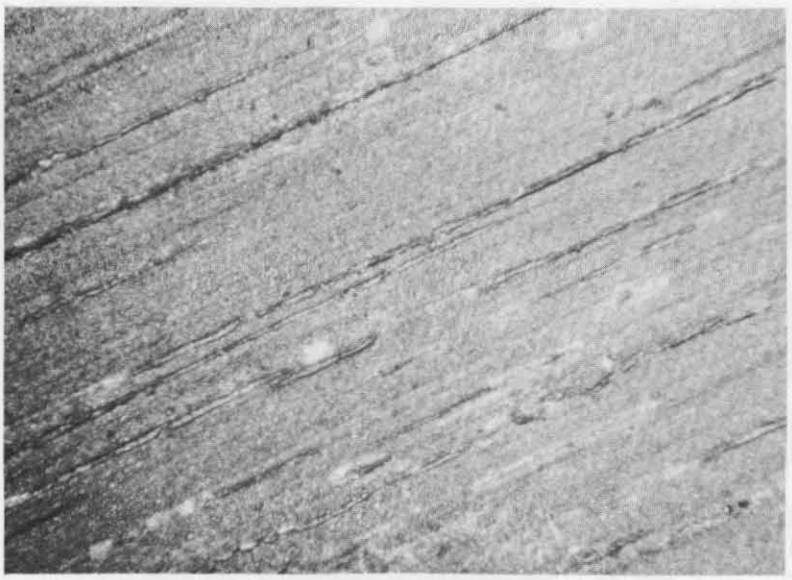

80X Oblique Illumination

FIGURE 28a. SURFACE OF A TDNiCr SPECIMEN CYCLICALLY OXIDIZED AT 1204°C FOR 50 HOURS IN AIR AT 1.01×10^5 N/M^2 (760 TORR) PRESSURE

The light regions are bare metal exposed by the spalling of the oxide on the final cooling cycle. The darker lines are thicker oxide and cracks, and lie parallel to the grinding marks on the original surface.

450X Oblique Illumination

FIGURE 28b. DETAIL OF THE SCALE SURFACE SHOWN IN FIGURE 28a

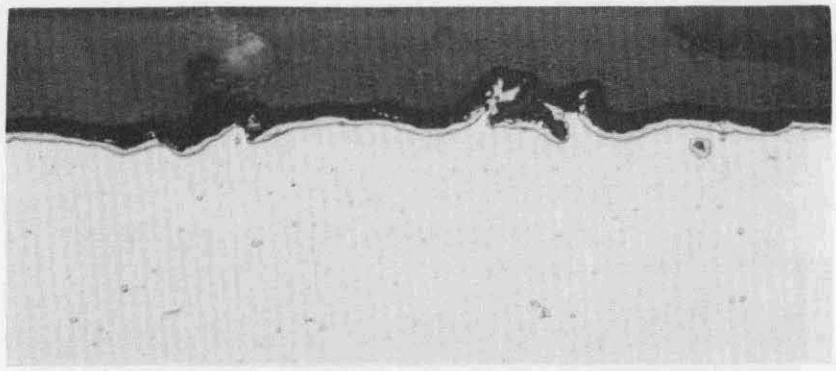

500X

FIGURE 28c. CROSS SECTION OF THE SAME SPECIMEN

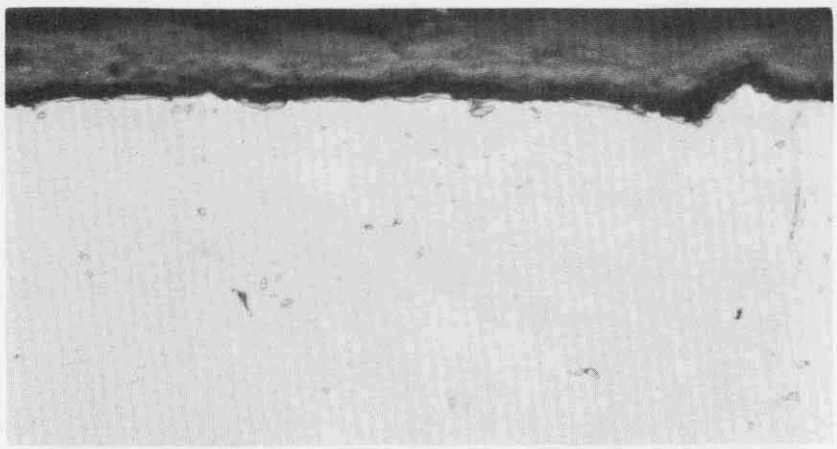

500X

FIGURE 29. CROSS SECTION OF A SPECIMEN OF TDNiCr CYCLICALLY OXIDIZED AT 1204°C IN AIR AT 1.33×10^3 N/M^2 (10 TORR) PRESSURE FOR 50 HOURS

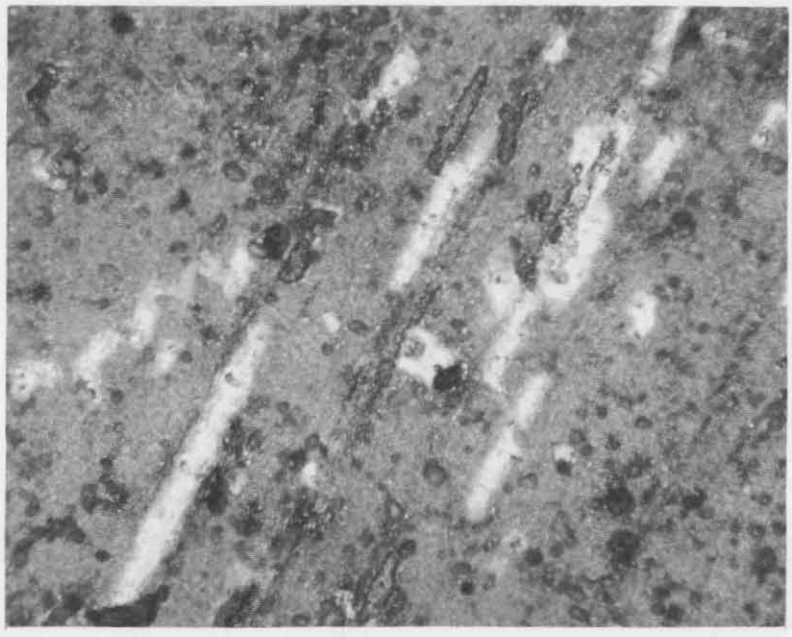

80X Oblique Illumination

FIGURE 30a. SURFACE OF A SPECIMEN OF TDNiCr - 4.95 Al CYCLICALLY OXIDIZED AT 1204°C IN AIR AT 1.01 X 10^5 N/M^2 (760 TORR) PRESSURE FOR 50 HOURS

The bright regions are bare metal from which the scale has spalled on the final cooling to room temperature; the darker regions are thicker oxide. Both lie parallel to the original grinding marks.

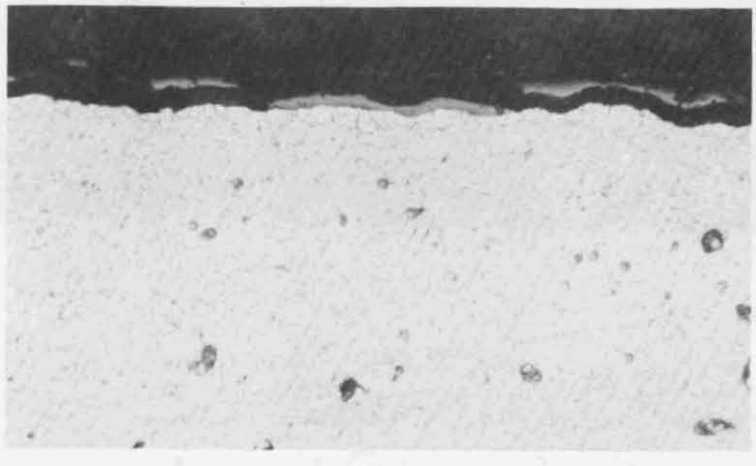

500X Etched

FIGURE 30b. CROSS SECTION OF THE SPECIMEN SHOWN IN FIGURE 30a

Note the fine-grained layer of metal immediately beneath the oxide.

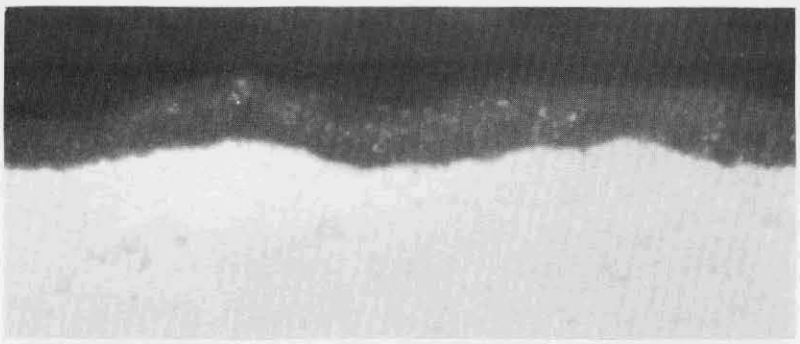

2000X Oil Immersion

FIGURE 30c. DETAIL OF THE INTERFACE FROM FIGURE 30b SHOWING THE FINE-GRAINED LAYER

Note the bright points visible in the oxide layer.

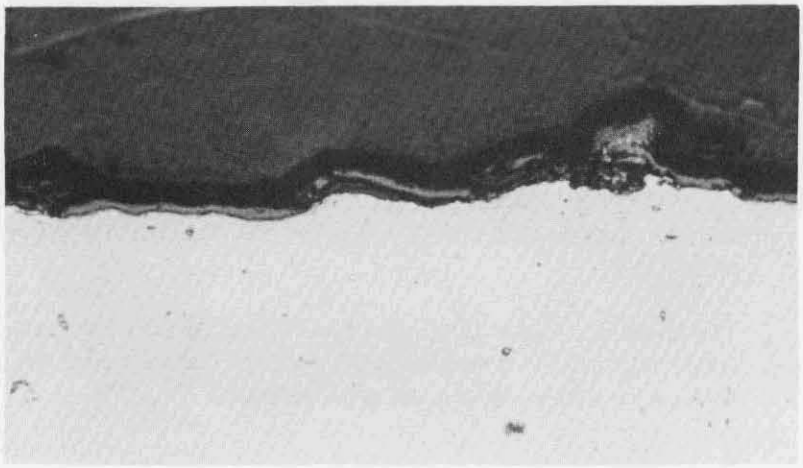

500X

FIGURE 30d. ANOTHER SECTION FROM THE SAME SPECIMEN, UNETCHED, SHOWING A LOCAL OXIDE GROWTH

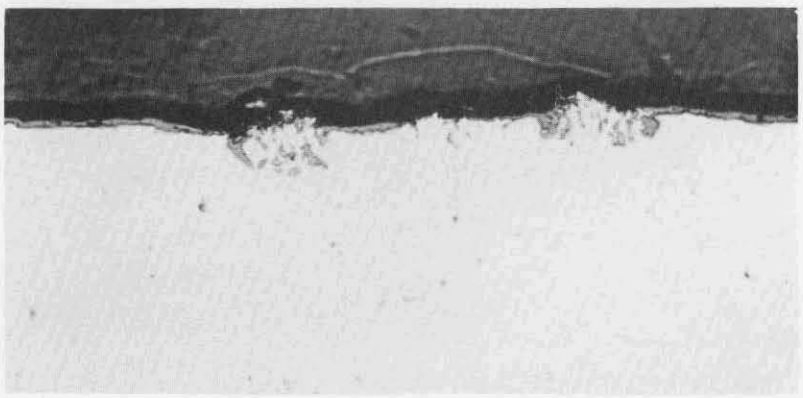

500X

FIGURE 30e. ANOTHER SECTION FROM THE SAME SPECIMEN, UNETCHED, SHOWING INTERNAL OXIDATION, APPARENTLY BENEATH HIGH SPOTS ON THE METAL SURFACE

at some time during the cyclic test, and has reduced the aluminum content of the substrate to the point at which internal oxidation can take place. Note that the internal oxidation shows signs of healing. It is also notable that these regions correspond to metal prominences rather than depressions, so either the rate of metal recession in these regions has been rather less than in the surrounding regions (which seems unlikely) or these regions correspond again to the high spots on the as-sanded metal surface. The marks in Figure 30a are in fact parallel to the sanding grooves.

Cyclic oxidation of a similar specimen at 1204°C (2200°F) in air at 1.33×10^4 N/m^2 (10 torr) pressure for 50 hours (Specimen 31) produces generally similar results. Figure 31a shows the generally uniform scale with a thin area of a different oxide on the outer surface, presumably $NiAl_2O_4$ spinel. Figure 31b shows a region where clearly the scale has fractured during the cyclic test, and a new protective layer is developing. Figure 31c shows a region where again the oxidation has depleted the aluminum content to the point at which internal oxidation of aluminum can proceed. The healing nature of the internal oxidation is apparent.

Figure 32a shows a cross section of a specimen of TDNiCr-5.8Al oxidized cyclically at 1204°C (2200°F) in air at 1.33×10^3 N/m^2 (10 torr) pressure (Specimen 35). The majority of the surface is covered with a uniform oxide layer, but local regions, again apparently corresponding to the high points on the as-prepared surface, show evidence of scale fracturing; and this again results in internal oxidation of the aluminum. Beneath the whole surface lies a band of pores or internal oxide, and it is extremely difficult on the basis of metallography to decide which they are. Figure 32b shows a detail at high magnification: the large dark areas immediately below the interface to the right are certainly internal oxidation of the aluminum; but the remaining features appear bright, which strongly suggests that they are in fact voids. Furthermore, internal oxide particles nearly always show an elongation in the direction of the oxygen flux, and these features appear to be equiaxed.

At 1093°C (2000°F) these "voids" are a much more common feature of the oxidation. Figure 33 shows a cross section of a specimen of TDNiCr-4.3Al oxidized isothermally at 1093°C (2000°F) in air at 1.01×10^5 N/m^2 (760 torr) pressure for 50 hours (Specimen 15): There is a thin, substantially uniform layer of oxide, and a relatively wide band of pores in the metal. These pores are definitely a consequence of oxidation, and not of the aluminizing treatment since they are absent in the as-aluminized specimens prior to oxidation. Figure 34 shows an exactly similar result for a specimen of TDNiCr-4.95Al oxidized isothermally under the same conditions (Specimen 22), and Figure 35 a specimen of TDNiCr-5.8Al (Specimen 33). Here the thin adherent scale has separated in places during metallographic preparation.

It is difficult to explain the orgin of these "voids". The thin adherent scale layer on all three specimens, presumably Al_2O_3, appears to be approximately 2 μm thick. This is equivalent to an oxygen absorption of 0.37 mg/cm^2; as seen from Figure 18 this agrees very well with the observed weight gain. The aluminum content of the scale is then 0.41 mg/cm^2, and if this is expressed in terms of "voids" in the matrix which has a density of approximately 7.9 g/cm^3, the volume of void formed will be 5.2×10^{-5} cm^3/cm^2. Examination of Figure 35 suggests that, very roughly, there are 3.25×10^6 voids beneath each cm^2 of surface, with an average diameter of about 2×10^{-4} cm. This corresponds to a total void volume of 1.3×10^{-5} cm^3/cm^2, which, in view of the crudities of the calculation, is very close to the required value.

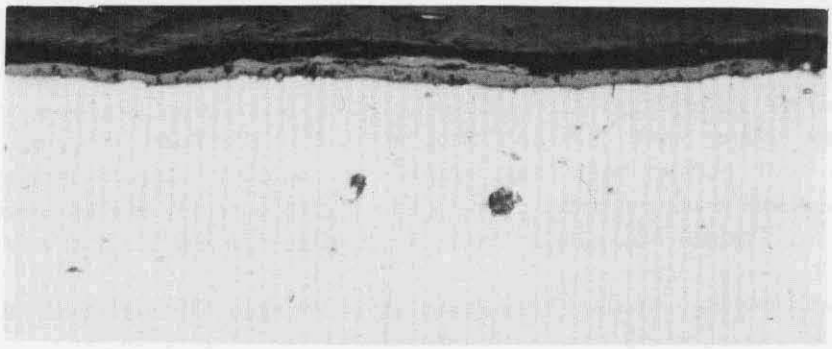

500X

FIGURE 31a. CROSS SECTION OF A SPECIMEN OF TDNiCr - 4.95 Al CYCLICALLY OXIDIZED AT 1204°C IN AIR AT 1.33 X 10^3 N/M^2 (10 TORR) PRESSURE FOR 50 HOURS

Note the outer layer of a second oxide (presumably $NiCr_2O_4$) at the center of the micrograph.

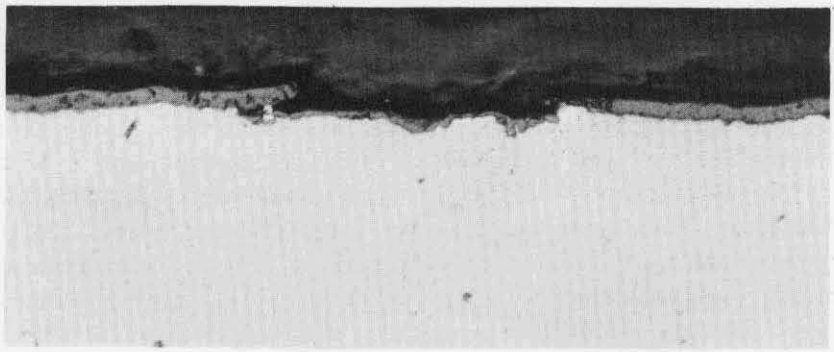

500X

FIGURE 31b. ANOTHER SECTION OF THE SAME SPECIMEN, SHOWING A REGION WHERE SCALE FAILURE HAS OCCURRED DURING THE TEST AND A NEW PROTECTIVE LAYER HAS DEVELOPED

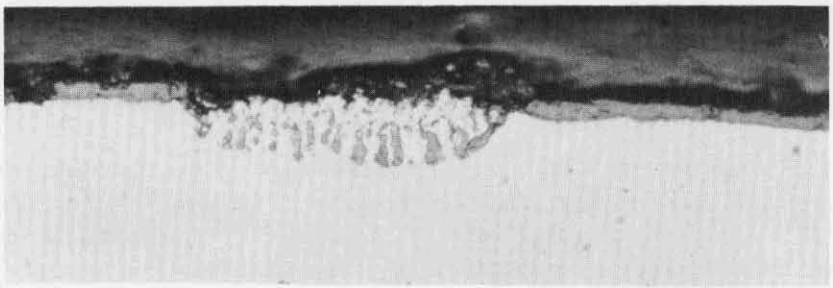

500X

FIGURE 31c. ANOTHER SECTION FROM THE SAME SPECIMEN, SHOWING INTERNAL OXIDATION BENEATH A BREAKDOWN OF THE PROTECTIVE SCALE

The internal oxidation shows signs of healing.

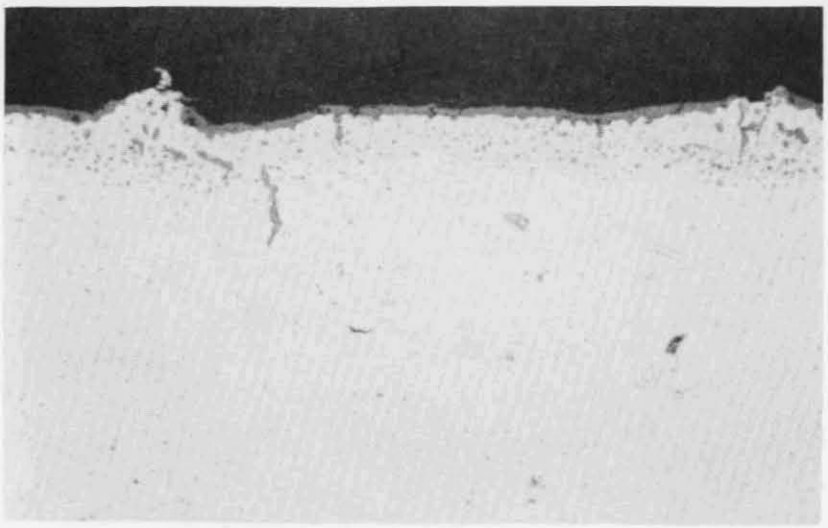

500X

FIGURE 32a. CROSS SECTION OF A SPECIMEN OF TDNiCr – 5.8 Al CYCLICALLY OXIDIZED AT 1204°C IN AIR AT 1.3×10^3 N/M^2 (10 TORR) PRESSURE FOR 50 HOURS, SHOWING BREAKDOWN OF THE OXIDE OVER HIGH SPOTS, AND ASSOCIATED INTERNAL OXIDATION

Note the band of voids or internal oxide particles in the metal below the oxide.

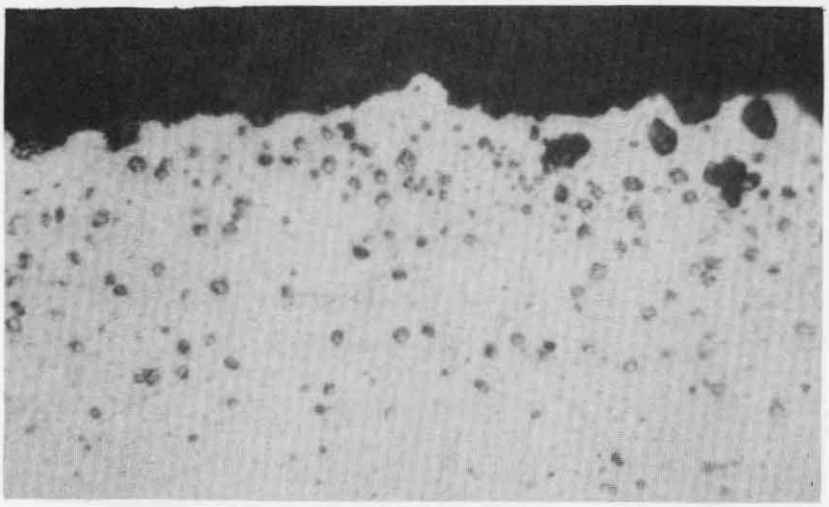

2000X Oil Immersion

FIGURE 32b. DETAIL OF THE METAL/OXIDE INTERFACE FROM THE SPECIMEN SHOWN IN FIGURE 32a.

The large dark areas in the metal immediately below the interface in the upper right are internal oxide. The bright appearance of the remaining features strongly suggests that they are voids.

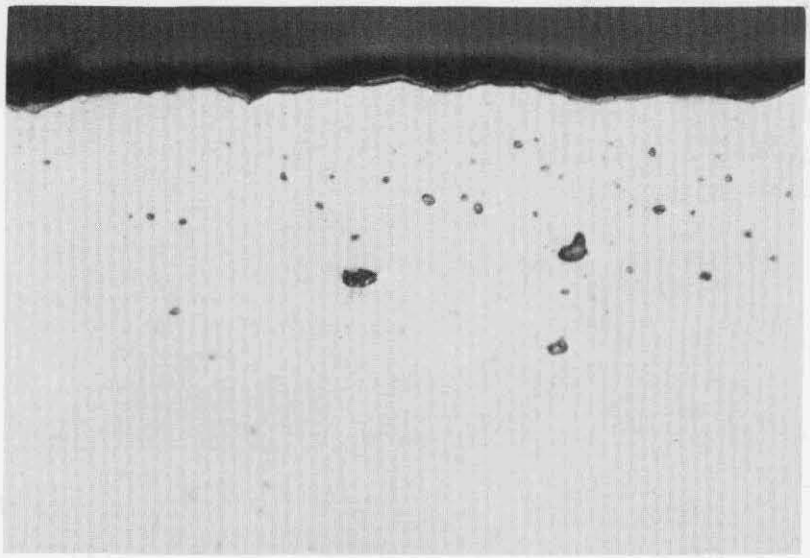

500X

FIGURE 33. CROSS SECTION OF A SPECIMEN OF TDNiCr - 4.3 Al OXIDIZED ISOTHERMALLY AT 1093°C (2000 F) IN AIR AT 1.01 X 10^5 N/M^2 (760 TORR) PRESSURE FOR 50 HOURS

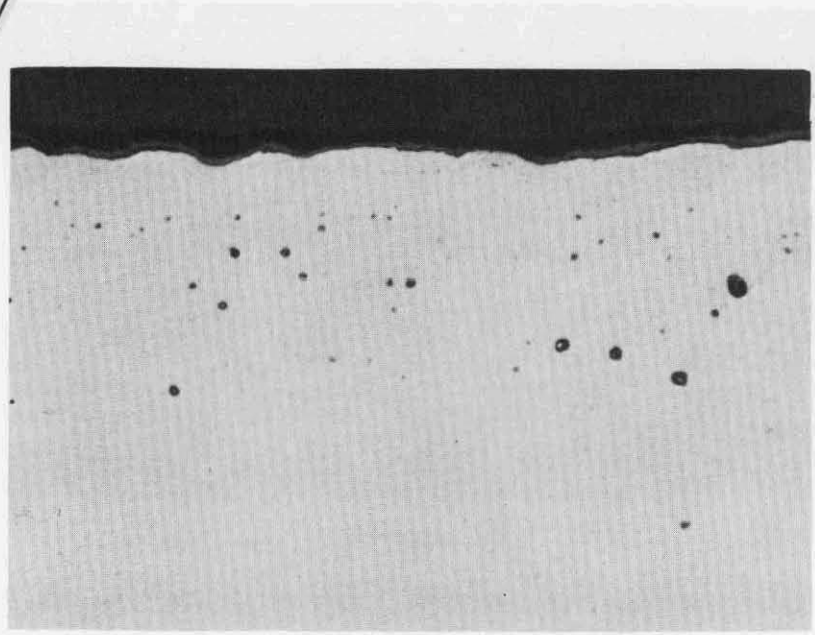

500X

FIGURE 34. CROSS SECTION OF A SPECIMEN OF TDNiCr - 4.95 Al OXIDIZED ISOTHERMALLY AT 1093°C IN AIR AT 1.01 X 10^5 N/M^2 (760 TORR) PRESSURE FOR 50 HOURS

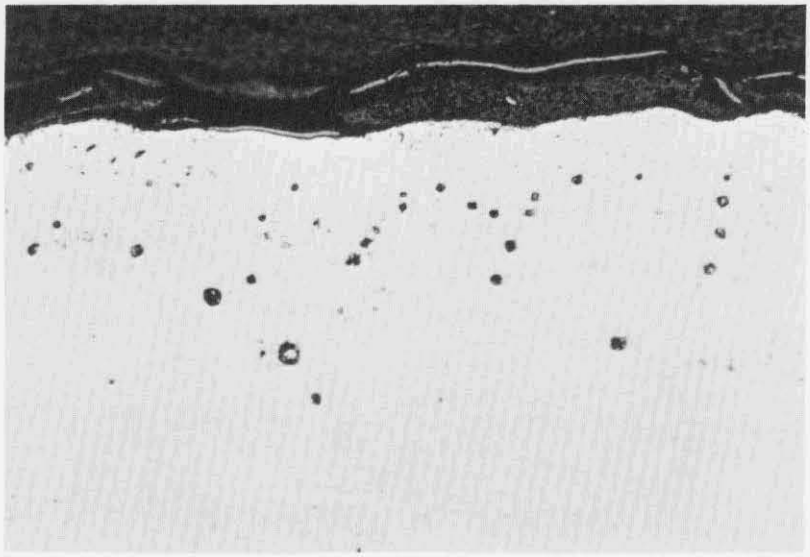

500X

FIGURE 35. CROSS SECTION OF A SPECIMEN OF TDNiCr-5.8Al OXIDIZED ISOTHERMALLY AT 1093°C IN AIR AT 1.01×10^5 N/m^2 (760 TORR) PRESSURE FOR 50 HOURS

The depth of the pore-containing region in Figures 33, 34, and 35 is approximately 50 μm, well within the diffusion layer, and the total aluminum content within this region is very approximately 1.5 mg/cm^2 of surface, approximately four times that consumed by the oxidation.

It appears therefore that all the data are qualitatively consistent with the view that the pores result from the removal of aluminum by the oxidation reaction, and this is consistent with the fact that aluminum diffusivities in the alloys are a factor of three or so higher than the rate of diffusion of chromium or nickel.

Attempts were made to measure the change in total thickness of the various alloys after oxidation. The oxidized specimens were mounted in epoxy next to a piece of the material which was sectioned from each coupon prior to oxidation. Care was taken to mount the specimens such that the plane of the sheets was normal to the mount face. The thicknesses of the oxidized and unoxidized specimens were measured by a traversing filar microscope at 200X, by using the traverse on a Tukon microhardness tester, with the specimen magnified 200X, and by measuring the thicknesses of the oxidized and unoxidized specimens from micrographs of the entire cross section taken at 600X. None of these techniques proved successful because the decrease in thickness was less than the sensitivity of the measuring techniques, i.e., < 10 μm. This is illustrated in Figure 36, which compares at 600X, micrographs of oxidized and unoxidized specimens of TDNiCr. The surface asperities, resulting from the belt-sanded finish cause changes in the effective thickness in excess of those due to oxidation.

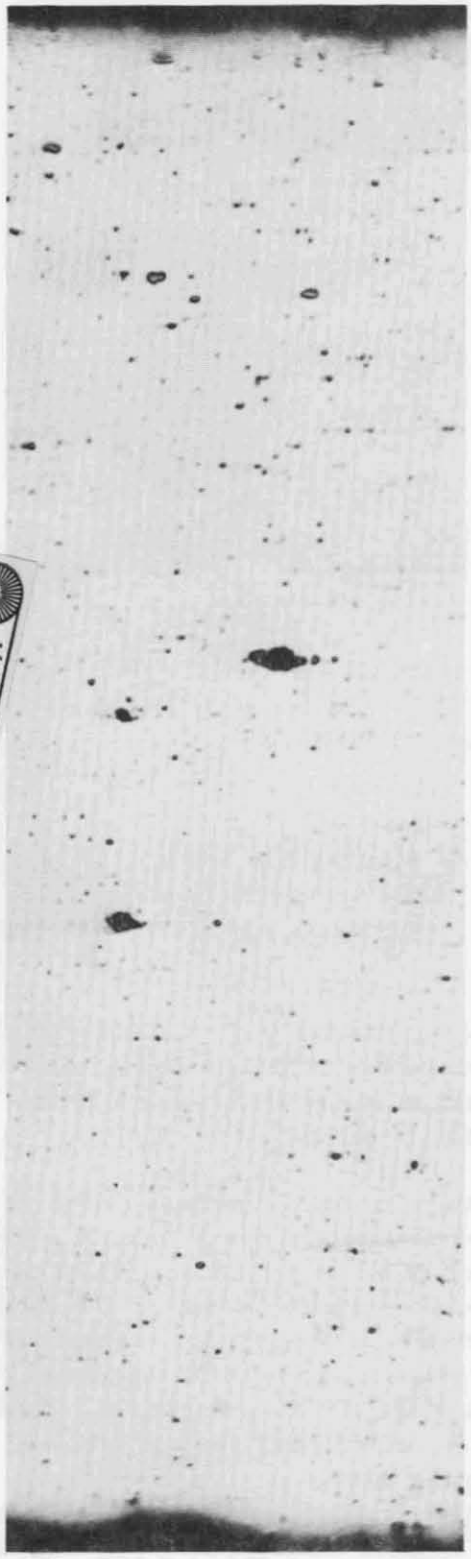

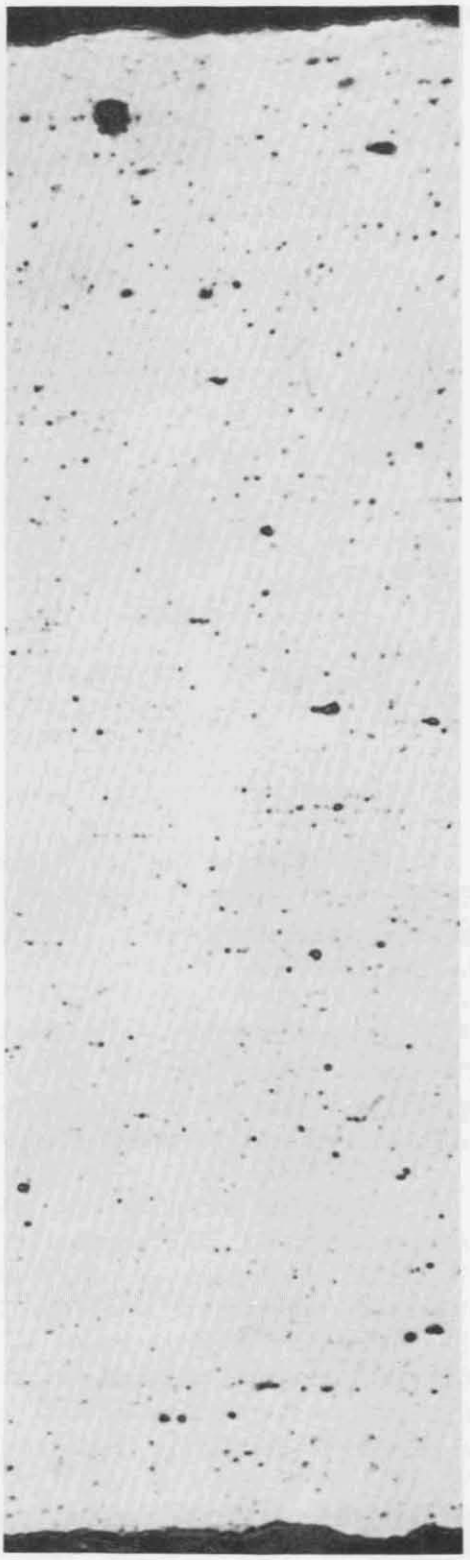

(a) Unoxidized

(b) Oxidized 50 hr at 1093°C (2000°F) in 1.01×10^5 N/m^2 (760 torr) air

FIGURE 36. CROSS SECTION OF TDNi-Cr BEFORE AND AFTER ISOTHERMAL OXIDATION, 600X

IV. MECHANICAL PROPERTIES

Bend Tests

To obtain some measure of forming limits for the various aluminized alloys produced in this investigation, a series of constrained bend tests were performed on specimens 2.54 cm (1 in.) long and 0.63 cm (0.25 in.) wide. The constrained bend test consists of forcing the bend sample to assume a sucessively sharper bend radius by bending between two matching dies, the male die having a 75 degree included angle, the tip radius of which is decreased progressively during the test. The degree of bending the sample can withstand without cracking (as observed under 10X magnification) is reported as the minimum bend radius. The minimum bend radius is expressed in terms of sheet thickness and is obtained by dividing the die radius of the last successful bend by the sample thickness to give a "T" value.

With the grinding scratches transverse to the bend direction, bend tests were performed on a series of samples consisting of TDNiCr without aluminum and containing 4.3, 4.9, and 5.8 weight percent aluminum. The samples were bent through a series of dies with radii of 9.52 mm (3/8 in.), 6.35 mm (1/4 in.), 4.76 mm (3/16 in.), 3.17 mm (1/8 in.), 2.38 mm (3/32 in.), 1.59 mm (1/16 in.), 1.19 mm (3/64 in.), 0.79 mm (1/32 in.), 0.40 mm (1/64 in.), and a "sharp" die, which is considered zero radius. Both the as-received TDNiCr and TDNiCr-5.8Al were successfully bent through the entire set of dies; cracks appeared only after bending in the "sharp" die. Thus, a "T" value of 1.2 was determined for these two alloys. Duplicate specimens of TDNiCr-4.3Al cracked on bending through the 0.40-mm (1/64 in.) die while the TDNiCr-4.9Al samples broke in two at the 0.40-mm (1/64 in.) and 0.79-mm (1/32 in.) dies. From these results the T values are 2.4 for TDNiCr-4.3Al and 2.3 or 3.5 for TDNiCr-4.9Al. The high T values for the TDNiCr-4.9Al alloy is in accord with the fact that this alloy contained a shallow aluminum concentration gradient with some aluminum even at the center of the specimens. The other aluminized alloys had aluminum-free sections in the mid-region of the test samples.

In addition to the above specimens, an as-received TDNiCrAlY specimen produced by Fansteel was subjected to the bend test. The sample broke in two at the 3.17-mm (1/8 in.) die, which gives a "T" value for this alloy of 12.50. This high "T" value suggests considerably less fabricability in the TDNiCrAlY alloy, which has a uniform aluminum concentration of 5.5 weight percent, as compared with the alloys aluminized by the pack process, which have a high aluminum concentration only in the near-surface region.

Bend tests were also performed on oxidized samples of TDNiCr, TDNiCr-5.8Al, and the Fansteel TDNiCrAlY, all of which were tested isothermally for 50 hours at 1204°C (2200°F) under 1.01×10^5 N/m^2 (760 torr) air. The "T" values obtained were 0.2, 2.4, and 3.9 for TDNiCr, TDNiCr-5.8Al, and TDNiCrAlY, respectively. In these tests, the TDNiCrAlY broke at the 1.19-mm/(3/64 in.) die, the TDNiCr-5.8Al cracked at the 0.40-mm (1.64 in.) die and the TDNiCr could be bent without cracking through the entire series of dies employed.

Tensile Tests

Room temperature tensile tests were made on TDNiCr and aluminized TDNiCr-5.8Al. Duplicate tests were performed both parallel and transverse to the rolling direction at a strain rate of 0.01 min^{-1}. The results in Table 4 indicate that aluminizing the TDNiCr caused no appreciable effect on its yield strength. The decrease in ultimate strength in the aluminized specimens, about 55 MN/m^2 (8,000 psi), was caused by the somewhat lower ductility. All specimens failed at maximum load and the work-hardening characteristics were similar in the two conditions.

TABLE 4. ROOM-TEMPERATURE MECHANICAL PROPERTIES OF TDNiCr AND ALUMINIZED TDNiCr (5.8Al AT SURFACE)

Orientation	0.2% Y.S. MN/m^2	0.2% Y.S. psi	UTS MN/m^2	UTS psi	% Total Elong.[a]
			TDNiCr		
Longitudinal	542	78,500	783	113,500	11.8
Longitudinal	526	76,500	800	116,000	13.6
Transverse	510	74,000	793	115,000	17.7
Transverse	-	-	759	110,000	20.0
			Aluminized TDNiCr		
Longitudinal	545	79,000	756	109,500	9.7
Longitudinal	543	78,800	724	105,000	7.4
Transverse	546	79,300	703	102,000	7.9
Transverse	526	76,500	711	103,000	10.2

(a) Elongation in 1-inch gage length.

DIFFUSION OF ALUMINUM AND CHROMIUM IN TDNiCr AND Ni-20Cr

Introduction

In an early study, Fleetwood[5] reported that diffusion of chromium in nickel that was dispersion hardened with 5 percent thoria was an order of magnitude faster than in pure nickel or Ni-20 weight percent Cr. The rapid diffusion was attributed to a very high density of dislocations and subgrain boundaries in the dispersion-strengthened alloy. Similarly Wenderott[20] has shown that diffusion of ^{51}Cr in Ni-20Cr containing 0.1 weight percent CeO_2 is nearly an order to magnitude faster at 1200°C (2192°F) than in the same alloy without the ceria addition.

The purpose of the present study was to determine diffusion rates for aluminum and chromium in NiCrAl and NiCrAlThO_2 alloys in order to establish the influence of thoria additions on the mobilities of these two species. If diffusivities of one or the other of the two are significantly affected by the thoria particles, it may be expected that oxidation mechanisms will be influenced.

Diffusion profiles for aluminum into TDNiCr and Ni-20Cr have been obtained by electron probe microanalysis on specimens aluminized at 1210°C (2210°F) for 16 hours and at 1260°C (2300°F) for 3.3 hours as described above, while diffusivities for chromium in various alloys have been obtained from experiments with the ^{51}Cr tracer on specimens annealed at temperatures in the range of 1038-1204°C (1900-2200°F) for 50 hours.

Experimental Procedures

The radioactive chromium was vacuum evaporated onto the alloy specimens from ^{51}Cr labelled chromium which was produced by neutron irradiation of high purity iodide chromium metal in the Battelle Research Reactor. The 1.59-cm (5/8 in.) square specimens were formed into couples and sandwiched with active faces in contact using molybdenum wires. Two sandwiches, consisting of TDNiCr and Ni-20Cr were then sealed in quartz capsules containing sufficient argon to give one atmosphere at the diffusion temperature. The diffusion anneals were conducted in a platinum-wire-wound resistance furnace for 50 hours. Upon completion of the anneal the specimens were removed and 0.317 cm (1.8 in.) was cut from each edge to eliminate the effects of any tracer that might have diffused down the sides of the specimens.

The specimens were then mounted in a micrometer-driven grinding block and diffusion profiles were obtained by grinding off layers of approximately 10 μm from the surface and counting the activity in the sections removed and the surface of the specimen after each grinding operation. Grinding was performed on 240-grit, kerosene-impregnated, metallographic paper and the thickness removed was measured using an electronic height gage and a micrometer.

For the experimental conditions of this investigation an infinitely thin layer of ^{51}Cr can be assumed to have been deposited on a semi-infinite solid. For such conditions the gradient of tracer concentration, C, at a distance x, beneath the original interface is given by

$$\delta \ln C / \delta x^2 = - 1/4Dt \quad , \tag{3}$$

where D is the diffusion coefficient in cm^2/sec and t is the time in seconds. Diffusion coefficients can be obtained by plotting the logarithm of the activity against the square of the distance from the initial interface, and setting the slope of the straight line so obtained equal to -1/4 Dt. Data obtained from diffusion anneals conducted at 1204°C (2200°F) under one atmosphere of argon are plotted in Figure 37 as counts per minute, cpm, versus x^2, where x = distance from the surface in μm. Similar results were obtained using data from either the sectioning method or the residual-activity technique (which are plotted in Figure 37).

Concentration profiles for aluminum in TDNiCr and Ni-20Cr after diffusion from the NiCrAl alloy for 16 hours at 1210°C (2210°F); i.e., aluminizing Treatment 2, are

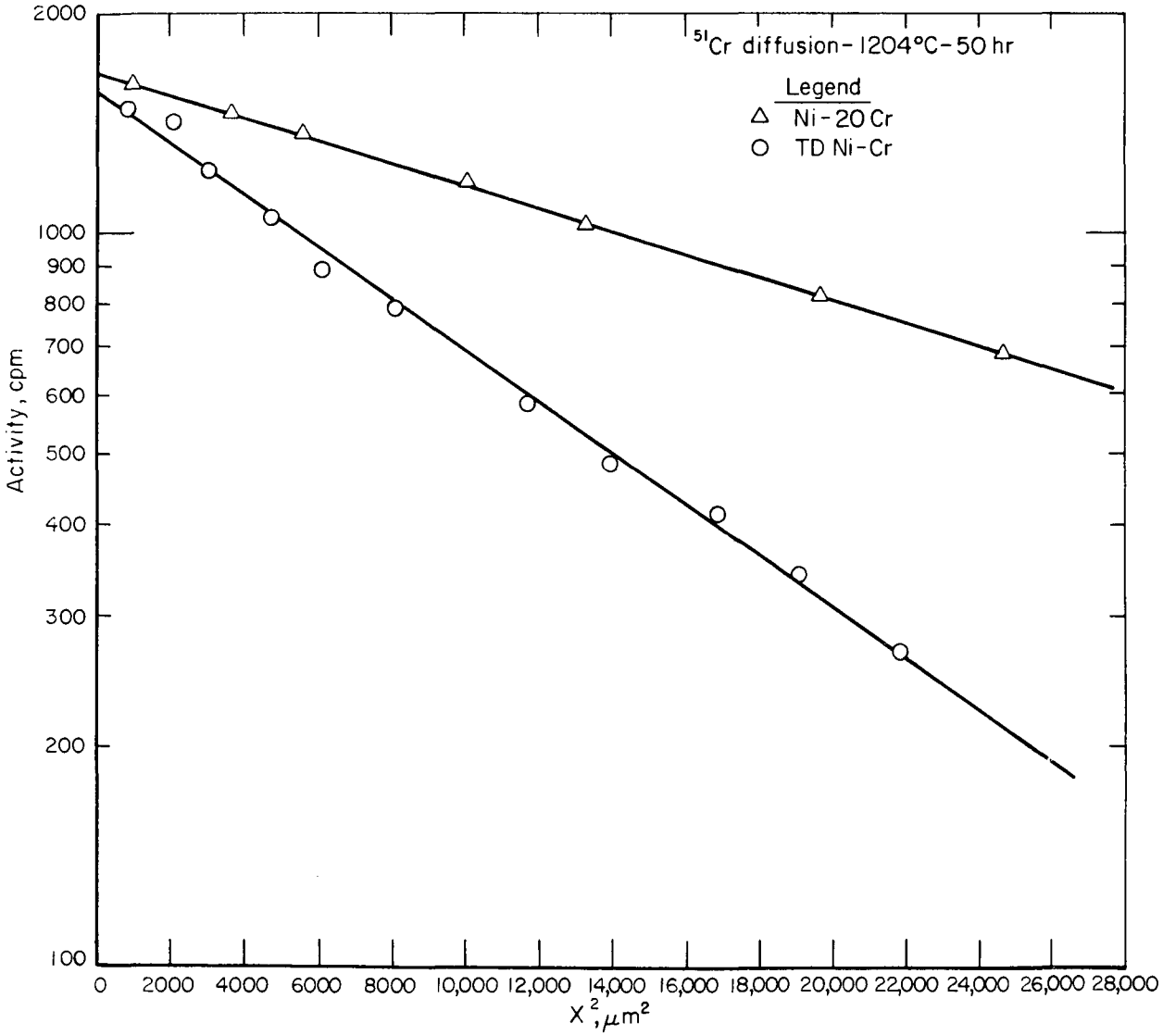

FIGURE 37. PENETRATION PROFILES FOR THE DIFFUSION OF ^{51}Cr IN TDNiCr AND Ni-20Cr AT 1204°C (2200°F)

shown in Figure 7 and 8. If it is assumed that the pack provided a continuous source at constant aluminum activity, then the profiles can be fit to the complementary error function solution to Fick's Second Law:

$$C(x) = C_S \left[1 - \text{erf} \frac{x}{2(Dt)^{1/2}} \right] , \quad (4)$$

where C(x) is the concentration at a distance, x, below the surface, C_S is the time-independent concentration of diffusant at the specimen surface, and t is the diffusion time.

Hall's method[21] can be employed to determine diffusion coefficients from the data if Equation 4 is valid. In this method $P = 50(2 - C/C_S) = 50[1 + \text{erf}\,(x/2(Dt)^{1/2}]$ is plotted versus $\lambda = [x/t^{1/2}]$ using probability paper to give a straight line of slope $h = 1/2D^{1/2}$. Typical plots of P versus λ are shown in Figure 38 for aluminum in TDNiCr and Ni-20Cr. The straight line obtained using this analysis for aluminum diffusion in TDNiCr is seen to intersect the origin at P = 50, indicating that concentration-independent diffusion has been observed. As shown in Figure 38, the profiles for aluminum in Ni-20Cr are not as clearly defined as those for TDNiCr, and the analysis of these data does not give linear behavior. That the nature of the profiles for aluminum in the two alloys is very similar suggests that aluminum diffusivities are nearly the same for TDNiCr and Ni-20Cr.

Results and Discussion

Chromium diffusivities have been measured for coarse-grained TDNiCr and TDNiCr-5.8Al with a grain-aspect ratio of 8.8, and on fine grained Ni-20Cr and Ni-20Cr-5.8Al prepared by the same method used to produce TDNiCr. The characterization of these alloys was discussed in the section on oxidation studies. Several diffusion coefficients have also been obtained for chromium migration in a fine grained TDNiCr, having a grain size on the order of 1 μm (see Figure 39).

Diffusion coefficients for ^{51}Cr in TDNiCr and Ni-20Cr obtained in this study are tabulated in Table 5 and are plotted in Figure 40. Also included in Figure 40 are results obtained by various investigators for chromium diffusion in thoriated nickel[5], and coarse grained Ni-20Cr.[22]

At least-squares analysis of the diffusion data, fit to an Arrhenius-type equation gave the following results for ^{51}Cr diffusion in coarse grained TDNiCr:

$$D_{Cr} = 0.92 \exp\left(\frac{-64.3 \text{ kcal/mole}}{RT}\right) \frac{\text{cm}^2}{\text{sec}} , \quad (5)$$

and, for diffusion of chromium in the fine grained Ni-20Cr:

$$D_{Cr} = 2,95 \times 10^{-3} \exp\left(\frac{-46.1 \text{ kcal/mole}}{RT}\right) \frac{\text{cm}^2}{\text{sec}} . \quad (6)$$

It is believed, on the basis of comparable activation energies and pre-exponential factors, that the present data for chromium diffusion in coarse grained TDNiCr are representative of true volume diffusion and that there is no real difference in rates in TDNiCr and coarse-grained Ni-20Cr. The higher diffusion coefficients, with low activation

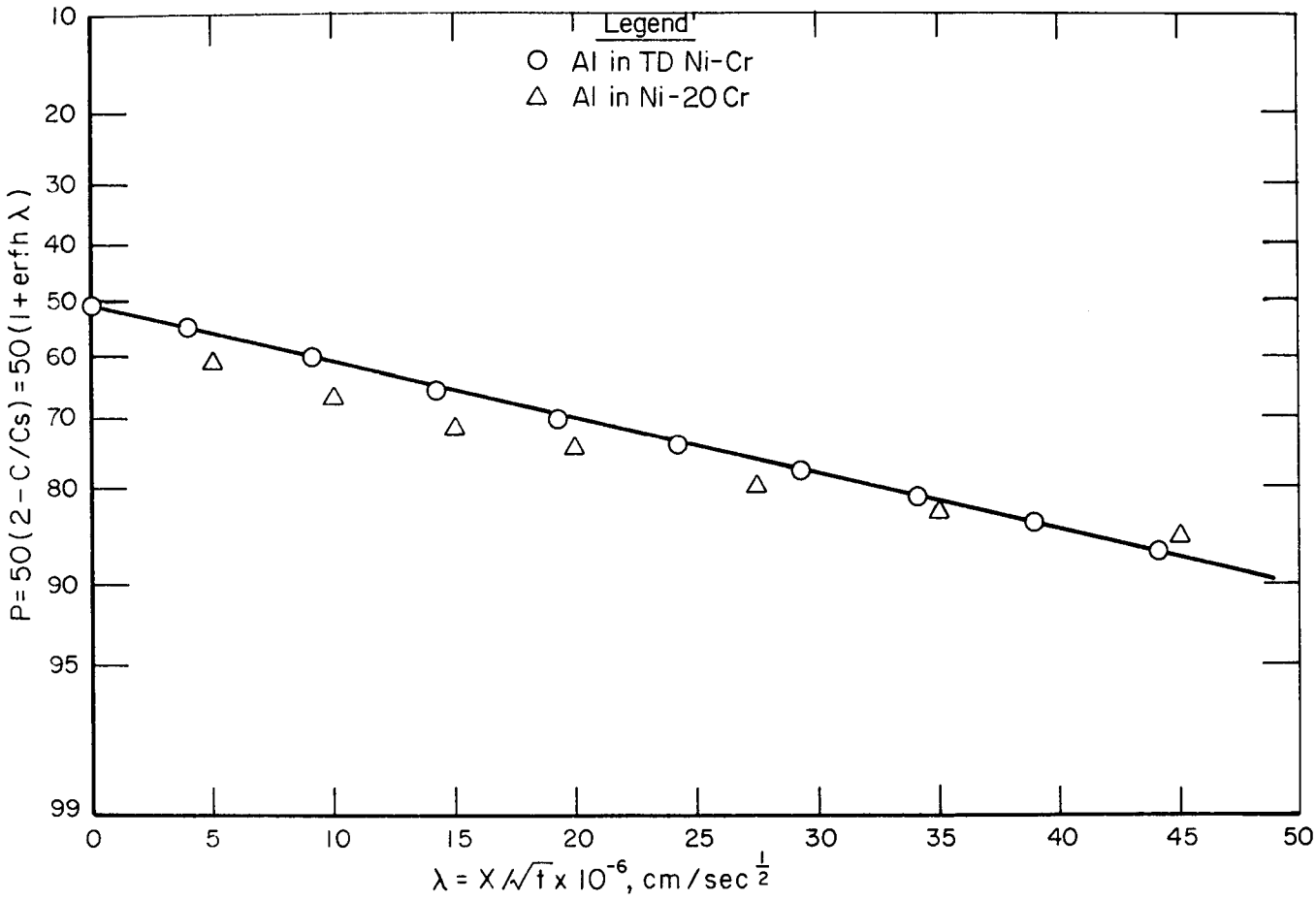

FIGURE 38. ALUMINUM DIFFUSION IN TDNi-Cr AND Ni-20Cr AT 1210°C (2210°F)

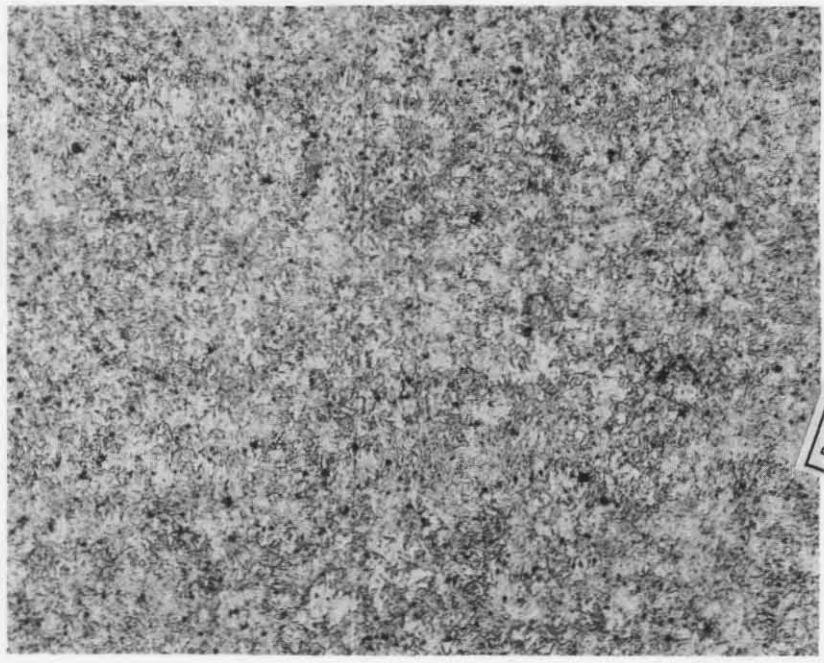

FIGURE 39. MICROSTRUCTURE OF FINE-GRAINED TDNi-Cr

energy and pre-exponetial, found in this study for chromium migration in fine-grained Ni-20Cr and TDNiCr are indicative of grain-boundary or other short-circuit contributions to the diffusivities. The grain size of the Ni-20Cr used in this study is 0.00076 cm (0.0003 in.), with many Cr_2O_3 inclusions. This is in contrast to the specimens used by Tyutyunnik and Estulin[23], for example, which had a grain size of 0.0041 cm, and those used by Monma, et al[22], which had grain sizes in the range of 0.1 to 0.4 cm. As mentioned above, the fine-grained TDNiCr, which yielded high D values for ^{51}Cr had a grain size of about 1μm.

The high diffusivities obtained by Fleetwood[5] using microprobe analysis may have been caused by some concentration-dependent diffusion; in the microprobe experiments chromium concentrations were as high as 50 weight percent at the specimen surface. Alternatively, the thoriated alloy used by Fleetwood may indeed have had a very high dislocation density that acted as short-circuit paths for diffusion and gave rise to the very low activation energy and preexponential found for chromium diffusion. Similar results were found for ^{51}Cr diffusion in fine-grained Ni-20Cr-3Y_2O_3, which was prepared by attritor milling of fine powders.[24]

Comparison of the diffusivities for ^{51}Cr in aluminized TDNiCr and Ni-20Cr at 1200°C (2192°F) with those for the alloys without aluminum, shows that the diffusion coefficients are the same for a given alloy, with or without aluminum. Thus no direct effect of thoria or of an aluminum (and simultaneously chromium) concentration gradient on chromium diffusion is evident at 1200°C (2192°F).

Diffusion coefficients were also determined for ^{51}Cr diffused into TDNiCr-5.8Al and Ni-20Cr-5.8Al at 1100°C (2012°F) for 50 hours under 1.01 x 10^5 N/m^2 (760 torr) argon. The values obtained were 3.17 x 10^{-11} cm^2/sec and 7.59 x 10^{-11} cm^2/sec for TDNiCr-5.8Al and Ni-Cr-5.8Al, respectively. The higher diffusion rate for the fine-grained ThO_2-free alloy is in accord with results for alloys without aluminum. For

TABLE 5. DIFFUSION COEFFICIENTS FOR ^{51}Cr IN TDNiCr, TDNiCr-5.8Al, Ni-20Cr-5.8Al, AND Ni-20Cr FOR 50 HOURS IN 1 ATM ARGON

Specimen	Alloy	Temperature C	Temperature F	D, cm^2/sec
T 1	TDNiCr	1200	2192	1.83×10^{-10}
T 2	TDNiCr	1200	2192	1.83×10^{-10}
N 1	Ni-20Cr	1200	2192	3.87×10^{-10}
T 5	TDNiCr	1100	2012	4.01×10^{-11}
N 3	Ni-20Cr	1100	2012	1.20×10^{-10}
T 7	TDNiCr	1038	1900	1.34×10^{-11}
T 8	TDNiCr	1038	1900	1.23×10^{-11}
N 5	Ni-20Cr	1038	1900	5.85×10^{-11}
N 6	Ni-20Cr	1038	1900	6.03×10^{-11}
T 9	TDNiCr	1149	2100	1.01×10^{-10}
T 10	TDNiCr	1149	2100	1.08×10^{-10}
N 7	Ni-20Cr	1149	2100	2.71×10^{-10}
N 8	Ni-20Cr	1149	2100	2.48×10^{-10}
T 13	TDNiCr-5.8Al	1200	2192	1.91×10^{-10}
T 14	TDNiCr-5.8Al	1200	2192	1.94×10^{-10}
N 11	Ni-20Cr-5.8Al	1200	2192	3.91×10^{-10}
N 9	Ni-20Cr-5.8Al	1093	2000	7.59×10^{-11}
N 10	Ni-20Cr-5.8Al	1093	2000	7.07×10^{-11}
T 11	TDNiCr-5.8Al	1093	2000	3.17×10^{-11}
T 15	TDNiCr (fine grained)	1050	1922	8.71×10^{-11}
T 17	TDNiCr (fine grained)	1150	2102	3.13×10^{-10}
T 18	TDNiCr (fine grained)	1150	2102	3.26×10^{-10}

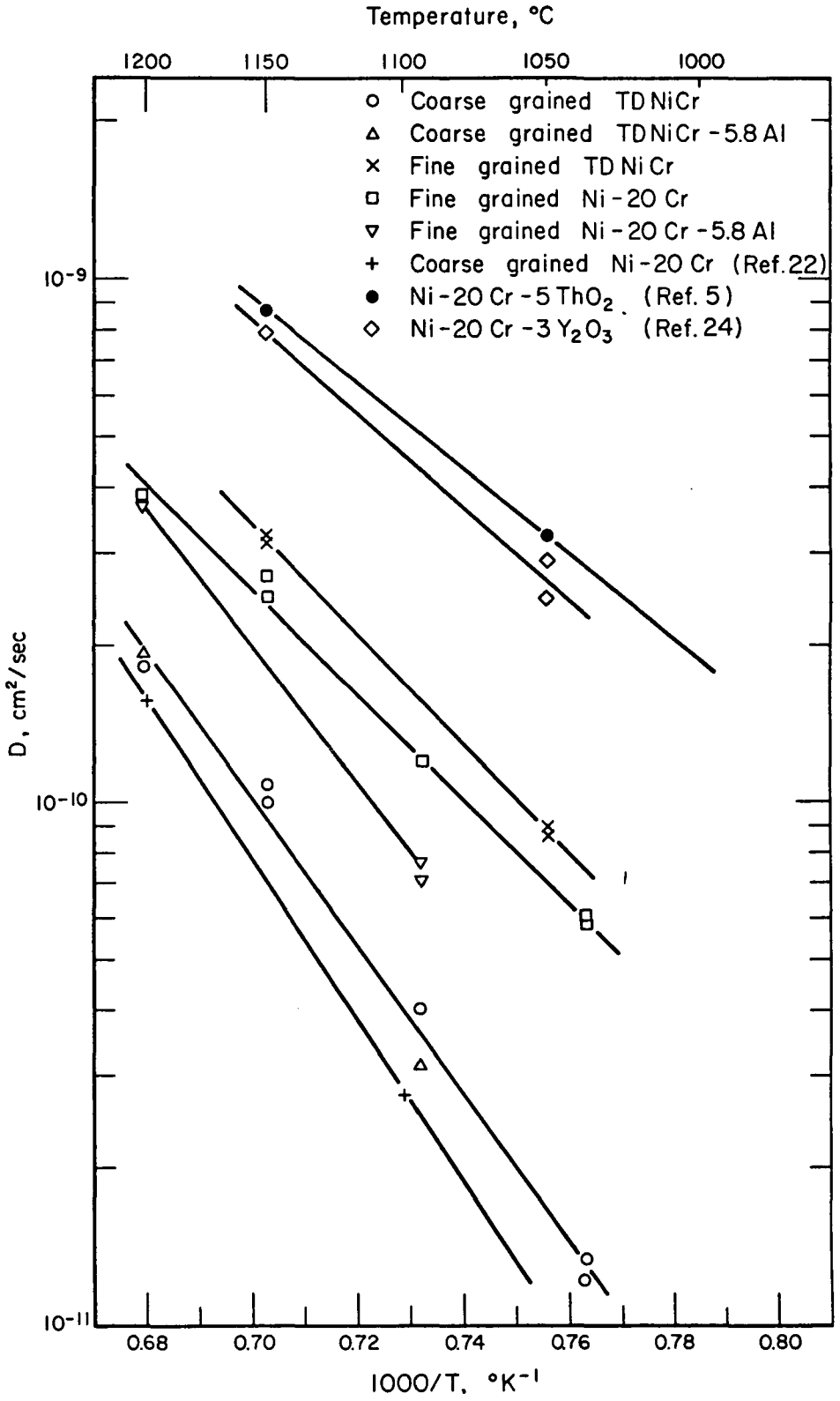

FIGURE 40. DIFFUSION COEFFICIENTS VERSUS RECIPROCAL OF ABSOLUTE TEMPERATURE FOR CHROMIUM DIFFUSION IN Ni-20Cr ALLOYS WITH AND WITHOUT DISPERSOID

both aluminized alloys, however, the diffusion rates are 30 to 60 percent lower than the values found in as-received material. This is in contrast to results obtained at 1200°C (2192°F) where the diffusion coefficients were the same for aluminized and as-received alloys. This difference may reflect the influence of the chromium-concentration gradient created during aluminizing. In the TDNiCr-5.8Al alloy, the surface concentration of chromium is 14.8 weight percent, and the concentration some 100 μm for the surface is approximately 20 weight percent. This gradient was quickly reduced at 1200°C (2192°F) where the diffusion rates are high, as mentioned in the section on oxidation studies. After oxidation of TDNiCr-5.8Al for 50 hours at 1100°C (2012°F), a distinct chromium-concentration gradient was still present, with the concentration decreasing from the center to the surface of the specimen.

The results obtained in this study suggest that a satisfactory explanation for the selective oxidation to produce Cr_2O_3 in thoriated Ni-20Cr alloys having the coarse grained, recrystallized structure characteristic of Fansteel TDNiCr cannot be based on enhanced diffusion of chromium in this alloy.

Diffusion coefficients for aluminum in TDNiCr and Ni-20Cr were obtained from the electron-microprobe profiles of specimens aluminized at 1210°C (2210°F) for 16 hours, and at 1260°C (2300°F) for 3.3 hours. The diffusion coefficient for aluminum in TDNiCr at 1210°C (2210°F) was 7.02×10^{-10} cm^2/sec. At 1260°C (2300°F) diffusion coefficients for aluminum in TDNiCr and Ni-20Cr were 1.30×10^{-9} and 2.67×10^{-9} cm^2/sec, respectively. Thus it is seen that aluminum diffusion is faster by a factor of two in the fine-grained Ni-20Cr than in the coarse-grained TDNiCr. This result is similar in magnitude to that found for chromium diffusion in these alloys using a tracer technique. The aluminum diffusivities are approximately a factor of three greater than the chromium diffusion coefficients both in TDNiCr and Ni-20Cr.

Few studies of diffusion in metals have included both aluminum and chromium diffusion. This is because of the lack of a suitable aluminum isotope. Thus comparisons of the present results with previous work is difficult. Diffusion of these two impurities in iron has been investigated, however[25, 26], and a sizable body of data for chromium diffusion in iron alloys is available.[27, 28]

Vignes, et al[25] used electron probe microanalysis to determine diffusion coefficients for aluminum in iron over the temperature range 800-1400°C (1472-2552°F). They measured diffusion in bcc iron (alpha) but in this temperature range it is the fcc gamma phase which is stable. They found that diffusivity does not vary with concentration, and the Hall method was used to obtain the relation:

$$D_{Al(Fe)} = 5.9 \exp[-57,700 \pm 1000)/RT] \quad . \tag{7}$$

For chromium diffusion in α iron in the temperature range of 775-875°C (1428-1608°F), Huntz, et al[26] found:

$$D_{Cr(Fe)} = 2.53 \exp[-(57,500)/RT] \quad . \tag{8}$$

For chromium diffusion in both Fe-1.7V and Fe-15Cr Pavlinov, et al[27] found:

$$D_{Cr} = 2.0 \exp[-(57,000)/RT] \quad , \tag{9}$$

while chromium diffusivities in Fe-12.3Cr and Fe-17.4Cr in the range of 900-1400°C (1652-2552°F) were found by Wolfe and Paxton[28] to fit relations of the form:

$$D_{Cr(Fe\text{-}12.3\ w/o\ Cr)} = 1.29\ \exp[-(55,200)/RT] \quad , \tag{10}$$

and

$$D_{Cr(Fe\text{-}17.4\ w/o\ Cr)} = 0.46\ \exp[-(52,500)/RT] \quad . \tag{11}$$

While direct comparisons with the present results are not possible, the large body of data suggest that aluminum diffusion is two to three times faster than chromium diffusion in fcc iron and iron-chromium alloys. This is similar to the behavior found in the present study for aluminum and chromium diffusion in TDNiCr and Ni-20Cr.

CONCLUSIONS

- A one-step pack process has been developed which permits the introduction of up to 6 weight percent aluminum into solid solution in the near-surface region of TDNiCr (Ni-20Cr-2ThO_2).

- Oxidation kinetics of TDNiCr at 1093°C (2000°F) and 1204°C (2200°F) in 1.33 x 10^3 N/m^2 (10 torr) and 1.01 x 10^5 N/m^2 (760 torr) air have been measured, and are in general accord with previous studies of the oxidation properties of this alloy.

- For all oxidation test conditions employed in this investigation, Al_2O_3 is the predominant constituent of scales which form on aluminized TDNiCr containing 5.8 weight percent aluminum at the surface (designated TDNiCr-5.8Al). Continuous weight increases are observed for this alloy for all tests (isothermal or cyclic) conducted in 1.01 x 10^5 N/m^2 (760 torr) or 1.33 x 10^3 N/m^2 (10 torr) air at 1204°C (2200°F) and 1093°C (2000°F).

- Continuous weight gains are observed for TDNiCr-4.95Al subjected to 50-hour isothermal oxidation tests, but weight losses occur during the course of 100-cycle tests in which the specimen is at temperature for 30 minutes and cooled for 20 minutes. This result, together with evidence from an analysis of the aluminum distribution in TDNiCr-4.95Al before and after oxidation, suggests that spallation occurs in the cyclic tests.

- TDNiCr-4.3Al does not have sufficient aluminum to form completely Al_2O_3 scales under the test conditions employed in this study. Weight losses are observed in both isothermal and cyclic tests at 1204°C (2200°F). These results suggest that the loss is due to scale spallation and to volatilization of Cr_2O_3 as CrO_3.

- The nature of the scale formed on pack aluminized TDNiCr depends on the aluminum surface concentration and on the distribution of aluminum through the alloy. For long-time oxidation resistance more protective Al_2O_3 scales may be produced on alloys containing shallow aluminum concentration profiles as compared with samples having high surface concentrations which decline sharply in the alloy.

- Analysis of aluminum profiles in pack-aluminized alloys suggests that after 50 hours at 1204°C (2200°F) the aluminum concentrations in all alloys tested in this program may be insufficient to provide protective Al_2O_3 scales in defected areas. Further experiments are necessary to decide whether or not this is the case.

- The oxidation kinetics for TDNiCr-5.8Al and NiCr-5.8Al in 50-hour isothermal tests are nearly identical. However, the ThO_2-free alloy is subject to severe spalling during cyclic tests, which does not occur for the thoriated alloy.

- Under certain conditions voids may occur during oxidation of aluminized alloys. Observations to date have not unambiguously distinguished between internal particles (such as Al_2O_3) or voids.

- Thickness changes due to oxidation could not be measured for the coarse belt-sanded finished specimens oxidized in this investigation.

- Results from a series of constrained bend tests and room-temperature tensile tests reveal little loss in ductility of pack aluminized TDNiCr as compared with that of the as-received TDNiCr.

- For a given grain size and temperature there is no difference in diffusivities for chromium diffusion in TDNiCr or Ni-20Cr. Diffusion coefficients increase with decreasing grain size for both alloys.

- Aluminum diffusivities are approximately three times higher than are chromium diffusion coefficients in TDNiCr and Ni-20Cr.

- The introduction of an aluminum gradient with a surface concentration of 5.8 weight percent to TDNiCr has no effect on chromium diffusion at 1200°C (2192°F), but it may depress chromium diffusivities at 1100°C (2012°F).

REFERENCES

1. R. Johnson and D. H. Killpatrick, "Dispersion-Strengthened Metal Structural Development", AFFDL-TR-68-130, Part I, July, 1968.

2. F. J. Centolanzi, "Hypervelocity Oxidation Tests of Thoria Dispersed Nickel Chromium Alloys", NASA-TM-X62,015 (February 11, 1971).

3. L. J. Klingler, P. G. Bailey, W. R. Weinberger, and S. Baranon, "Development of Dispersion Strengthened Nickel-Chromium Alloy (Ni-Cr-ThO_2) Sheet for Space Shuttle Vehicles", NASA Contract NAS3-13490, Fansteel Inc., Baltimore, Maryland.

4. G. R. Wallwork and A. Z. Hed, "The Oxidation of Ni-20 wt. % Cr-2 ThO_2", J. Oxidation of Metals, 3, 229(1971).

5. M. J. Fleetwood, "The Diffusion of Chromium Into Nickel-Thoria", J. Inst. Metals, 94, 218 (1966).

6. J. Stringer, I. G. Wright, B. A. Wilcox, and R. I. Jaffee, "Oxidation and Hot Corrosion of Ni-Cr and Co-Cr-Base Alloys Containing Rare Earth Oxide Dispersions", Final Report to Naval Air Systems Command, N00019-71-C-0079, October 20, 1971.

7. W. P. Gilbreath, "Preliminary Studies of the Oxidation of TDNi-20Cr in Static Flowing, and Dissociated Oxygen at 1100°C and 130 Nm^{-2}", NASA-TM-X-62,064 (August 18, 1971).

8. H. Lewis, Jour. Int. d'Etude sur l'ox. des Met., Serai, Brussels (October, 1965).

9. C. S. Tedmon, Jr., "The Effect of Oxide Volatilization on the Oxidation Kinetics of Cr and Fe-Cr Alloys", J. Electrochem. Soc., 113, 766 (1966).

10. C. E. Lowell, D. L. Deadmore, S. J. Grisaffe, and I. L. Drell, "Oxidation of Ni-20Cr-2ThO_2 and Ni-30Cr-1.5Si at 800°, 1000°, and 1200°C, NASA TDN-6290 (April, 1971).

11. C. S. Giggins and F. S. Pettit, "The Oxidation of TDNiC (Ni-20Cr-2 vol. pct. ThO_2) Between 900° and 1200°C", Met. Trans., 2, 1071 (1971).

12. W. C. Hagel, "Factors Affecting the High Temperature Oxidation of Chromium", Trans. ASM, 56, 583 (1963).

13. C. E. Lowell, "A Scanning Electron Microscopy Study of the Surface Morphology of TDNiCr Oxidized at 800°C to 1200°C", NASA TMX-67867 (June 8, 1971).

14. H. H. Davis, H. C. Graham, and I. A. Kvernes, "Oxidation Behavior of Ni-Cr-1ThO_2 Alloys at 1000° and 1200°C", J. Oxidation of Metals, 3, 431 (1971).

15. H. C. Graham and H. H. Davis, "Oxidation/Vaporization Kinetics of Cr_2O_3", J. Am. Ceram. Soc., 54, 89 (1971).

16. B. A. Wilcox, A. H. Clauer, and W. B. Hutchinson, "Structural Stability and Mechanical Behavior of Thermomechanically Processed Dispersion Strengthened Nickel Alloys", NASA CR-72832 (March 18, 1971).

17. B. A. Wilcox and R. I. Jaffee, "Direct and Indirect Strengthening Effects of ThO_2 Particles in Disperson-Hardened Nickel", Trans. Japan Inst. Met., 9, 575 (1968).

18. C. S. Giggins and F. S. Pettit, "Oxidation of Ni-Cr-Al Alloys Between 1000° and 1200°C", J. Electrochem. Soc., 118, (1971).

19. R. C. Cook, D. H. Timbres, and L. F. Norris, "Improvement of the Oxidation Resistance of Dispersion Strengthened Nickel-Chromium Alloys", AFML-TR-70-247 (October, 1970).

20. B. Wenderott, "On The Effect of Trace Elements in Nickel-Chromium, Heat-Resistant Alloy", Z. Metall., 56, 63 (1965).

21. L. D. Hall, "An Analytical Method of Calculating Variable Diffusion Coefficients", J. Chem. Phys., 21, 87 (1953).

22. K. Monma, H. Suto, and H. Oikawa, "Diffusion of Ni^{63} and Cr^{51} in Nickel-Chromium Alloys", J. Japan Inst. Metals, 28, 188 (1964).

23. A. D. Tyutyunnik and G. V. Estulin, "The Effect of Microstructure on Chromium Diffusion in Nickel-Based Alloys", Phys. Metals, Metallog. USSR, 4, 146 (1957).

24. M. S. Seltzer, unpublished research.

25. A. Vignes, J. Philibert, M. Badia, and J. Levasseur, "The Use of the Electron Microprobe for the Determination of Impurity Diffusion Coefficients", Second National Conference on Electron Microprobe Analysis, Paper No. 20, Boston, Mass., 1967.

26. A. M. Huntz, M. Aucouturier, and P. Lacombe, "Measurement of Volume and Intergranular Diffusion Coefficients of Radioactive Chromium in Alpha Iron", C. R. Acad. Sci., Paris, Ser. C, 265, 554 (1967).

27. L. V. Pavlinov, E. A. Isadzanov, and V. P. Smirnov, "Diffusion of Chromium in Alloys of Iron with Vanadium and Chromium", Phys. Met. and Metall., 25 (5), 206 (1968).

28. R. A. Wolfe and H. W. Paxton, "Diffusion in BCC Metals", Trans. Met. Soc. AIME, 230, 1426 (1964).

29. C. E. Lowell and W. A. Sanders, "Mach 1 Oxidation of Thoriated Nickel Chromium at 1204°C (2200°F)", NASA TDN-6562, November, 1971.

30. F. J. Centolanzi, H. B. Probst, L. E. Lowell, and N. B. Zimmerman, "Arc Jet Tests of Metallic TPS Materials", NASA TM X-62,092, October, 1971.

31. W. A. Sanders and C. A. Barrett, "Oxidation Screening at 1204°C (2200°F) of Candidate Alloys for the Space Shuttle Thermal Protection System", NASA TM X-67864, October, 1971.

NEW TECHNOLOGY

The research in this investigation has provided New Technology in the area of pack aluminizing. This technology is described in detail in pages 7 to 19, and was the subject of a New Technology Report submitted to the Technology Utilization Officer, NASA-Lewis Research Center, on August 18, 1971.

DISTRIBUTION LIST FOR SUMMARY REPORT

Contract NAS-3-14326

Addressee	No. of Copies
NASA Headquarters 600 Independence Avenue, S. W. Washington, D. C. 20546 Attention: G. Deutsch (RR-1)	1
NASA-Lewis Research Center 21000 Brookpark Road Cleveland, Ohio 44135 Attention: Aeronautics Proc. Section MS 77-3	1
Technology Utilization Office, M.S.3-19	1
Audit Branch, MS 500-303	1
Dr. G. Santoro, MS 49-1	4
F. H. Harf, MS 49-1	3
Dr. H. Probst, MS 49-1	1
J. C. Freche, MS 49-1	1
S. Grisaffe, MS 49-1	1
M. Quatinetz, MS 49-1	1
C. Blankenship, MS 105-1	1
R. W. Hall, MS 105-1	1
Professor Robert A. Rapp Department of Metallurgy The Ohio State University Columbus, Ohio 43210	1
Fansteel Metallurgical Corporation 5101 Tantalum Place Baltimore, Maryland 21216 Attention: Dr. L. Klingler	1
Metals and Ceramics Information Center (MCIC) Battelle Memorial Institute 505 King Avenue Columbus, Ohio 43201	1
Aerospace Research Laboratories Metallurgy and Ceramics Research Lab. Building 450 (ARZ) Wright-Patterson AFB, Ohio 45433 Attention: Dr. N. M. Tallan	1
Dr. H. C. Graham	1
Dr. H. Davis	1
McDonnel Douglas Corporation Materials Research Division 3000 Ocean Park Boulevard Santa Monica, California 90406 Attention: Dr. D. Killpatrick	1

Addressee	No. of Copies
Defense Documentation Center (DDC) Cameron Station 5010 Duke Street Alexandria, Virginia 22314	1
Chief, Bureau of Naval Weapons Department of the Navy Washington, D. C. 20350 Attention: RRMA-2/T. F. Kearns	1
RRMA/I. Machlin	1
NASA-Langley Research Center Langley Station Hampton, Virginia 23365 Attention: Technical Library	1
NASA-Manned Spacecraft Center Structures and Mechanics Division 2101 Webster-Seabrook Road Houston, Texas 77058 Attention: Library	1
U. S. Army Aviation Materials Lab. Fort Eustis, Virginia 23604 Attention: John White, Chief, SMOFE-APG	1
Jet Propulsion Laboratory 4800 Oak Grove Drive Pasadena, California 91103 Attention: Library	1
NASA-Ames Research Center Moffet Field, California 94035 Attention: Library	1
Dr. W. Gilbreath	1
Dr. F. Centolanzi	1
NASA-Goddard Space Flight Center Greenbelt, Maryland 20771 Attention: Library	1
NASA-Flight Research Center P. O. Box 273 Edwards, California 93523 Attention: Library	1
Air Force Institute of Technology Civil Engineering School Wright-Patterson AFB, Ohio 45433 Attention: Dr. James R. Myers	1

DISTRIBUTION LIST
(Continued)

Addressee	No. of Copies
Avco Lycoming Division Materials Laboratories Department 550 South Main Street Stratford, Connecticut 06497 Attention: Dr. W.R. Freeman, Jr.	1
Bell Telephone Laboratories Department of Metallurgical Engineering Room 1A-106 Murray Hill, New Jersey 07974 Attention: Dr. J. H. Swisher	1
Bendix Research Laboratories Materials and Processes Department 10-1/2 Mile Road Southfield, Michigan 48075 Attention: S. K. Rhee	1
Cabot Corporation Stellite Division Technology Department 1020 West Park Avenue Kokomo, Indiana 46901 Attention: Dr. S. T. Wlodek	1
Curtiss-Wright Corporation Materials Engineering Department One Passaic Street Wood-Ridge, New Jersey 07075 Attention: Dr. Sam Wolsin	1
University of Delaware Department of Chemical Engineering Newark, Delaware 19711 Attention: Professor C. E. Birchenall	1
Ford Motor Company Materials Development Department Turbine Operations 20000 Rotunda Drive Dearborn, Michigan 48121 Attention: Yesh P. Telang	1
General Electric Company Materials and Processes Laboratory Schenectady, New York 12305 Attention: Dr. Chester T. Sims	1
General Electric Company Material and Process Technology Laboratories Thomson Laboratory 1000 Western Avenue Lynn, Massachusetts 01905 Attention: Dr. M. Kaufman	1
General Electric Company Oxidation/Corrosion Laboratory Materials Development Engineering Gas Turbine Department No. 53-337 Schenectady, New York 12305 Attention: Harvey von E. Doering	1
General Electric Company Research and Development Center Metallurgy and Ceramics Laboratory P. O. Box 8 Schenectady, New York 12301 Attention: Dr. C. S. Tedmon, Jr. Dr. Alan U. Seybolt	1 1
General Electric Company Materials and Process Technology Laboratory Aircraft Engine Group Building 500-M87 Cincinnati, Ohio 45215 Attention: Dr. William C. Hagel	1
General Electric Company Materials and Processes Laboratory Aircraft Engine Group Evendale, Ohio 45218 Attention: Dr. R. E. Allen	1
The International Nickel Company Paul D. Merica Research Laboratory Materials System Section Sterling Forest Suffern, New York 10901 Attention: Dr. J. W. Schultz	1
Little, A. D., Inc. R&D Division, Materials Section Cambridge, Massachusetts 02140 Attention: Dr. Joan B. Berkowitz	1
Lockheed Missiles and Space Company Palo Alto Research Laboratories Metallurgy and Composites, D/52-31, B/204 3251 Hanover Street Palo Alto, California 94304 Attention: Dr. T. E. Tietz	1
Naval Air Development Center Mechanical Metallurgy Branch (MAMM-4) Metallurgical Division Aero Materials Department Warminster, Pennsylvania 18974 Attention: Robert G. Mahorter	1

DISTRIBUTION LIST
(Continued)

Addressee	No. of Copies
Naval Ship Research and Development Laboratory Metals and Composites Division Code A815 Annapolis, Maryland 21402 Attention: Walter L. Wheatfall, Sr.	1
New York State University Dept. of Materials Science College of Engineering Stony Brook L.I., New York 11790 Attention: Professor L. Seigle	1
North American Rockwell Corporation Science Center Thousand Oaks, California 91360 Attention: Dr. Neil Paton	1
Northwestern University Department of Materials Science The Technological Institute Evanston, Illinois 60201 Attention: Prof. J. Bruce Wagner, Jr.	1
Olin Corporation Metals Research Laboratories 91 Shelton Avenue New Haven, Connecticut 06511 Attention: Dr. M. J. Pryor	1
Pennsylvania State University Metallurgy Section M. I. Building University Park, Pennsylvania 16802 Attention: Prof. G. Simkovich	1
Phillips Petroleum Company Research and Development Department Phillips Research Center Building C-7 Bartlesville, Oklahoma 74003 Attention: R. M. Schirmer	1
Pratt and Whitney Aircraft Division of United Aircraft Corp. Advanced Materials Research and Development Laboratory Middletown, Connecticut 06457 Attention: Dr. F. S. Pettit Dr. G. W. Goward	1 1

Addressee	No. of Copies
Solar Division International Harvester Company Process Research Department (Mail Zone R-1) 2200 Pacific Highway San Diego, California 92112 Attention: A. R. Stetson	1
Sylvania Electric Products, Inc. Chemical and Metallurgical Division High Temperature Composites Laboratory 70 Cantiague Road Hicksville, New York 11802 Attention: Lawrence Sama	1
Systems Research Laboratories, Inc. Physical Sciences Division 7001 Indian Ripple Road Dayton, Ohio 45440 Attention: Dr. W. C. Tripp	1
TRW, Inc. Equipment Group 23555 Euclid Avenue Cleveland, Ohio 44117 Attention: Dr. J. V. Peck	1
United Aircraft Research Laboratories High Temperature Materials Research 400 Main Street East Hartford, Connecticut 06108 Attention: Dr. Michael A. DeCrescente	1
United States Steel Corporation Applied Research Laboratory, MS-16 P. O. Box 38 Monroeville, Pennsylvania 15146 Attention: Dr. W. E. Boggs	1
United States Steel Corporation Physical Chemistry Section Edgar C. Bain Laboratory for Fundamental Research Research Center Monroeville, Pennsylvania 15146 Attention: Dr. Howard W. Pickering	1
University of California at Los Angeles Materials Department 6531 Boelter Hall Los Angeles, California 90024 Attention: Professor D. L. Douglass	1

DISTRIBUTION LIST
(Continued)

Addressee	No. of Copies
Vanderbilt University Department of Materials Science and Metallurgical Engineering Nashville, Tennessee 37203 Attention: Professor B. D. Lichter	1
Westinghouse Electric Corporation Astronuclear Laboratory Metals Science Section P. O. Box 10864 Pittsburgh, Pennsylvania 15236 Attention: Dr. R. C. Svedberg	1
Westinghouse Electric Corporation Westinghouse Research Laboratories Churchill Borough Pittsburgh, Pennsylvania 15235 Attention: Dr. Earl A. Gulbransen	1
Atomic Energy of Canada Limited Chalk River Nuclear Laboratories Materials Science Branch Chalk River, Ontario Canada Attention: Dr. B. Cox	1
McMaster University Department of Metallurgy Hamilton, Ontario Canada Attention: Professor W. W. Smeltzer	1
Sentralinstitutt for Industriell-51 Blindern, Forskingvien 1 Oslo 3, Norway Attention: Dr. P. Kofstad	1
University of Manchester Institute of Science and Technology Chem. Eng. P. O. Box 88, Sackville Street Manchester M60 1QD Attention: Dr. G. C. Wood	1
School of Metallurgy University of New South Wales Kensington Australia Attention: Prof. G. R. Wallwork	1